QUANTIFICATION OF SYNERGIES BETWEEN ENERGY EFFICIENCY FIRST PRINCIPLE AND RENEWABLE ENERGY SYSTEMS

D5.1

Excess heat potentials of industrial sites in Europe

(Revised version)

Documentation on excess heat potentials of industrial sites including open data file with selected potentials

Project

Acronym	**sEEnergies**
Title	Quantification of Synergies between Energy Efficiency First Principle and Renewable Energy Systems
Coordinator	Aalborg Universitet
Reference	846463
Type	Research and Innovation Action (RIA)
Programme	HORIZON 2020
Topic	LC-SC3-EE-14-2018-2019-2020 - Socio-economic research conceptualising and modelling energy efficiency and energy demand
Start	01 September 2019
Duration	30 months
Website	https://seenergies.eu/

Consortium

Aalborg Universitet (AAU), Denmark
Hogskolan i Halmstad (HU), Sweden
TEP Energy GmbH (TEP), Switzerland
Universiteit Utrecht (UU), Netherlands
Europa-Universität Flensburg (EUF), Germany
Katholieke Universiteit Leuven (KULeuven), Belgium
Norges Miljø- og Biovitenskapelige Universitet (NMBU), Norway
SYNYO GmbH (SYNYO), Austria
Fraunhofer-Gesellschaft zur Förderung der angewandten Forschung e.V. (Fraunhofer), Germany

Deliverable

Number	**D5.1**
Title	**Documentation on excess heat potentials of industrial sites including open data file with selected potentials (Revised version)**
Lead beneficiary	Fraunhofer
Work package	WP5
Dissemination level	Public
Nature	Other
Due date	28.02.2020
Submission date	28.02.2020 (31.12.2020)
Authors	**Tobias Fleiter (Fraunhofer ISI)** **Pia Manz (Fraunhofer ISI)** **Marius Neuwirth (Fraunhofer ISI)** **Felix Mildner (Fraunhofer ISI)** **Urban Persson (HU)** **Katerina Kermeli (UU)** **Wina Crijns-Graus (UU)** **Cathelijne Rutten (formerly UU)**
Contributors	
Reviewers	**Brian Vad Mathiesen (AAU)** **Ulrich Reiter (TEP Energy)**
Revision note	An SQL script error in the final modelling step to group the calculated number of industrial sites with spatial matches to actual district heating areas (DH-A) was found post submission. The correct number of industrial sites with such 1st rank matches within the used 10 km search radius is 866 (of which 752 with data on annual excess heat volumes) and not 499 (466 with data) as stated in the original version. The correction of this error is reflected here in the revised version mainly in Table 26, Table 29, Table 30, Figure 20, and associated text paragraphs. The main significance of the correction is that the potential for external excess heat recovery in current district heating systems was underestimated by an approximate factor 0.66: for example, at cooling of flue gases to 95 ˚C and at current rates of internal heat recoveries, the potential amounts to 230 PJ per year and not to 151 PJ per year as stated in the original report. Apart from this correction, no other major changes made in this version.

© 2020 sEEnergies | Horizon 2020 – LC-SC3-EE-14-2018-2019-2020 | 846463

Acknowledgement: This project has received funding from the European Union's Horizon 2020 Research and Innovation Programme under Grant Agreement No 846463.	**Disclaimer:** The content of this publication is the sole responsibility of the authors, and in no way represents the view of the European Commission or its services.

© 2020 sEEnergies | Horizon 2020 – LC-SC3-EE-14-2018-2019-2020 | 846463

Executive Summary

Facilities of energy-intensive industries including those for the production of steel, cement, paper, glass, chemicals and others are spread across Europe. The combination of high flue gas temperatures, continuous operation and highly concentrated point sources make the excess heat from such industrial plants a very attractive source for district heating. Despite this, excess heat sources from industry are currently only rarely exploited and major potentials are being wasted.

Here, we aim to contribute by providing the most detailed, comprehensive assessment of the excess heat potentials available for Europe. More specifically, we aim to analyse the available excess heat from heavy industry in Europe and assess its suitability for use in district heating systems. Our approach uses GIS-based mapping of 1608 industrial sites in Europe combined with a process-specific assessment of their excess heat potential. The heat sources are then matched with data on heat demand density and existing as well as potential district heating networks. The scope of this analysis covers the major industrial excess heat sources (large heavy industry facilities) and the most important excess heat streams: flue gases.

Our results show a total potential of 425 PJ of excess heat available at a temperature of 95°C, with 960 PJ available at a lower temperature (25°C). This equals about 4% and 9% of total industrial final energy demand in 2015, respectively.

Matching this potential with a GIS analysis of heat demand densities and current district heating systems reveals that 230 PJ of excess heat could be used within a 10km range at a temperature of 95°C, which is compatible with most existing district heating systems. As district heat today has a total final energy consumption of 1,945 PJ, this means that about 12% of district heating in the EU28 could be supplied by excess heat sources from energy-intensive industries.

While this is already a substantial potential, many excess heat sources remain untapped, particularly in countries with low district heating use. We therefore projected future district heating systems based on a GIS analysis of heat demand densities for all EU28 countries. The results indicate that district heating systems would be economically viable in most urban areas in Europe and could cover as much as 65% of heat demand in buildings in the residential and service sectors. This represents an enormous increase compared to today's use of district heating. If district heating networks were expanded, they could use almost all the available excess heat from the industrial sites analysed. 98% of these are within 10km, allowing the exploitation of 415 PJ of heat at 95°C.

In the future, low-temperature district heating systems, often referred to as 4th generation district heating, are expected to diffuse further, which will increase the amount of excess heat available. For example, at a temperature of 25°C, the exploitable excess heat potentials will more than double from 415 PJ (95°C) to 940 PJ (25°C). This low-temperature heat could either be used in cold district heating systems with decentralised heat pumps, or in centralised large-scale heat pumps to supply district heating systems at higher temperatures.

To summarize, our analysis reveals a significant potential of mostly untapped excess heat from energy-intensive industries that could be used in district heating systems as well as a huge potential to increase the use of district heating systems in Europe. Combining excess heat sources and the deployment of district heating systems should therefore be a central element in the transition towards a sustainable and CO_2-neutral heating and cooling sector in Europe. However, the analysis also shows that industrial

excess heat alone will not be sufficient, and the major heat source for district heating will need to come from renewable energy sources (locally, this might be different in highly industrialised areas).

It should be emphasized that the bottom-up approach used inherently underestimates the available potentials, because it focuses on the largest point sources, major processes and flue gases as the most attractive excess heat streams. Although the analysis covers the most attractive potentials, including additional excess heat sources would increase the potentials available, particularly at lower temperatures. However, it should also be considered that some of the excess heat might be used via internal heat recovery before it is delivered to a district heating system.

Contents

Figures

Tables

Acronyms & Abbreviations

Term	Description
BFG	Blast furnace gas
BOF	Basic oxygen furnace
C	Carbon
CO	Carbon monoxide
CO_2	Carbon dioxide
CH_4	Methane
C_2H_6	Ethane
C_3H_8	Propane
C_4H_{10}	Butane
COG	Coke oven gas
Cp	Specific heat
DH	District heating
DH-A	Actual District Heating areas
DH-E	Expected District Heating areas
DRI	Direct reduced iron
EAF	Electric arc furnace
GIS	Geographical Information Systems
GJ	Gigajoule
h	Enthalpy
H_2	Hydrogen
H_2O	Water
HRE4	Heat Roadmap Europe 4
HUDHC	Halmstad University District Heating and Cooling database
kJ	Kilojoule
kmol	kilomole
m	Mass rate
MWh	Megawatt hour
NOx	Nitrogen oxide

© 2020 sEEnergies | Horizon 2020 – LC-SC3-EE-14-2018-2019-2020 | 846463

NUTS	Nomenclature of Territorial Units for Statistics (French: *Nomenclature des unités territoriales statistiques*)
NACE	Statistical Classification of Economic Activities in the European Community (French: *Nomenclature statistique des activités économiques dans la Communauté européenne)*
N_2	Nitrogen
EU ETS	European Union Emissions Trading System
E-PRTR	European Pollutant Release and Transfer Register
GHG	Greenhouse Gas
LHV	Low Heating Value
S	Sulfur
SEC	Specific energy consumption
SOx	Sulfur oxide
UA	Urban Areas
UMZ	Urban Morphological Zones

1 Introduction

Facilities from the energy-intensive industries including the production of steel, cement, paper, glass, chemicals and others are spread across Europe. Together they account for about 20% of Europe's energy consumption. Driven by economies of scale, individual plants have enormous energy needs due to upscaled process design and, mainly operate at temperatures above 1000°C. Due to high capital costs, all these plants are run in 3-shifts operation and only pause for maintenance needs. High energy costs as share of total production costs of 10-20% led to substantial improvements in energy efficiency in the past century in these industries. Still, many plants from the energy-intensive industries show substantial unused energy losses in the form of excess heat. A particularly large source of excess heat are the flue gasses resulting from combustion of fuels in furnaces and boilers. Individual projects (e.g. cement, refinery, steel, paper) throughout Europe show that the use of such excess heat sources and the integration in district heating grids is economically viable. Indeed, the high flue gas temperature and the continuous operation as well as they highly concentrated point sources make excess heat from industrial plants a very attractive source for district heating. This source, however, is currently typically neglected by city and district heating planners and large potentials remain wasted.

Here, we aim to contribute with the most detailed and the most comprehensive assessment of excess heat potentials available for Europe. More specifically, we aim to analyse the available potential for excess heat from the energy-intensive industries in Europe and assess the suitability for its use in district heating grids. Our approach uses a GIS-based mapping of about 1608 industrial sites in Europe combined with a process-specific assessment of their excess heat potential. The heat sources are then matched with heat demand density data and potential and existing district heating grids. The scope of this analysis contains the major industrial excess heat sources (large heavy industry facilities) and the most important excess heat streams: The flue gasses.

This report is structured along the three major analytical steps: The estimation of excess heat potentials (1), the allocation of excess heat potentials to industrial sites (2) and the matching with potential and existing district heating grids (3). Finally, we present results and derive conclusions. The report is accompanied by a data set containing the dataset with the 1608 excess heat sources in Europe.

1.1 Visualisation and public sharing of output dataset

The two major outputs from this work, the georeferenced industrial sites dataset[1] and the district heating areas dataset (expected and actual), are published as web map layers at the **sEEnergies D5.1 Web-App hosted by Europa-Universität Flensburg** (Fleiter et al., 2020):

https://tinyurl.com/sEEnergies-D5-1

Figure 1 provides a screenshot of both layers in zoomed-out view at this browser-based Web-App.

Both datasets are further available for download at the **sEEnergies Open Data hub** (sEEnergies, 2020):

https://tinyurl.com/sEEnergies-Hub

[1] The dataset contains a total of 1842 sites, of which 1608 sites show quantified excess heat potentials. For the remaining sites excess heat potentials could not be quantified, but might exist as well.

At this site, the datasets are visible on a map but also available for download in geospatial and tabular form. The datasets are published under the Creative Commons CC BY 4.0 license.

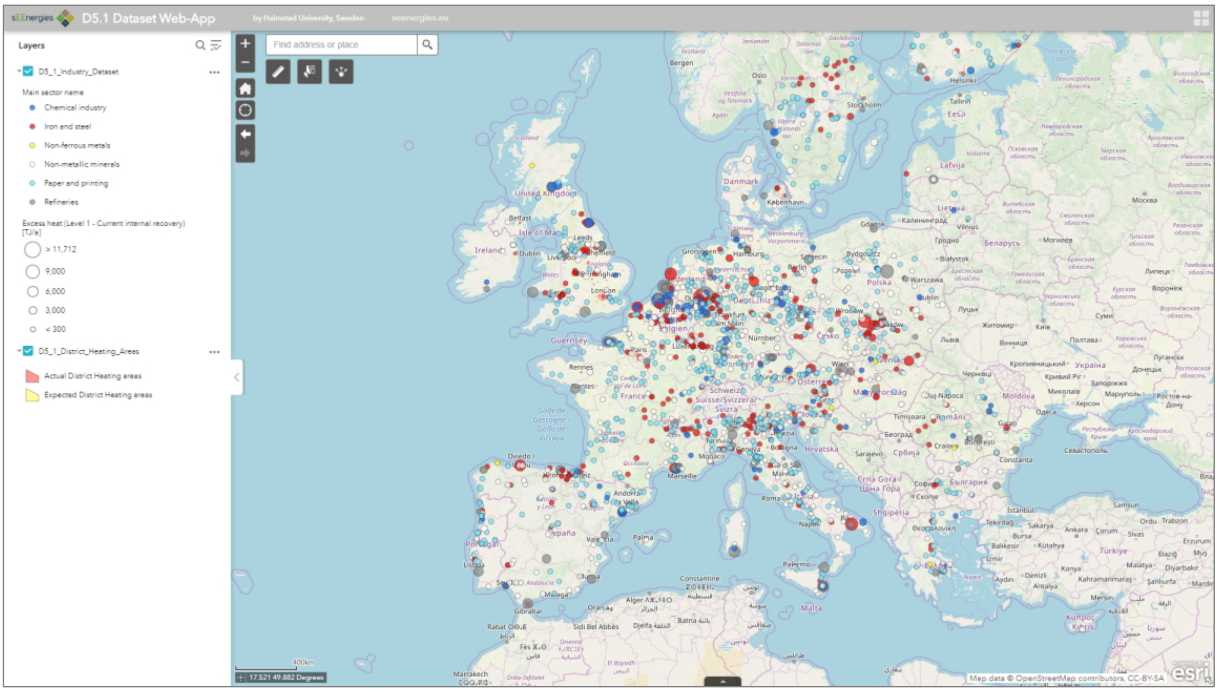

Figure 1: Screenshot 1: sEEnergies D5.1 Dataset Web-app with the industry dataset and the district heating areas dataset in zoomed-out view

Table 1 provides an overview of table properties for the attribute fields included in the district heating areas dataset.

Table 1: Properties of the district heating areas dataset accessible at the sEEnergies ArcGIS Hub site

Field Name	Description	Data type	Map Pop-up display
OBJECTID	Unique feature object identifier	Long Integer	Yes
Placename_assigned	Name	Short Text	Yes
CNTR_CODE	Two-digit country code	Short Text	Yes
NUTS_ID	NUTS3 Code	Short Text	Yes
NAME_ASCI	NUTS3 Name	Short Text	Yes
HD_345_GJ	Annual residential and service sector heat demands of area (Heat demand density classes 3-5) [GJ/a]	Double	No
HD_345_TJ	Annual residential and service sector heat demands of area (Heat demand density classes 3-5) [TJ/a]	Double	Yes
HD_345_PJ	Annual residential and service sector heat demands of area (Heat demand density classes 3-5) [PJ/a]	Double	No
Type	Indicator for actual district heating area ("DH" = Yes, "NULL" = No)	Short Text	Yes
CityID	District heating dataset city identifier (CityID)	Long Integer	Yes
GazetteerName	District heating dataset city name	Short Text	Yes
CountOfSystemID	Count of district heating systems per CityID	Long Integer	Yes
TARGET_FID_12	District heating dataset system identifier (SystemID)	Long Integer	Yes
Shape_Length	Circumference [m]	Double	Yes
Shape_Area	Area [m2]	Double	Yes
Shape	Geometry (polygon)	Short Text	No

Figure 2 shows a screenshot of both layers in zoomed-in view at the browser-based Web-App, with layer legends to the left and a map pop-up opened for the actual district heating area of Düsseldorf.

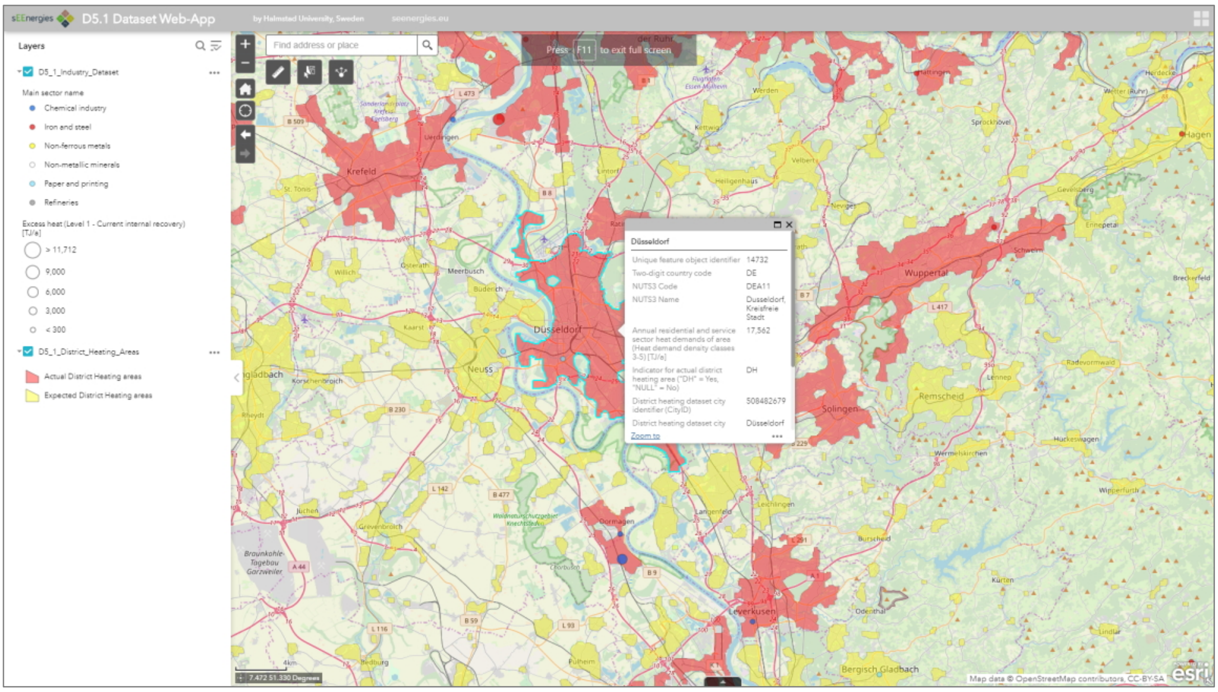

Figure 2: **Screenshot 2: sEEnergies D5.1 Dataset Web-app with the industry dataset and the district heating areas dataset in zoomed-in view, with Map Pop-up opened for Düsseldorf (district heating areas dataset)**

Table 2 provides an overview of table properties for the attribute fields included in the georeferenced industrial sites dataset.

Table 2: **Properties of the georeferenced industrial sites dataset accessible at the sEEnergies ArcGIS Hub site**

Field Name	Description	Data type	Map Pop-up display
OBJECTID	Unique feature object identifier	Long Integer	Yes
SiteId	Industrial dataset site identifier	Double	Yes
CompanyName	Company name	Short Text	Yes
StreetNameAndNumber	Street address	Short Text	Yes
Country	Two-digit country code	Short Text	Yes
EU28	Member State of the EU28? (Yes/No)	Short Text	No
Eurostat_Name	Main sector name	Short Text	Yes
Latitude	Site coordinates (Latitude)	Double	No
Longitude	Site coordinates (Longitude)	Double	No
NUTS1ID	NUTSID (Level 1 code)	Short Text	No
NUTS3ID	NUTSID (Level 3 code)	Short Text	Yes
Excess_Heat	Excess heat data? (Yes/No)	Short Text	Yes
level_1_Tj	Excess heat (Level 1 - Current internal recovery) [TJ/a]	Double	Yes
level_2_Tj	Excess heat (Level 2 - Current internal recovery) [TJ/a]	Double	Yes
level_3_Tj	Excess heat (Level 3 - Current internal recovery) [TJ/a]	Double	Yes
level_1_r_Tj	Excess heat (Level 1 - Max internal recovery) [TJ/a]	Double	Yes
level_2_r_Tj	Excess heat (Level 2 - Max internal recovery) [TJ/a]	Double	Yes
level_3_r_Tj	Excess heat (Level 3 - Max internal recovery) [TJ/a]	Double	Yes
level_1_Pj	Excess heat (Level 1 - Current internal recovery) [PJ/a]	Double	No
level_2_Pj	Excess heat (Level 2 - Current internal recovery) [PJ/a]	Double	No
level_3_Pj	Excess heat (Level 3 - Current internal recovery) [PJ/a]	Double	No
level_1_r_Pj	Excess heat (Level 1 - Max internal recovery) [PJ/a]	Double	No
level_2_r_Pj	Excess heat (Level 2 - Max internal recovery) [PJ/a]	Double	No
level_3_r_Pj	Excess heat (Level 3 - Max internal recovery) [PJ/a]	Double	No
Shape	Geometry (point)	Short Text	No

2 Overview of the approach

2.1 Overview of the data flow and calculations

The main objective of this deliverable is to calculate excess heat potentials from the energy-intensive industry sectors for the entire EU and estimate the share of these potentials that can be used in district heating systems. The analysis is to be conducted considering the georeferenced location of heat sources (industrial plants) and heat sinks (existing and potential future district heating systems).

The analysis consists of three major steps.

1. We first calculate excess heat potentials for specific industrial processes based on exhaust temperatures and relate them to the physical production (unit: GJ excess heat/t product output). The potentials are calculated regardless of the geographical context, but with specific knowledge of the industrial process.
2. In a second step, we allocate the excess heat potentials to geographical locations, meaning the current industrial sites/plants for each specific process. While no such data set with production capacity on a site level is publicly available, we construct a new data set by combining several individual data sets on emissions reporting as well as sectoral asset information. As a result, excess heat potentials are available for about 1608 major industrial sites throughout Europe.
3. In a third step, the excess heat potentials are matched with today's and future potential district heating systems by applying spatial GIS analyses. We calculate the amount of excess heat that can be realistically supplied to district heating networks.

2.2 Definition of excess heat potentials

The main purpose of the resulting excess heat potentials is their use in other sectors via district heating systems. Thus, the potentials are defined according to the temperature needs of district heating systems, as summarized in Table 3. As the availability of excess heat for external uses also depends on how much excess heat is used internally on the same site, e.g. for preheating materials, we distinguish two categories of potentials:

- **Current situation**: Many industrial processes already utilize waste heat recovery systems. This potential considers today's diffusion rate of the internal heat recovery technologies currently installed in the EU. This is assessed individually for each process considered. The calculated waste heat potentials represent the excess heat potential currently available for external use, if internal use of waste heat remains on today's levels.
- **Full internal use of excess heat**: We assume a 100% diffusion of internal waste heat recovery systems (e.g. for preheating materials), thereby reducing the remaining available excess heat for external use. This potential is more future oriented and assumes that internal excess heat use is always preferable over external heat use.

The second distinction of excess heat potentials concerns the maximum heat attainable from industrial gas streams when they are cooled down to the following reference temperatures:

- **25°C**: to estimate the maximum waste heat attainable if an exhaust gas is cooled to ambient temperatures. This can potentially be used as a heat source for large scale heat pumps feeding into 3rd or 4th generation district heating grids.

- **55°C**: to estimate the maximum waste heat attainable if an exhaust gas is cooled to 55°C. This can potentially be used directly in 4th Generation district heating grids that work on a lower temperature.
- **95°C**: to estimate the maximum waste heat attainable if an exhaust gas is cooled to 95°C. This can potentially be used directly in typical 3rd generation DH grids, which corresponds to many of the common district heating systems in place in Europe today.

The following table shows, how the two potential categories are combined.

Table 3: Definition of excess heat potentials and labels used throughout the report

	Level 1 - 25°C	Level 2 - 55°C	Level 3 - 95°C
Current situation	Level1	Level2	Level3
Full internal use of excess heat assumed	Level1_r	Level2_r	Level3_r

This analysis focuses on the exhaust streams from main energy intensive industrial processes to capture the most significant high-quality excess heat sources. Excess heat sources beyond the waste heat losses from exhaust gases, such as waste heat from solid streams (e.g. hot coke, rolled steel, hot clinker), liquid streams (e.g. wastewater in the paper production), cooling water, radiation heat losses (e.g. furnace openings) or conduction heat losses (heat lost from equipment surfaces) are not included although the analysis would benefit from such inclusion. Figure 3 shows the main sources of waste heat from industrial furnaces.

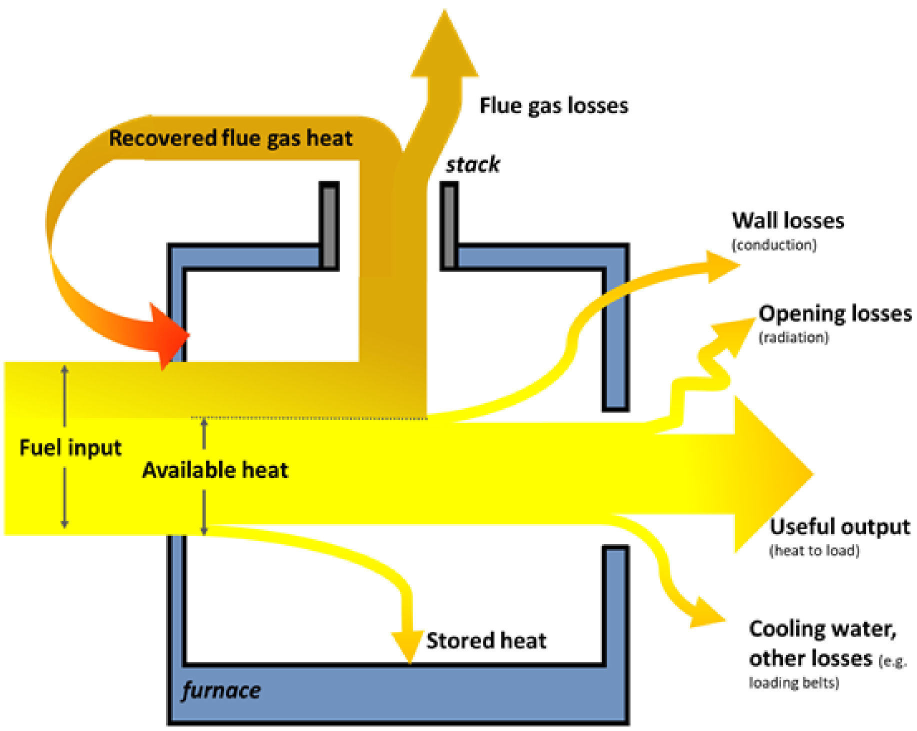

Figure 3: Typical heat losses in industrial furnaces (adjusted from BCS, 2008)

2.3 Literature overview on estimating industrial excess heat potentials

The estimation of (industrial) excess heat potential is an emerging research area and the number of studies which have previously proposed methodologies are limited (see e.g. Brückner et al. 2014).

An overview of methodologies used in existing literature for the estimation of waste heat potential is given in Table 4. The most sophisticated methods introduced early are used by McKenna & Norman (2010) and the BCS (2008) for the U.S. Department of Energy. Both methodologies are similar in the fact that they estimate excess heat potentials by comparing the input energy of a process to the energy that is released at the exhaust and estimating the maximum amount of recoverable work from this exhaust gas. A process-based method presented by Bühler et al. (2016, 2017 and 2018) uses energy and exergy analysis to determine the annual excess heat potential for 80% of industrial energy demand in Denmark based on several available data sources. This energy analyses is based on the fuel, heat and electricity demand of industrial sectors.

The main difference between the presented methodologies is the calculation method applied. McKenna & Norman (2010) take conservative estimates from literature for the fraction of input energy which is released at the exhaust and assume that 50% of this energy is recoverable. The input energy is then calculated on site level back calculating this from the amount of emissions emitted from a site using EU ETS data. BCS (2008) take a more quantitative approach by calculating the composition of the exhaust gas based on the input fuels and calculating the total enthalpy of the exhaust gas based on this composition. Bühler et al. (2016) base the heat recovery potential on sectoral energy input and use process specific energy and exergy efficiencies to calculate exergy losses. The site specific energy consumption for each of the 22 processes is distributed by site production data.

For an emission-based estimation of industrial waste heat potential, the methodology of BCS (2008) seems more relevant since it is based on calculations with process parameters rather than rough estimates. Therefore, it can be considered to yield more consistent and comparable results between sub-sectors. However, as a far more precise approach is the consideration of actual production data of each site as used by Bühler et al. (2016). This approach is more data intensive, but enables the further calculation like of sub-annual availability of excess heat together with high resolution spatial analyses for the integration of industrial excess heat into district heating systems (Bühler et al. (2018)).

Table 4: Overview of methodologies used in previous literature for the quantification of waste heat potential

Reference	Scale	Data sources	Summary of methodology used	Type of potential	Suitability
Boddy et al. (1994)	U.K.	Literature values from 1985 and before	Ratios of thermal input energy into a process that can be regained and at which temperature per tons of product produced from a U.S. survey from 1974.	Technical potential	Data used for waste heat potential are outdated.
Bonilla et al. (1997)	Basque (Spain)	Data base of the Basque Government's energy agency	Quantification of waste heat in GJ per ton of product based on energy and material flow diagram of representative industrial processes.	Theoretical potential	Requires in-depth analysis of all the material and energy flows in each process.
Lopez et al. (1998)	Basque (Spain)	Data base of the Basque Government's energy agency	Quantification of waste heat in GJ per ton of product based on energy and material flow diagram of representative industrial processes.	Theoretical potential	Requires in-depth analysis of all the material and energy flows in each process.
Glatzel et al. (2001)	Germany	Expert estimation	Expert estimation at 40% of the industrial process heat.	Technical potential	Quantitative methodology is preferred
Land et al. (2002); Cronholm et al. (2009)	Sweden	Empiric values from district heating association, data from government statistics agency and previous waste heat potential study	Excess heat delivery per used fuel for companies (< 3 GWh equivalent of oil use per year and close to settlements) in industrial sub-sectors, then extrapolated to the whole of Sweden. Estimation based on qualitative assessment of all data available.	Technical potential (focus on DH)	Qualitative methodology for excess heat delivery per used fuel too unclear.
Kattenstein et al. (2002)	North Rhine-Westphalia (Germany)	Unclear	Waste heat to input energy ratio for different industrial sectors at 70 °C and 120 °C developed based on data from the city of Duisburg and then extrapolated to the whole state of North Rhine-Westphalia.	Unclear	Methodology is too unclear.
Energetics (2004)	U.S.	Expert judgement, literature values and pilot projects	Upstream waste heat quantified by applying equipment loss factors to the energy systems (e.g. 3% loss in fuel and electricity distribution lines and pipes). Downstream waste heat quantified by multiplying thermal energy use with the efficiency of a specific process.	Theoretical potential	Generalized loss factors for processes.
Ecoheatcool (2006)	Europe	Land et al. (2002)	Energy factors from Land et al. (2002) were applied to other countries (e/g/ 3.4% of input energy can be retrieved as waste heat for the paper industry).	Technical potential	Energy factors taken from another study
BCS (2008)	U.S.	Literature review and expert interviews	Quantification of fraction of waste heat loss relative to energy input taking the waste heat (as a function of the exhaust gas mass flow rate and its enthalpy which is dependent on the chemical composition and temperature) as a ratio to the energy input.	Theoretical potential	Emission-based approach with excess heat factors suitable for estimation based on industrial sectors
Blesl et al. (2008)	Baden-Württemberg (Germany)	Literature values and empirical data of individual companies	Calculation of annual thermal demand subtract part that is used for space heating. The rest is potential annual waste heat, divide by load hours gives the potential waste heat output.	Theoretical potential	Methodology too simple/rough for adequate estimation of the waste heat potential.
McKenna (2009); McKenna & Norman (2010); Hammond & Norman (2012)	UK	UK National Allocation Plan for the EU ETS, with capacity and SEC data	Use emission data to estimate total site fuel and electricity use, then transform to heat load taking the efficiency of fuels to heat and the load factor into account. Transformed to recoverable potential with a weighted Carnot factor and fraction of exhaust energy compared to the input energy.	Technical potential	Methodology takes places on site-level but could be performed on aggregated national capacity level.

Reference	Scale	Data sources	Summary of methodology used	Type of potential	Suitability
Enova (2009)	Norway	Survey	69% of industrial companies in Norway answered survey with regard to their waste heat potential in different temperature ranges.	Unclear	Survey is not suitable for execution in sEEnergies.
Pehnt et al. (2010)	Germany	Enova SF (2009), Energetics (2004)	Waste heat quantities from Enova SF (Norway) & Energetics (U.S.) were transformed to relative amounts of waste heat per sub-sector and then applied to the energy consumptions in these German sub-sectors.	Unclear	Energy factors taken from another study
Blesl et al. (2011)	Baden-Württemberg (Germany)	Literature values and empirical data of individual companies	Estimation of waste heat potential by determining potential waste heat as a ratio of the energy input based on literature research of the relevant processes and combining this with the capacity of companies in the region.	Technical potential	Methodology remains too unclear from report.
Ammar et al. (2012)	U.K.	Boddy et al. (1994)	Waste heat quantities taken from Boddy et al. (1994)	Technical potential	Data used for waste heat potential are outdated.
Element Energy et al. (2014)	U.K.	Literature review, expert interviews	Estimation made by combining (heat) source and (heat) sink databases. These databases contain data on available rejected heat flows per unit of production for representative processes and sub-processes, characterized on heat carrier medium, temperature ranges, mass flow and a compatibility factor. The site database then scales that data based on assumptions of output at site level.	Technical and economic potential	Methodology requires in-depth analysis on site level.
Persson et al. (2014)	Europe	Pollutant register (E-PRTR)	Application of emission factors and default recovery efficiency to calculated primary energy supplies per sector	Theoretical potential	Unclear how default recovery efficiencies have been established.
Bühler et al. (2016;2017;2018)	Denmark	Energy and exergy efficiencies based on literature review, site specific production data used for distribution of national energy demand	Energy and exergy flow for 22 processes. Statistical data about energy carrier use for these processes are obtained from the Danish Energy Agency. For 2284 sites of the industrial sector production data and excess heat potentials are calculated. Also considers temporal aspects in matching heat sources and sinks..	Technical and economic potential	Numerous data needs to be collected for each country, process structure in each sector is presumed to be the same
Brückner et al. (2017)	Germany	Pollutant register (PRTR)	Bottom up estimation of excess heat per site from CO_2-emission data for Germany (PRTR). Extensive plausibility analysis for this dataset. Same methodology for excess heat estimation as Kattenstein et al. (2012)	Unclear	Methodology is too unclear.
Aydemir et al. (2019)	Baden-Württemberg (Germany)	German pollutant register	Estimation of excess heat potentials is based on CO2 emissions of point sources.	Technical potential	Could be used in sEEnergies, because pollutant data is available
Popovski et al. (2018)	Portugal Matosinhos	Site data	Used specific data from individual site and developed detailed site-specific assessment of local heat source characteristics and potential heat sinks	Economic potential	Not applicable, because too detailed - rather for individual sites

3 Excess heat potentials on process level

3.1 Method

In this analysis, we adopt the bottom-up approach applied by BCS (2008) to calculate the unrecovered waste heat from exhaust gases in the different industries. In the following sections, we describe the methodology used:

The energy lost to exhaust gases (E_x) is a function of the exhaust gas mass flow rate (m_{ex}) and its enthalpy (*h(t)*). The enthalpy is a function of the exhaust gas chemical composition and temperature, as shown in Eq.1:

$$E_{ex} = m_{ex} \cdot h(t) = m_{ex} \cdot \sum(t)(x_i h_i(t))_{ex} \quad (1)$$

Where, x_i is the mass fraction of each component in the exhaust and $h_i(t)$ its enthalpy.

By assuming that all gases (except H_2O) are ideal gases, the enthalpy of each gas component can be calculated based on the specific heat capacity of each component ($C_{p,i}(t)$) (Eq.2):

$$h_i(t) = \int_r^T C_{p,i}(t)dt \quad (2)$$

Where, *r* is the reference temperature and *T* is the temperature of the exhaust. The enthalpies can also be calculated from steam tables. The enthalpy is not an absolute term and needs to be calculated against a reference state (e.g., room temperature). In this analysis, we calculate the enthalpy of exhaust gas streams at the three following reference temperatures:

1. 25°C to estimate the maximum heat attainable if gas is cooled to ambient temperatures;
2. 55°C to estimate the maximum heat attainable if gas is cooled to 55°C;
3. 95°C to estimate the maximum heat attainable if gas is cooled to 95°C.

In current industrial practices, exhaust gases are typically not cooled below 149°C in order to avoid condensation of waste streams (BCS, 2008). In addition, other temperature restrictions, particular to a specific exhaust stream might be in place. For example, in the case of the highly corrosive exhaust gases of glass furnaces, the gases can be cooled to a minimum temperature of 265°C as at lower temperatures they condensate. In this analysis, we note such restrictions for every stream but do not take them into account for the calculation of the unrecovered waste heat. This is because the heat from gas streams with highly chemical activity or very high temperatures could still be recovered but it would require more advanced techniques and different materials, such an assessment is however out of the scope of this analysis.

Finally, the fraction of the waste heat lost in the exhaust (E_x) and the energy input (E_{in}) is equal to (Eq.3):

$$\frac{E_{ex}}{E_{in}} = \frac{\frac{m_{ex}}{m_{fuel}} \sum(x_i h_i(t))_{ex}}{h_c} \quad (3)$$

Where, m_{fuel} is the fuel mass flow rate and h_c is the heating value of the fuel used. In this analysis, we use the lower heating value (LHV).

3.2 Data

© 2020 sEEnergies | Horizon 2020 – LC-SC3-EE-14-2018-2019-2020 | 846463

Exhaust gas composition (mass fraction x_i)

The mass fraction of each component in the exhaust, x_i, depends on the composition of the fuel used and the air to fuel ratio. Basic combustion equations were determined for all fuel components (e.g. methane, ethane, carbon, etc.) assuming full combustion and an air to fuel ratio of 10%[2]. For example, in the case of carbon:

$C+1.1(O_2+3.76\ N_2) \rightarrow CO_2+0.1O_2+4.13N_2$

The fuels used in this analysis and their assumed compositions are shown in Table 5.

Table 5: Assumed fuel compositions (% volume) (BCS, 2008; IEA, 2000)

		Natural gas	Coal	Coke oven gas	Blast furnace gas	Coke	Refinery fuel gas
Methane	CH_4	93%	0%	37%	0%	0%	44%
Ethane	C_2H_6	4%	0%	5%	0%	0%	9%
Propane	C_3H_8	1%	0%	0%	0%	0%	10%
Butane	C_4H_{10}	0%	0%	0%	0%	0%	16%
Nitrogen	N_2	1%	1%	0%	50%	0%	0%
Water	H_2O	0%	8%	0%	0%	0%	0%
Carbon dioxide	CO_2	1%	0%	2%	21%	0%	1%
Carbon	C	0%	72%	0%	0%	88%	0%
Hydrogen	H_2	0%	4%	52%	3%	4%	17%
Sulfur	S	0%	2%	0%	0%	3%	0%
Carbon monoxide	CO	0%	0%	4%	26%	0%	0%
Rest:		-	12%	-	-	5%	2%

Mass flow rate (mex/mfuel)

The m_{ex} is equal to the sum of m_{fuel} and m_{air}. Thereby, the m_{ex}/m_{fuel} ratio can be calculated based on the fuel chemical composition and the assumed added combustion air. The air required for full combustion (with a 10% air to fuel ratio) is found from the basic combustion equations.

Enthalpy (hi)

The enthalpy of each of the exhaust gas components is a function of their specific heat capacities (see Eq. 2). Specific heats are a function of temperature (Eq.4):

$$C_p = a + bT + cT^2 + dT^3 \quad (4)$$

The temperature used must be in Kelvin and the unit is kJ/kmol.

For ideal gases, the constants *a*, *b*, *c* and *d* per exhaust gas component are given in Table 6:

Table 6: Constants a, b, c, and d for selected ideal gases

Substance	Formula	a	b	c	d
Nitrogen	N_2	28.9	-0.00157	0.00000808	-2.9E-09
Oxygen	O_2	25.48	0.0152	-0.00000716	1.3E-09
Carbon dioxide	CO_2	22.26	0.0598	-0.000035	7.5E-09
Water vapor	H_2O	32.24	0.00192	0.0000106	-3.6E-09
Sulfur dioxide	SO_2	25.78	0.058	-0.0000381	8.6E-09
Hydrogen	H_2	29.11	-0.001916	0.000004003	-8.7E-10
Carbon monoxide	CO	28.16	0.001675	0.000005372	-2.2E-09
Methane	CH_4	19.89	0.05024	0.00001269	-1.1E-08
Ethane	C_2H_6	6.9	0.1727	-0.00006406	7.3E-09

[2] For a higher air to fuel ratio, the exhaust mass flow rate to the fuel mass flow rate (m_{ex}/m_{fuel}) increases, increasing thereby the estimated waste heat losses.

Water vapor does not follow ideal gas behavior at low pressures. Thereby, the enthalpy change was taken from steam tables for the corresponding partial pressure. At atmospheric pressure the partial pressure of water vapor is equal to the molar fraction of water in the exhaust gas mixture.

3.3 The glass industry

There are several furnace types used for glass melting. In 2005 in the EU, regenerative furnaces were the furnaces most used, accounting for approximately 85% of glass melting capacity. Then, followed the recuperative type of furnaces (8%), the oxy-fuel (4%) and the electric furnaces (2%) (European IPPC Bureau, 2013b). The fuel predominantly used in European countries is natural gas responsible for 65% of fuel use, with the rest being fuel oil (European IPPC Bureau, 2013b). In this analysis, we assumed that all furnaces were fired with natural gas.

Without waste heat recovery the exhaust gases from glass melting furnaces would exceed the 2,400°C. In regenerative furnaces, heat is recovered to heat the combustion air dropping the exhaust gas temperature at about 320-540°C. Recuperative furnaces are in general less energy efficient with exhaust temperatures at approximately 980°C. Direct, oxy-fuel and electric boost melters have exhausts with temperatures of 1,300°C, 1,430°C and 430°C, respectively (BCS, 2008).

In addition to combustion air preheating, waste heat from the flue gases could be recovered for batch/cullet preheating or for steam/electricity generation. When a batch preheater is used, the temperature of the flue gases drops to approximately 200°C. Thereby, if all melters used batch preheating the waste heat availability would decrease considerably.

To avoid material agglomeration, the temperature of the flue gasses that enter the batch heat exchanger cannot be higher than 550-600°C (European IPPC Bureau, 2013b). Thus, for the direct, recuperative and oxyfuel melters, the flue gases need to be cooled down prior to entering the batch preheater. If not possible to utilize on site, waste heat could be potentially available for district heating from the cooling of the flue gases to about 550°C. This potential could however disappear with the use of advanced batch preheaters. In these preheaters, the flue gases would be able to enter the batch preheater at high temperatures (1,200-1,400°C) with minimal or no required cooling (European IPPC Bureau, 2013b). Cullet preheating is currently limited in the container glass industry (European IPPC Bureau, 2013b). It is estimated that about 40% of container glass furnaces use this technology[3].

Table 7 shows the estimated waste heat losses for the different furnaces used in the glass industry, with and without batch preheating systems, and for different reference temperatures, based on the method described in Section 3.1.

Main barrier in heat recovery from glass furnace off-gas is that the off gases contain sulfates making heat recovery at temperatures below 270°C challenging as the sulfates deposit on the heat exchanger surfaces (BCS, 2008).

[3] In the Heat roadmap Europe project, the diffusion rate for this technology was estimated at 60% for 2030 (HRE4, 2017).

Table 7: Estimated exhaust gas waste heat losses from glass melting furnaces

	Exhaust gas temperature (°C)[4]	Fuel SEC[2] (GJ/tonne)	% of fuel input lost as waste heat			Assumed current diffusion rate (%)	Assumed full internal use diffusion rate (%)
			25°C level 1	55°C level 2	95°C level 3		
Container glass							
Recuperative	980	6.2	60%	47%	45%	60%	0%
Recuperative, with batch/cullet preheat	200	4.6	19%	7%	5%	40%[3]	100%
Regenerative	430	5.2	30%	18%	16%	60%	0%
Regenerative, with batch/cullet preheat	200	3.8	19%	7%	5%	40%[3]	100%
Oxy-fuel[1]	1400	5.2	35%	30%	29%	60%	0%
Oxy-fuel [1], with batch/cullet preheat	200	3.8	8%	3%	2%	40%[3]	100%
Flat glass							
Recuperative	980	9.2	60%	47%	45%	100%	0%
Recuperative, with batch/cullet preheat	200	7.8	19%	7%	5%	0%[3]	100%
Regenerative	430	7.5	30%	18%	16%	100%	0%
Regenerative, with batch/cullet preheat	200	6.4	19%	7%	5%	0%[3]	100%
Oxy-fuel [1]	1400	5.6	35%	30%	29%	100%	0%
Oxy-fuel [1], with batch/cullet preheat	200	4.8	8%	3%	2%	0%[3]	100%

[1] Although the exhaust gas temperature is higher than in the exhaust gases from other glass melting furnaces, the mass flow rate is lower resulting in less waste heat (BCS, 2008). We estimate the mass rate at approximately 40% of the mass flow rate in the other furnaces.
[2] To estimate the SECs per technology with and without batch/cullet preheating, we used the fuel use reported in HRE4 (2017) as an average, and we assumed that for 40% of the production it is 15% lower and for 60% of the production 15% higher. The typical energy savings from batch/cullet preheating are around 10-20% (European IPPC Bureau, 2013b).
[3] In 2010, the batch/cullet preheating was not widely used in the EU primarily due to the high investment costs and potential space limitations (European IPPC Bureau, 2013b). In addition, its application was limited to the container glass industry (European IPPC Bureau, 2013b). We hereby assume that 40% of the container glass industry has this technology installed while in the flat glass industry the diffusion rate is 0%.
[4] We have rounded the values when switching from °F to °C.

If we would also consider the waste heat from cooling the flue gases to 550°C prior to entering the batch preheater, the waste heat availability would increase by an additional 24%, 43% and 21% in recuperative furnaces, direct melters, and oxy-fuel burners, respectively.

3.4 The cement industry

The most energy intensive step in cement making is the clinker calcination in cement kilns, accounting for approximately 90% of the total energy use and practically all fuel use (Worrell et al., 2013). The type of kiln used is dictated by the moisture content off the raw material (limestone). Dry kilns are generally more energy efficient than wet kilns as the water evaporation requirements are reduced. The fuel primarily used is coal although alternative fuels have gained important shares in total fuel use. In this analysis, for simplicity reasons we assumed that all kilns are fired with coal.

Heat from the kiln exhaust gases is commonly used in cyclones to preheat the meal fed to the kiln achieving significant energy savings. The more preheater stages used the lower the exhaust gas temperature. Dry kilns with no heat recovery have an exhaust temperature of approximately 450°C. When four preheater stages are used the temperature drops to 300-400°C (European IPPC Bureau, 2013c) and when the stages are increased to five or six the temperature drops to 200-300°C (BCS, 2008).

The kiln-off gases that exit the top preheater stage are normally used for raw material drying (European IPPC Bureau, 2013c). If raw material drying is not needed, the medium-low temperature heat contained in the kiln-off could be used for electricity generation (alternative cycles such as Kalina and Organic Rankine Cycle) or for supplying hot water (European IPPC Bureau, 2013c). Low temperature heat from the clinker cooler can also be used for heat recovery, however in this analysis we mainly focused on the heat recovery from flue gases.

Table 8 shows the estimated waste heat losses for the different cement kilns, with and without preheater and precalciner systems, and for different reference temperatures, based on the method described in Section 3.1.

Main difficulty in recovering heat from kiln off-gas is that the off-gases from burning coal (high sulfur content) can condensate in the heat exchanger at temperatures below 177°C (BCS, 2008).

Table 8: Estimated exhaust gas waste heat losses from cement kilns

	Exhaust gas temperature (°C)[3]	Fuel SEC[1] (GJ/tonne)	% of fuel input lost as waste heat[2]			Assumed current diffusion rate (%)	Assumed full internal use diffusion rate (%)
			25°C level 1	55°C level 2	95°C level 3		
Wet	340	5.5	20%	15%	13%	n/a	100%
Dry	450	4.5	27%	22%	20%	n/a	0%
Dry+preheater	340	3.7	21%	17%	14%	n/a	0%
Dry+4 stage preheater+precalciner	340	3.3	22%	17%	15%	n/a	0%
Dry+5-6 stage preheater+precalciner	250	3.0	17%	12%	10%	n/a	100%

[1] Source: HRE4 (2017) except for "Dry+5-6 stage preheater+precalciner" where the SEC of the most energy efficient kiln is used (CSI/ECRA, 2017).
[2] Except from the combustion off-gases from burning coal, process CO_2 emissions from clinker calcination are also released that contribute in the calculation of the exhaust gas enthalpy. For every tonne of clinker approximately 0.55 tonnes of process CO_2 are released. It can be noted that the calculated waste heat lost is higher in "dry+4 stage preheater+precalciner" kilns than in the "dry+preheater" kilns although the exhaust gas temperatures are the same. This is because, the specific energy consumptions are different between kilns, which leads to variations in the exhaust gas composition (i.e. different shares of process related and combustion related products).
[3] We have rounded the values when switching from °F to °C.
n/a: not applicable as the production volumes are known for each kiln technology.

3.5 The iron and steel industry

Table 11 shows the estimated waste heat available from exhaust gases or other significant gas streams that are generated from the manufacture of iron and steel. The processes included and that are briefly described in the following paragraphs are: i) coke ovens, ii) blast furnaces, iii) basic oxygen furnaces (BOFs), and iv) electric arc furnaces (EAFs).

3.5.1 Coke ovens

Coke ovens have two sources of sensible waste heat loss: i) the heat contained in the cooled coke oven gas (COG) and ii) the heat contained in the off-gases generated from burning COG (BCS, 2008).

The sensible heat losses from COG are significant. The COG exits the coke oven at a high temperature, ranging between 650 and 1,000°C however, because it is highly contaminated with tars and other materials that can build up on the surface of heat exchangers, the sensible heat is commonly lost (BCS, 2008). In the European industries it is common to clean the COG and then use it as a fuel internally or externally but without any recovery of the sensible heat (European IPPC Bureau, 2013a).

There are however techniques available for waste heat recovery but due to the high capital costs they are not widely implemented. The minimum allowable temperature in the heat exchanger is 450°C, as at lower temperatures tar condenses and leads to soot formations on the heat exchanger surfaces. So here we assume that at 450°C is also the COG temperature when a heat exchanger is used.

To recover the sensible heat from the off-gases, a regenerator is commonly used. The recovered heat is used to preheat the incoming combustion air. The flue gases leave the regenerator at about 200°C, a temperature sufficiently high for further heat recovery.

Table 11 shows the estimated waste heat losses from coke ovens. The waste heat in off-gases was calculated based on the method described in Section 3.1 and by assuming that all fuel used is COG. The sensible heat in COG cannot be calculated based on the above method as the COG composition cannot be calculated based on the complete combustion of the fuel source. The COG enthalpy was thereby estimated based on the typical composition of COG (see Table 5) and the average temperature (about 800°C without heat recovery and 450°C with heat recovery).

3.5.2 Blast furnaces

Sensible heat in blast furnaces can be recovered from two gas streams: i) the generated blast furnace gas (BFG) and ii) the blast stove exhaust. Although older blast furnaces had high exhaust temperatures of about 400°C, newer furnaces have improved heat transfer and the generated gases are at lower temperatures. The BFG gas has a temperature of about 200°C and the exhausts from the blast stove are at about 250°C. When additional heat recovery is used, the exhaust temperature drops to approximately 130°C (BCS, 2008).

Using the waste gases of the hot blast stove to preheat the host blast stove fuel or the combustion air is considered best available technology (European IPPC Bureau, 2013a). Since the off-gases are relatively clean, heat recovery from the off-gases is considered a more common practice (BCS, 2008).

Table 11 shows the estimated waste heat losses from blast furnaces. The sensible heat in blast stove off-gases was calculated based on the method described in Section 3.1 and by assuming that all fuel used is BFG enriched with COG. The sensible heat in BFG cannot be calculated based on the above method as the BFG composition cannot be calculated based on the complete combustion of the fuels. The BFG enthalpy was thereby estimated based on the typical composition of BFG (see Table 5) and an average temperature of about 220°C.

3.5.3 Basic oxygen furnaces

The gases leaving the basic oxygen furnace are very hot, with temperatures typically ranging between 1,600 and 1,800°C and have a high heating value of approximately 0.84 GJ/tonne steel (IEA, 2007). Thereby, BOF gases offer great opportunities for the recovery of both the sensible heat and the chemical energy. However, the sensible heat of BOF gases is often not recovered. This is because BOF gases are considered dirty gases with contaminants such as iron oxides, fluorides, SOx and NOx present, they have high temperatures and their generation is not continuous. This makes heat recovery challenging with many facilities simply flaring BOF off-gases (BCS, 2008).

The two main heat recovery processes, with wide implementation, are classified as the combustion and the non-combustion processes. In the combustion process, air is added to combust the CO and H_2 and the waste heat energy is recovered in a waste heat boiler for steam production. In the non-combustion process, the CO and H_2 combustion is inhibited and the gas is stored for later use as a fuel after first it is being cleaned. Before cleaning, a waste heat boiler is used to recover the sensible heat and generate high pressure steam. The non-combustion process is considered more efficient as both waste heat and fuel are recovered (European IPPC Bureau, 2013). The BOF gas temperature in this case is reduced to about 250°C (Ray et al., 2005).

In the EU, the suppressed combustion process (non-combustion process) is the most used however, there are still some plants that simply flare BOF gases (European IPPC Bureau, 2013a). In addition, there are plants that use partial suppressed combustion or other gradations of the above technologies. In this analysis we assume a diffusion rate of 70% for the suppressed combustion process.

Table 11 shows the estimated waste heat losses from basic oxygen furnace off-gases. The sensible heat cannot be calculated based on the above method as the off-gas composition cannot be calculated based on the complete combustion of the fuels. The off-gas enthalpy was thereby estimated based on the typical composition of the BOF off-gases (see Table 9) and an average temperature of 1,700°C when heat recovery is not used and 250°C when heat recovery is used.

Table 9: Typical composition of basic oxygen furnace off-gas (BCS, 2008)

Substance		% volume
Nitrogen	N_2	13%
Oxygen	O_2	0%
Carbon Dioxide	CO_2	14%
Water vapor	H_2O	0%
Sulfur Dioxide	SO_2	0%
Hydrogen	H_2	6%
Carbon Monoxide	CO	68%
Methane	CH_4	0%
Ethane	C_2H_6	0%

3.5.4 Electric arc furnaces

Electric arc furnaces are traditionally fed with ferrous scrap (e.g., postconsumer, process cut offs) but also with iron sources such as hot metal and direct reduced iron (DRI). EAFs, similarly to the blast furnaces in the primary production steel route, remove the carbon, silicon and other impurities.

The off--gases from EAFs are at high temperatures ranging from 1,370-1,925°C (BCS, 2008). The most common method used for waste heat recovery is scrap preheating saving approximately 5-25% of the total EAF consumption (BCS, 2008; European IPPC Bureau, 2013a). With scrap preheating the temperature of the off-gases is reduced to approximately 200°C (BCS, 2008).

Because the off-gases from EAFs vary strongly in composition, temperature and flow-rate, to estimate the available sensible heat in off-gases in Table 11 we do not use the method described in Section 3.1. Instead, we base our estimates on industry observations that about 20% of the furnace energy input is lost as waste heat, of which, 50% is lost in the form of sensible heat and 50% in the form of chemical energy (BSC, 2008). This would mean that for an energy use of 1 GJ/tonne steel, 0.12 GJ/tonne are lost as sensible heat from the exhaust. The ratio of sensible heat losses for different exhaust and reference temperatures was estimated based on the assumed off-gas composition shown in Table 10.

Table 10: Typical composition of electric arc furnace off-gases (BCS, 2008)

Substance		% volume
Nitrogen	N_2	57%
Oxygen	O_2	0%
Carbon Dioxide	CO_2	14%
Water vapor	H_2O	0%
Sulfur Dioxide	SO_2	0%
Hydrogen	H_2	11%
Carbon Monoxide	CO	18%
Methane	CH_4	0%
Ethane	C_2H_6	0%

Table 11: Estimated exhaust gas waste heat losses from the iron steel industry

	Exhaust gas temperature (°C)[10]	Fuel SEC[1] (GJ/tonne)	% of fuel input lost as waste heat			Assumed current diffusion rate (%)	Assumed full internal use diffusion rate (%)
			25°C level 1	55°C level 2	95°C level 3		
Coke ovens							
Sensible heat in COG	820	-	0.98[2]	0.95[2]	0.91[2]	100%[5]	0%
Sensible heat in COG, after heat recovery	450	-	0.47[2]	0.44[2]	0.40[2]	0%	100%
Waste heat in off-gases	200	1.6	44%	13%	9%	100%	100%
Blast furnaces							
Sensible heat in BFG	220	-	0.42[3]	0.36[3]	0.27[3]	100%	100%
Blast stove exhaust, no heat recovery	250	1.5[4]	13%	10%	8%	50%	0%
Blast stove exhaust, with heat recovery	130	1.4[4]	6%	4%	2%	50%[6]	100%
Basic oxygen furnace							
Sensible heat in BOF off-gases, no heat recovery	1700	-	0.56[3]	0.55[3]	0.54[3]	30%	0%
Sensible heat in BOF off-gases, with heat recovery	250	-	0.02[3]	0.02[3]	0.01[3]	70%[7]	100%
Electric arc furnace							
Electric arc furnace no recovery	1200	1.8[8]	12%	12%	12%	70%	0%
Electric arc furnace with recovery	200	1.5[8]	2%	1%	1%	30%[9]	100%

[1] When not mentioned otherwise, the fuel SEC values were taken from HRE4 (2017).
[2] The unit is in GJ/tonne coke.
[3] The unit is in GJ/tonne steel.
[4] The fuel use in blast stoves accounts for 10-12% of overall fuel use in blast furnaces (Energetics, 2004). In HRE4 (2017) the fuel use in blast furnaces was estimated at about 12 GJ/tonne steel.
[5] The sensible heat from COG is commonly wasted due to how dirty it is (European IPPC Bureau, 2013a), we hereby assume that 100% of the production capacity does not recover it.
[6] The blast stove exhaust is relatively clean and can be used in recovery technologies without great difficulties (BCS, 2008). We hereby assume that 50% of the production capacity already recovers it.
[7] We assume a diffusion rate of 70% as according to the European IPPC Bureau (2013a) many plants use waste heat recovery while only few flare the off-gases.
[8] For an energy use of 1.8 GJ/tonne in EAFs the energy use when scrap preheating is used is about 5-25% lower (BCS, 2008; European IPPC Bureau, 2013a). We use an average of 15%.
[9] In HRE4 (2017), the maximum diffusion rate of this technology for 2050 was assumed to be 55%. We here assume a current diffusion rate of 30%.
[10] We have rounded the values when switching from °F to °C.

3.6 The primary aluminium industry

Primary aluminium production is a multistage process. Initially, the extracted bauxite ore is digested and refined into alumina in the Bayer process, and then alumina is transformed with the Hall-Héroult process into aluminium in an electrolytic cell. The molten aluminium is cast into ingots which are transferred and further processed in aluminium foundries. Aluminium can also be produced from scrap in the secondary production route.

Aluminium smelting is very electricity intensive consuming approximately 14.9 MWh/tonne aluminium (HRE4, 2017). Off gases, approximately 1.5 tonnes CO_2/tonne aluminium, are emitted due to anode reactions and air burning (BCS, 2008). The off-gases are however responsible for only a small part of total heat losses with the most significant coming from the electrolytic cell surface. As in this analysis the focus is on the exhaust gases, Table 12 shows only the waste heat available from the CO_2 off-gases.

The sensible heat cannot be calculated with the method described in Section 3.1 as it relies on the complete combustion of the fuels and in the electrolytic cell electricity is consumed. The off-gas enthalpy was thereby estimated from the typical composition of the off-gases (100% CO_2) and an average off-gas temperature of 700°C (BCS, 2008).

Table 12: Estimated exhaust gas waste heat losses from the aluminium smelting industry

	Exhaust gas temperature (°C)	Electricity SEC (GJ/tonne)	% of fuel input lost as waste heat[1]			Assumed current diffusion rate (%)	Assumed full internal use diffusion rate (%)
			25°C level 1	55°C level 2	95°C level 3		
Primary aluminium	700	54	1.1	1.0	1.0	100%[2]	100%

[1] The unit is in GJ/tonne aluminium.
[2] No significant efforts for heat recovery from the smelter off-gases (BCS, 2008).

3.7 Pulp and paper industry

The main processes in paper and paperboard manufacture are pulp making, bleaching, chemical recovery, pulp drying and paper making. To produce pulp there are several processes used with main being the chemical (or else known as Kraft pulping), the semi-chemical, and the waste paper pulp process. Pulp production comprises the most energy intensive process step in the whole paper and paperboard production chain (Xu et al., 2012).

Electricity is used throughout the plant but it is not as significant as the fuel use. The largest fuel consumers are the boilers that are used for steam and electricity generation. Steam is used in large quantities for pulping, evaporation, paper making and other operations. The fuel most used is black liquor followed by hog fuel and natural gas. Natural gas and oil are mainly used for direct process heating in lime kilns (Kramer et al., 2009). In this analysis we assume that 100% of fuel use in pulp and paper making is in boilers and that the fuel used is black liquor. Only exception we make is the fuel used in lime kilns for the recovery of chemicals in the chemical pulping process where we assume that 100% of the fuel used is natural gas.

Lime kilns are usually equipped with low temperature chain heat exchangers for heating the solids with the exhaust gases. The temperature of the kiln exhaust gases is in this way significantly lowered from about 650°C to less than 200°C (Hough, 1985 as cited in Lundqvist, 2009).

Exhaust temperatures from industrial boilers depend on the steam pressures needed for the various processes. In this analysis, we make the same assumption with BCS (2008), that the average exhaust temperatures are 260°C with no heat recovery and when an economizer is used, the temperature drops to 150°C when conventional fuels and 180-200°C when byproduct fuels are used. Economizers are quite common in large industrial boilers.

Table 14 shows the estimated waste heat losses from pulp and paper manufacturing processes. Except for the lime kilns that are used in chemical pulping, the sensible heat in all other processes cannot be calculated based on the method in Section 3.1 as black liquor compositions vary strongly from site to site depending on the type of wood, alkali charge and pulp yield (Fakhrai, 2002). The off-gas enthalpy was thereby estimated based on the information available on the composition of off-gasses from burning black liquor (see Table 13).

Table 13: Typical composition of off-gases from burning black liquor (Vakkilainen, 2002)

Substance		% volume
Nitrogen	N_2	58%
Oxygen	O_2	3%
Carbon Dioxide	CO_2	16%
Water vapor	H_2O	23%
Sulfur Dioxide	SO_2	0%
Hydrogen	H_2	0%
Carbon Monoxide	CO	0%
Methane	CH_4	0%
Ethane	C_2H_6	0%

Table 14: Estimated exhaust gas waste heat losses from the pulp and paper industry

	Exhaust gas temperature (°C)	Fuel SEC (GJ/tonne)	% of fuel input lost as waste heat			Assumed current diffusion rate (%)	Assumed full internal use diffusion rate (%)
			25°C level 1	55°C level 2	95°C level 3		
Pulp making							
Chemical pulping, no boiler heat recovery	260	12.3[1]	9%	3%	3%	30%	0%
Chemical pulping, with boiler heat recovery	177	10.3[1]	8%	2%	1%	70%[5]	100%
Lime burning, no heat recovery[2]	650	2.2[3]	52%	36%	34%	30%	0%
Lime burning, with heat recovery[2]	200	1.4[3]	24%	8%	6%	70%	100%
Mechanical pulping, no boiler heat recovery	260	2.2[4]	9%	3%	3%	30%	0%
Mechanical pulping, with boiler heat recovery	177	1.9[4]	8%	2%	1%	70%[5]	100%
Recovered fibres, no boiler heat recovery	260	0.6[4]	9%	3%	3%	30%	0%
Recovered fibres, with boiler heat recovery	177	0.5[4]	8%	2%	1%	70%[5]	100%
Paper making							
Board & packaging paper, no boiler heat recovery	260	5.7[4]	9%	3%	3%	30%	0%
Board & packaging paper, with boiler heat recovery	177	4.9[4]	8%	2%	1%	70%[5]	100%
Graphic paper, no boiler heat recovery	260	8.4[4]	9%	3%	3%	30%	0%
Graphic paper, with boiler heat recovery	177	7.2[4]	8%	2%	1%	70%[5]	100%
Tissue paper, no boiler heat recovery	260	8.1[4]	9%	3%	3%	30%	0%
Tissue paper, with boiler heat recovery	177	6.9[4]	8%	2%	1%	70%[5]	100%

[1] Estimated from the fuel use reported in HRE4 (2017), after excluding the energy use in lime kilns, 1.8 GJ/tonne, and accounting for the share of production that uses boiler economizers and the share that does not. When economizers are used, 5-10% of the fuel use can be saved (Kermeli et al., 2017).

[2] Except from the combustion off-gases from natural gas in lime kilns, process CO_2 emissions are also released that contribute in the calculation of the exhaust gas enthalpy. For every tonne of lime approximately 0.75 tonnes of process CO_2 are released (U.S. EPA, 2009). The specific energy consumption is also needed in this case to calculate the exhaust gas composition as the share of the process related to the combustion related products needs to be defined. Typical energy intensities of lime kilns range between 6 and 9 MJ/ton CaO (Norbom, 1985 as cited in Lundqvist, 2009). For every tonne of air-dried pulp about 240 kg of lime are required (Ecofys et al., 2009), we thereby estimate an energy consumption in lime kilns of approximately 1.8 GJ/tonne pulp.

[3] The typical energy use is 6-9 GJ/ton CaO (Norbom, 1985 as cited in Lundqvist, 2009). Here we assume that the lower end is with waste heat recovery and the higher end without waste heat recovery. For every tonne of air-dried pulp about 240 kg of lime are required (Ecofys et al., 2009).

[4] Estimated from the fuel use reported in HRE4 (2017), while also accounting for the share of production that uses boiler economizers and the share that it does not. When economizers are used, 5-10% of the fuel use can be saved (Kermeli et al., 2017).

[5] Economizers recover the waste heat in the flue gases to heat the boiler feed. Because economizers are considered a common waste heat recovery measure in large boilers used in the pulp and paper industries (Kermeli et al., 2017), we assume a slightly higher current diffusion rate than the one estimated for steam boilers in the EU for 2013 (64%) (Dengler et al., 2016).

3.8 The chemical industry and the refineries

For this analysis, to calculate the availability of waste heat from the flue gases we need to know: i) the exhaust gas temperature of the main processes where fuel is used, ii) either the type of fuel used (typical composition) or the composition of the exhaust gases and, iii) how much energy is consumed per process. The chemical industry is quite complex with many different products generated and many small furnaces in operation for which information is scarce. Since industrial systems are very diverse, but often have major steam systems in common, we target boiler flue gases for the industries for which information on fuel use for steam generation is known.

We have hereby limited this analysis to industries that relevant information was available or partially available. In the following paragraphs we show the estimates of the waste heat potentials from flue gases in ethylene production and the waste heat potentials from only the boiler flue gases in the ammonia and chlorine industries and in refineries. The estimates on waste heat availability can be seen in Table 15.

3.8.1 Ethylene production

Ethylene is a key petrochemical used for the manufacture of many chemicals. Ethylene furnaces are used to crack hydrocarbon feedstocks at very high temperatures (760-870°C) (BCS, 2009). The hot flue gases are typically recovered to produce steam needed to drive the large compressors for gas handling and distillations. After the heat recovery systems, the flue gas temperature is decreased to about 150°C (Hendricks and Choate, 2006).

In naphtha cracking most of the fuel consumed, about 2/3, is used in the ethylene furnace, while the remaining 1/3 is used in the separation and compression processes (Boulamanti and Moya, 2017). Usually this is in the form of steam, we hereby assume that the remaining 1/3 of fuel is consumed in boilers.

Table 15 shows the estimated waste heat losses from ethylene furnaces and boilers calculated based on the method described in Section 3.1. It is assumed that all fuel used is natural gas. The waste heat potentials in boilers were calculated based on an exhaust temperature of 260°C when there is no heat recovery and of 150°C when there is waste heat recovery.

3.8.2 Ammonia and chlorine production, and refineries

The chemical industry and refineries are industries where a large part of the fuel used is for generating steam. In ammonia production, about 40% of the fuel used for energy purposes goes to boilers for steam generation (U.S. DOE, 2002). In chlorine production, both for the membrane separation and the diaphragm processes the biggest part of fuel use is also for steam generation (Jörissen et al., 2011). Here we assume that 100% of fuel consumption in chlorine production goes to boilers. In addition, about 52% of the flue used in refineries is consumed in boilers (U.S. DOE, 2002).

Table 15 shows the estimated waste heat losses from the boiler exhaust in ammonia and chlorine production and in refineries calculated based on the method described in Section 3.1. In the case of ammonia and chlorine we assume that all fuel used is natural gas while in the case of refineries refinery fuel gas. The waste heat potentials in boilers were calculated based on an exhaust temperature of

260°C when there is no heat recovery and of 150°C (natural gas fuel) and 177°C (refinery fuel gas) when there is waste heat recovery.

Table 15: Estimated unrecovered waste heat from exhaust gases in the ethylene industry and from boiler exhaust gases in the ammonia and chlorine industries and from refineries

	Exhaust gas temperature (°C)	Fuel SEC (GJ/tonne)	% of fuel input lost as waste heat			Assumed current diffusion rate (%)	Assumed full internal use diffusion rate (%)
			25°C level 1	55°C level 2	95°C level 3		
Ethylene							
furnace	150	23.9	17%	4%	3%	100%	100%
boiler, no recovery	260	13.3[1]	22%	10%	8%	30%	0%
boiler, with recovery	150	11.4[1]	17%	4%	3%	70%[2]	100%
Ammonia							
boiler, no recovery	260	5.1[1]	22%	10%	8%	30%	0%
boiler, with recovery	150	4.4[1]	17%	4%	3%	70%[2]	100%
Chlorine_diaphragm							
boiler, no recovery	260	3.6[1]	22%	10%	8%	30%	0%
boiler, with recovery	150	3.1[1]	17%	4%	3%	70%[2]	100%
Chlorine_membrane							
boiler, no recovery	260	1.2[1]	22%	10%	8%	30%	0%
boiler, with recovery	150	1.0[1]	17%	4%	3%	70%[2]	100%
Refineries[3]							
Refinery basic, no boiler heat recovery	260	1.60[1]	29%	11%	9%	30%	0%
Refinery basic, with boiler heat recovery[4]	177	1.4[1]	24%	6%	4%	70%[2]	100%
Refinery gasoline focused, no boiler heat recovery	260	2.0[1]	29%	11%	9%	30%	0%
Refinery gasoline focused, with boiler heat recovery[4]	177	1.7[1]	24%	6%	4%	70%[2]	100%
Refinery diesel focused, no boiler heat recovery	260	2.3[1]	29%	11%	9%	30%	0%
Refinery diesel focused, with boiler heat recovery[4]	177	2.0[1]	24%	6%	4%	70%[2]	100%
Refinery flexible, no boiler heat recovery	260	2.1[1]	29%	11%	9%	30%	0%
Refinery flexible with boiler heat recovery[4]	177	1.8[1]	24%	6%	4%	70%[2]	100%

[1] Estimated from the fuel use reported in HRE4 (2017), while also accounting for the share of production that uses boiler economizers and the share that does not. When economizers are used, 5-10% of the fuel use can be saved (Kermeli et al., 2017).
[2] Economizers recover the waste heat in the flue gases to heat the boiler feed. Because economizers are considered a common waste heat recovery measure in large boilers used in the chemical industries and in refineries (European IPPC Bureau, 2015), we assume a slightly higher current diffusion rate than the one estimated for steam boilers in the EU for 2013 (64%) (Dengler et al., 2016).
[3] In refineries, the fuel used is refinery fuel gas that has a different composition than natural gas. This leads to different waste heat potentials from the boiler flue gases compared to the ethylene, ammonia and chlorine industries where natural gas is assumed to be the fuel in use.
[4] In boilers fired with byproduct fuels, such as refinery fuel gas, the minimum final exhaust temperature after waste heat recovery is more likely to be higher compared to when conventional fuels are used (BCS, 2008).

3.9 Results

Table 16 shows the waste heat availability summations per industrial sector when the diffusion rates and specific energy consumptions per technology shown in Tables 7, 8, 11, 12, 14 and 15 are considered.

For example, in the recuperative furnaces used in the container glass industry, the waste heat available is estimated at 2.6, 1.9 and 1.8 GJ/tonne in the “Current situation” scenario for the three different reference temperatures, 25°C, 55°C and 95°C respectively. When the exhaust gases are cooled from 982°C to 25°C (see Table 7), 60% of the fuel used, that is 3.7 GJ/tonne, is wasted. When batch/cullet preheating is used, the waste heat availability is significantly reduced as the temperature of the exhaust gases is significantly lower. The waste heat available from cooling the gases from 200°C to

25°C (see Table 7) is estimated at 19% of the fuel use, that is 0.9 GJ/tonne. Considering that 60% of the container glass production does not use batch/cullet preheating and the rest does, we estimate that the waste heat available for recuperative furnaces in the container glass industry is 2.6 GJ/tonne. In the "full internal use of excess heat" scenario where all furnaces are assumed to have cullet/batch preheating the waste heat availability drops to 0.9 GJ/tonne. Similarly, all the summations have been made for the different industrial sub-sectors and the results are shown in Table 16.

Table 16: Estimated unrecovered waste heat in GJ/tonne from exhaust gases in the different industries under the "current situation" and the "full internal use of excess heat" scenarios

	Current situation			Full internal use of excess heat		
	25°C	55°C	95°C	25°C	55°C	95°C
	level 1	level 2	level 3	level 1	level 2	level 3
Glass Industry						
Container glass						
Recuperative	2.6	1.9	1.8	0.9	0.3	0.2
Regenerative	1.2	0.7	0.6	0.7	0.3	0.2
Oxy-fuel	1.2	1.0	0.9	0.3	0.1	0.1
Flat glass						
Recuperative	5.5	4.4	4.2	1.5	0.5	0.4
Regenerative	2.3	1.3	1.2	1.2	0.4	0.3
Oxy-fuel	2.0	1.7	1.6	0.4	0.1	0.1
Cement Industry						
Wet	1.1	0.8	0.7	1.09	0.8	0.7
Dry	1.2	1.0	0.9	0.51	0.4	0.3
Dry+ph+pc (4 stage PH)	0.7	0.6	0.5	0.51	0.4	0.3
Dry+ph+pc (5-6 stage PH)	0.5	0.4	0.3	0.51	0.4	0.3
Iron and Steel Industry						
Coke ovens	1.7	1.2	1.1	1.2	0.6	0.6
Blast furnaces	0.6	0.5	0.3	0.5	0.4	0.30
Basic oxygen furnace	0.2	0.2	0.2	0.0	0.0	0.0
Electric arc furnace	0.2	0.2	0.1	0.0	0.0	0.0
Aluminium Industry						
Primary aluminium	1.1	1.0	1.0	1.1	1.0	1.0
Pulp and Paper Industry						
Pulp making						
chemical pulping	1.5	0.6	0.5	1.1	0.3	0.2
mechanical pulping	0.2	0.0	0.0	0.1	0.0	0.0
recovered fibres	0.0	0.0	0.0	0.0	0.0	0.0
Paper making						
Board & packaging paper	0.4	0.1	0.1	0.4	0.1	0.1
Graphic paper	0.6	0.2	0.1	0.5	0.1	0.1
Tissue paper	0.6	0.2	0.1	0.5	0.1	0.1
Chemicals Industry						
Ethylene	6.3	1.8	1.1	6.0	1.5	0.9
Ammonia	0.9	0.3	0.2	0.7	0.2	0.1
Chlorine_diaphragm	0.6	0.2	0.1	0.5	0.1	0.1
Chlorine_membrane	0.2	0.1	0.0	0.2	0.0	0.0
Refineries						
Refinery basic	0.4	0.1	0.1	0.3	0.1	0.1
Refinery gasoline focused	0.5	0.1	0.1	0.4	0.1	0.1
Refinery diesel focused	0.5	0.2	0.1	0.5	0.1	0.1
Refinery flexible	0.5	0.2	0.1	0.4	0.1	0.1

4 Allocate specific excess heat potentials to individual industrial sites

4.1 Overview

The objective of this task is to obtain a dataset of industrial sites in EU27 + United Kingdom (EU28). Each data entry of an industrial production site contains the name of the company and site, the geographical location, the industrial sector as well as process-specific data like yearly emission values, manufactured goods and corresponding production process, yearly production or production capacity. The industrial database includes mainly industrial sectors of the basic material industry like steel and aluminium manufacturing, non-metallic materials (cement, glass), chemicals (ethylene, chlorine, ammonia), pulp and paper industry and refineries. These industrial subsectors account for about 62% of the total industrial energy demand (Eurostat 20202a), therefore the database covers the main and biggest industrial energy consumers in the EU, having also high excess heat regarding the quality and quantity of heat. The allocation to geographical locations enables the analysis of possible feeding in of excess heat into district heating systems.

For the estimation of georeferenced excess heat potentials from industrial processes the following data of the listed industrial sites are required:

- coordinates or at least the address of the site,
- industrial subsector together with production processes, or in some cases sufficient information on the manufactured goods,
- and annual production data or at least production capacity.

As no publicly available database of industrial sites includes all the information needed for process-specific allocation of production data, a new dataset based on a combination of several different datasets is created. This database matches information of emission reporting and sectoral asset databases.

While other datasets of georeferenced excess heat potentials are available, they basically calculate excess heat potentials only based on the emission intensity of the sites using pollution registries like the EU ETS (European Environment Agency, 2020a) and the E-PRTR (European Environment Agency, 2020b). Compared to such approaches, we use a methodology that allows a substantially more precise calculation of excess heat potentials and has three major advantages:

1. We add data on the physical production of each site in tonnes of e.g. steel (where other studies use CO_2 emissions). The production allows a much more precise estimation of energy needs and excess heat availability than the CO_2 emissions do.
2. We add information on the specific product/process (where other studies only identify the sector). Specific information on the process/product allows a detailed estimation of exhaust gas temperature and thus, resulting excess heat potentials
3. We add additional sites that are not included in E-PRTR or EU ETS emission registries. This particularly holds for smaller sites e.g. in the pulp and paper industry.

In the following, first the input datasets together with the information they cover, second the matching methodology with the consolidation process and finally the excess heat potential calculation is described.

4.2 Input data for the industrial site database

Several available industrial databases are considered for the creation of a new dataset of individual industrial sites including information about geographical location. In general, two different types of input datasets can be distinguished. On the one hand, there are pollutant and emission registers, which aim for publishing the emissions; on the other hand, sectoral databases including production process and annual production for single assets, which are commercially available. Table 17 gives an overview about the details provided in the datasets. It illustrates that the information provided by the original databases is heterogeneous, especially regarding sectoral differentiation (4-digit NACE code, ETS activity or plant type), the resolution of location (from coordinates, address, to city or just country) and production capacity and effective production.

Table 17: Content of datasets used to develop the georeferenced industrial database (Source: based on Manz et al. 2018)

Dataset	Company		Geographical data			Plant			Quantity produced/emitted		
	Company name	Asset name	Address	Country	Coordinates	Product	Plant Type	Age	Effective production	Production capacity	Emissions
E-PRTR	x	x	x	x	x	x			Few		x
EU ETS	x	x		x		x					x
Cement	x	x	Few	x			x		Few	x	
Paper	x	x		x	x	x	x		x		
Steel	x			x			x	x		x	
Glass	x		x	x		x	x		x		
Ethylene	x		Few	x		x	x			x	
Chlorine	x		Few	x		x	x			x	
Ammonia	x		Few	x		x	x			x	
Aluminium				x		x	x			x	
Refineries	x		Few	x		x	x	x	x	x	

In the following, the input datasets are described in detail.

European Pollutant Release and Transfer Register (E-PRTR): The E-PRTR database contains coordinates, pollutants including greenhouse gas (GHG) emissions for industrial sites and other sources that emit pollutants to air, water and land above an indicated threshold value in the EU. The industrial activities are classified by four-digit NACE codes (French: *Nomenclature statistique des activités économiques dans la Communauté européenne,* the Statistical Classification of Economic Activities in the European Community). Its objective is to establish uniform and publicly accessible national pollutant release and transfer registers in all Member States of the European Union. The published CO_2-values are commonly used for estimations of the energy use of the georeferenced sites and thus for excess heat potential modelling e.g. by McKenna and Norman 2010, Bühler et al., 2016 and Brückner et al., 2017. Base year 2015.

European Union Emissions Trading System (EU ETS) from EUTL: The EU emission trading system (ETS) is one of the main measures introduced by the EU to achieve cost-efficient reductions of greenhouse gas emissions and reach its targets under the Kyoto Protocol and other commitments. The data for this dataset comes mainly from the EU Transaction Log (EUTL). It covers about 45% of the total emissions of CO_2 equivalents in the EU by including major emission sources like power plants, aviation and most of industrial sectors. The dataset indicates only addresses of the company headquarters and defines the industrial subsectors by 40 different activities that represent the produced product. Base year 2015.

Global Cement Directory: The commercially available dataset covers cement plants worldwide and is published annually. The site information includes annual production capacity data, contact details and basic process information like wet or dry method and number of kilns. Base year 2015.

RISI Pulp and Paper: Fastmarkets RISI analyses the global pulp, paper and wood products market. The dataset of the pulp and paper asset database of global companies and mills is available online; registering is subject to a fee. The database indicates the coordinates of sites, the annual production and further information like produced products. Base year 2014.

VDEh Steel: The German Steel Institute VDEh updates continuously the Plantfacts database that can be purchased for a fee. It covers industrial steelmaking sites and lists them by type of process together with details on materials used and production capacity for each process. The age and year of reconstruction of most of the installations are included. Base year 2016.

glassglobal Plants: This online database covers the worldwide glass producing industry. The registration is subject to a fee to assess the data. Included are the statistics about flat, container and tableware glass types together with the type of furnaces and annual and daily production. Base year 2015.

Eurochlor Chlorine Industry Review: The commercially available dataset is published every two years. It includes general information about the industry as well as an asset dataset of chlorine-producing sites. The annual production capacity for each of the membrane, diaphragm, mercury and other processes is indicated. Base year 2015-2016.

Ethylene/Steam Cracker, Ammonia, Aluminium, Refineries: The data are a combination of publicly available data on production capacity, annual production per country like PRODCOM (Eurostat, 2020b) and extensive internet research for individual companies in the EU producing Ethylene, Ammonia, Aluminium and petrochemicals. Base year 2016.

4.3 Methodology for matching the input datasets

The combination of the mentioned datasets covering the emissions of industrial sites together with sector specific datasets covering production data enables the creation of a detailed georeferenced database. The approach is depicted in Figure 4. First, the two emission datasets are combined, forming a basic dataset, and later information from the sector specific datasets are included.

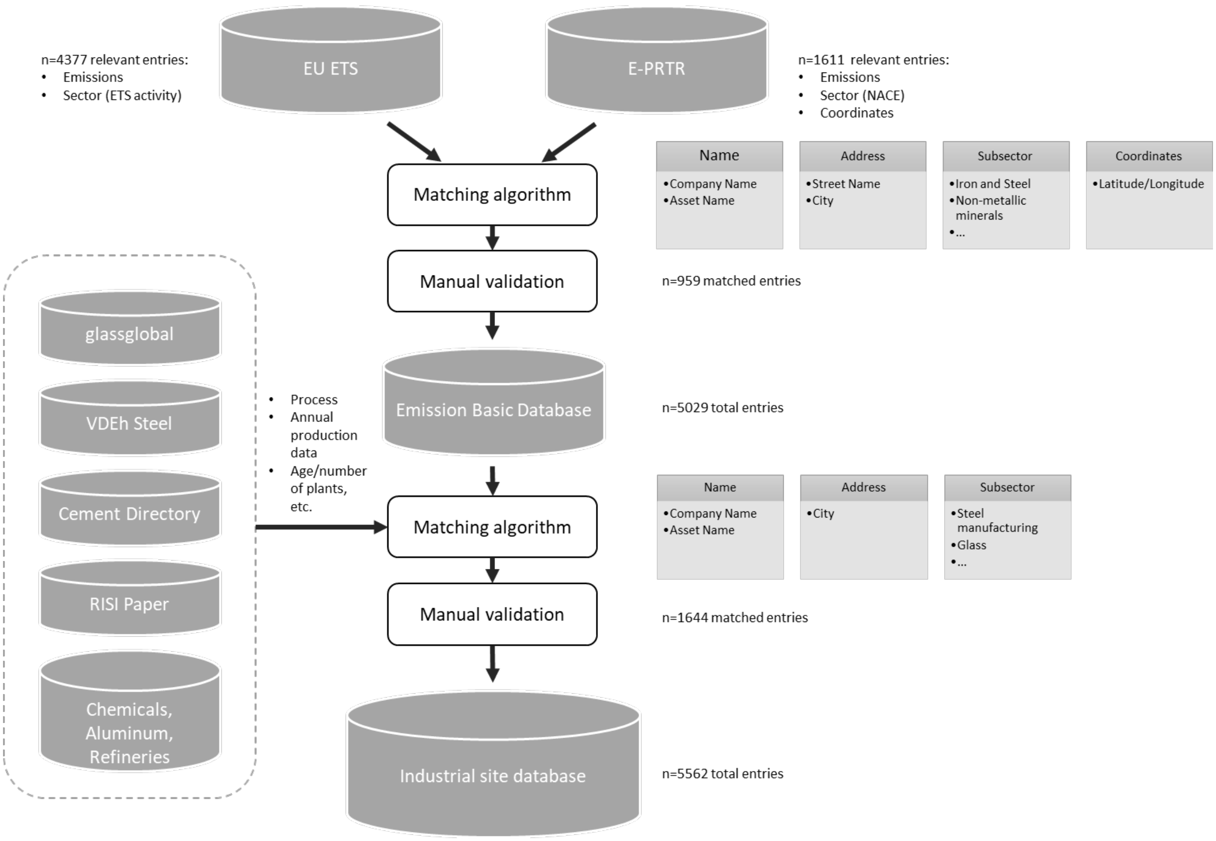

Figure 4: Data flow for establishing the georeferenced industrial site database

The challenge in combining the heterogeneous datasets are mainly to match corresponding entries of one location in the datasets to form one entry in the final database. By this process, the several information provided by the different datasets like emissions and production capacity are combined and listed together. For the matching an algorithm in C# is established that compares all the entries between two input datasets and calculates a matching score for the best three matching entries (Fydrich, 2017). Thus, the datasets are merged one after the other. The matching algorithm considers several indicators like company name, location and sector/activity for each country and is adapted for each new input dataset, according to the information provided. A matching score ranging from 0 to 100 is calculated for possible matches of two datasets and adapted considering the available information in each new input dataset. Afterwards, the possible matches with a high matching score have to be confirmed manually. This laborious process is made more cumbersome because of the difficulties mentioned in the following section of validation. In the worst case, only the company name is a valid indicator of whether this entry is the same in both databases.

4.3.1 Matching EU ETS and E-PRTR

Combining these two databases by matching individual plants has two advantages: It georeferences the EU ETS sites that could be matched with E-PRTR sites as well as includes industrial sites that may be missing in one of the two database. The number of relevant entries, i.e. industrial sites emitting greenhouse gases (GHG), is 1,611 in E-PRTR and over 4,377 in EU ETS. These numbers are obtained after excluding non-relevant sectors (like aviation and energy sector) and non-European countries as well as non-GHG emissions. After the manual confirmation of the matching possibilities, in total 959 entries are matched from both databases, leaving 652 entries from E-PRTR and 3418 entries in EU ETS unmatched. This is mainly because differing threshold values both for production as well as for emissions exist. These unmatched entries are added to the Emission Basic Database. The unmatched entries from EU ETS need to be georeferenced, either by address or by manual research on the companies' websites. In total, the Emission Basic Database has 5029 entries, which forms the basis for matching of the sector specific databases. This Emission Basic Database stores the emission values from both input datasets for different years, but uses the EU ETS values as a default if both values exist for one entry.

4.3.2 Matching of sector specific datasets

Data of annual production or production capacity of the sites can be obtained by including sectoral databases. From the seven different datasets covering the relevant industrial sectors, information about 2177 sites can be retrieved. From these, 1644 sites are matched either to sites coming from both EU ETS or E-PRTR or just one of them. That means the 533 entries from the sectoral databases, which cannot be matched to the emission basic database, need again to be georeferenced manually. The reasons why these are not included in the emission databases are not completely solved and is subject to further research and quality checks. Most of these entries include small production sites or sites using mainly biomass especially in the paper industry, some are also shut-down and decommissioned sites. There are 71 plants from the cement sector, 35 from the steel sector, 28 from the glass sector and 204 from the paper sector remaining unmatched. These unmatched entries from the sectoral databases represent maximum 13%, average 8% of the total production capacity per process. Furthermore, there are 3385 entries from ETS and E-PRTR, which cannot be matched with the sectoral datasets. These entries are, with a few exceptions, other sectors/products than the ones included in the respective sectoral datasets. The matched entries from the sectoral databases cover average about 90% of the sectoral emissions per sector as recorded by EU ETS. To include more sectoral matches and production capacities, other sectoral information and datasets need to be considered. Note, that all sites that include data about annual production are georeferenced in the industrial sites database, either by matching them to entries from E-PRTR with coordinates or by manual internet research.

4.3.3 Validation of data

The combination of different datasets facilitates the validation of the data listed in the datasets by comparing single entries with each other, filling data gaps with information from other datasets and crosschecking the recording methodology of the different datasets. The major issues that came up in the process are the following:

1. Asset data for EU ETS and E-PRTR: installations vs. sites

The definition of an asset differs in the main emission datasets. The EU ETS lists all installations emitting CO_2 as single entries, while E-PRTR summarizes mostly all installations at one site as one asset entry. The CO_2 emissions are summarized respectively, as well as installations of one company at one site but with different processes are summarized under one entry. Consequently, in the matching process of the two emission datasets, several EU ETS entries are often matched to one single E-PRTR entry.

2. CO_2 equivalents of EU ETS and E-PRTR: differences by definition

After matching the entries of the two emission databases, the emission data of the 959 matched entries can be compared to assess structural differences of emission documentation in the two datasets. Even though only 20% of the entries in EU ETS can be matched with E-PRTR entries, the matched emission values represent over 70% of all industrial EU ETS emissions. This is because facilities with a high output of emissions are likely to be represented in both databases. The sectoral emissions are depicted in Figure 5.

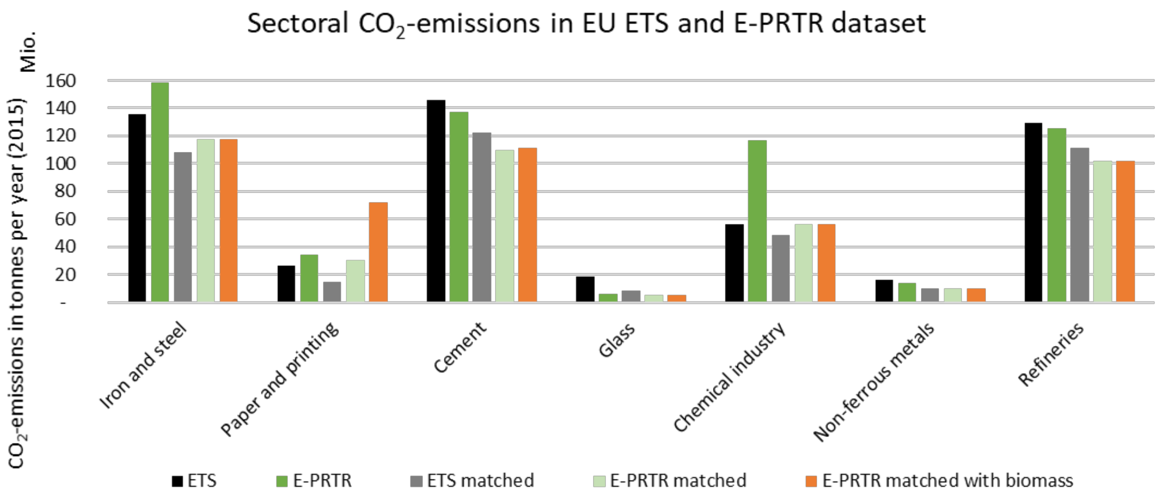

Figure 5: Sectoral CO_2 emissions in the E-PRTR and EU ETS datasets and in the Emission Basic Database

Even though the majority of industrial CO_2 equivalent emissions is represented in both databases and companies are actually obliged to report identical CO_2 emissions to both datasets, two main reasons for the differing of emission values can be identified. First, it has to be taken into account that EU ETS lists only one value of CO_2 equivalents per asset, which is calculated without the emissions coming from the combustion of biomass but take into account the N_2O from several chemical products and PFCs from aluminium production. In the E-PRTR database, the CO_2 emissions from fossil fuels and biomass are recorded separately as well as another five different greenhouse gases (HFCs, CH_4, N_2O, PFCs and SF_6) which enables the comparison of the CO_2 equivalents without the consideration of biomass combustion and with consideration of respective N_2O and PFCs emissions for the entries in the E-PRTR database. Second, the threshold values for emissions differ to be recorded in the emission database. This is exacerbated as the definition for asset differ. This is also the reason for the high number of unmatched entries. In EU ETS, all CO_2 equivalent emission for each industrial installation of the covered industrial sector are counted (opt-out exceptions for small installation need to be applied for); in E-PRTR threshold values for each pollutant (e.g. 100 kt CO_2 per year) as well as for production for some NACE activities exist. That justifies the high number of unmatched EU ETS entries. Vice versa some companies that emit e.g. pollutants other than GHG together with a low value of CO_2 emissions are recorded in E-PRTR, but not in EU ETS.

After taking these aspects into account, the deviation of the emissions decrease, depending on the industrial subsector. Deviations in emissions of 50% and 65% remain in the paper sector and glass sector, respectively. In the other sectors, deviations are below 10%. Possible causes for these deviations may be the high numbers of smaller companies and differing system boundaries, e.g. the inclusion of on-site electricity generation units together with measurement and calculation methods and the differing threshold values for single units. These possible explanations are amplified by the differing definition of an asset mentioned above, since e.g. thresholds for one single installation lead to inclusion in the register earlier than for entire sites. For further analysis, the CO_2 equivalents from the EU ETS are used.

3. Process installations in one location: defined differently in sectoral databases

In some cases, the entries in the final industrial database are inconclusive regarding the production processes included. Often, the information is sourced from three different input dataset: the EU ETS, E-PRTR and the respective sectoral dataset indicating the production capacity. The definition of processes and products itself differs, as well as the depth of defining the processes of that installation: EU ETS uses one of thirty defined ETS activities mainly focusing on products, while E-PRTR includes 4-digit NACE code, which is not congruent or overlaps with the ETS activities in some cases and vice versa. Both input datasets have in general no information about the production processes of the indicated product. The different product and process definitions can lead to the fact, that e.g. the emissions of one steel site are not totally consistent with the production capacity for steel making, sintering and coking installation or vice versa.

Another difficulty arising from differing process definitions is the calculation of excess heat potentials. The specific energy consumption and excess heat calculation relying on the production processes and the annual production are based on specific definitions of production processes. The processes included from the sectoral databases amongst others are clinker calcination dry, semidry and wet, mechanical pulp, chemical pulp, several paper grades, flat and container glass, coking, electric arc furnaces and oxygen steel, chemicals and refineries (for a comprehensive overview refer to table 16 in chapter 3). The different definition of system boundaries of production processes in the several sectoral databases can be a challenge. Furthermore, some sectoral datasets indicate the annual production, others the production capacity. As the calculation of excess heat potentials is directly linked to the physical annual production, the production capacity has to be multiplied by national utilization rates per production process. Sectoral national datasets like PRODCOM (Eurostat 2020b) serve as benchmark values.

4. Data quality: Formats, gaps and manual validation

The writing and format of strings like company names and addresses differ because of differences in language (English vs. local language), spelling (typos, usage of local letters) and different alphabets (Greek, Cyrillic, Latin). This leads to many formatting issues as well as matching problems.

Addresses and coordinates in the input datasets are often wrong or slightly off the actual location. One major issue is that EU ETS often lists the address of the companies' headquarters instead of the site; minor issues are for example missing street numbers, which lead to coordinates located in the centre of the street. Manual crosschecking of matched sites together with internet research is necessary. Entries from input sites that had no match with the E-PRTR do not include the coordinates. When the complete address is known, an automatized look-up tool could often gain the coordinates, but otherwise checking with the company's website was unavoidable. Furthermore, another issue is that company names change because of acquisition by other companies, which is not updated in all datasets.

Even though the sectoral databases are extensive, there are still non-matched entries from EU ETS and E-PRTR that are reasonable. Vice versa, several entries from the sectoral databases cannot be matched to the emission database. This leads to the question if they do not have relevant CO_2 emissions or if the emissions reported in the EU ETS are not relevant for the processes listed in the sectoral databases. This point is not yet resolved for many unmatched entries.

4.4 Georeferenced industrial sites and site-specific excess heat potentials

4.4.1 Structure of the final industrial site database

The industrial site database is established as a SQL database, which has *Sites* as the main table, covering 5562 industrial sites in the EU27 + United Kingdom (EU28), Switzerland, Norway and Iceland. The relations of the database entities are shown in Figure 6. One important feature of this database is the separate tables of sites and plants, which enables the easy storage and access of either plant specific or site specific characteristics. Note, that these 5562 entries do not cover necessarily all the information possible, like coordinates, production process and especially annual production. Nevertheless, it is the declared aim of the database to fill these data gaps as thoroughly as possible. The table *OriginDatabases* stores the original IDs from the input datasets and enables easy updates of relevant information. The plants, that have capacities connected to the *Plant* table, also relate to a specific production process. However, this is only true for sites that are matched with entries from sector specific datasets. For these entries, the database enables fast access to process-specific production capacities that are georeferenced with coordinates stored in the table *GeoPositions*.

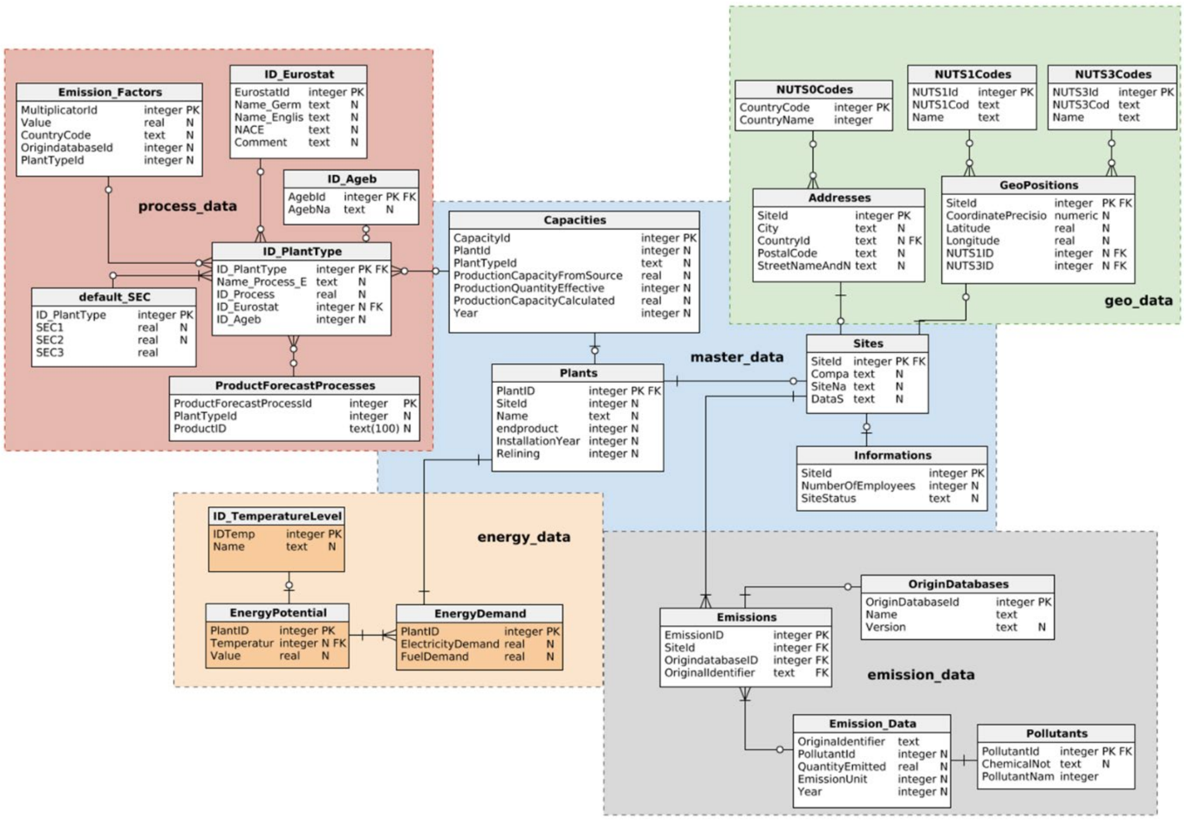

Figure 6: Relations of SQL database industrial sites

The national production data per year are listed in Table 18 for selected processes of the included processes in this study.

Table 18: Selected production data for EU28 and relevant process as listed in the industrial sites database in kt/a

	Production process, annual production in kt/a												
	Glass industry		Cement industry		Steel industry			Paper industry		Chemicals			
MS	Container glass	Flat glass	Clinker, wet	Clinker, dry	Coke oven	Blast furnace	Electric arc furnace	Mechanical pulp	Paper production	Ethylene	Ammonia	Chlorine, diapragm	Chlorine, membrane
AT	310	-	-	3154	2673	4446	761	424	5233	450	463	-	67
BE	117	522	1302	2938	3888	3987	4158	-	1620	972	360	-	791
BG	321	210	1523	1523	-	-	900	-	28	-	347	-	-
CY	-	-	-	594	-	-	-	-	-	-	-	-	-
CZ	395	560	-	3506	36	2825	563	-	398	-	-	-	74
DE	2659	2318	938	17764	5030	28044	13786	1202	29158	4909	2863	999	3355
DK	73	-	-	-	-	-	-	-	65	-	455	-	-
EE	84	-	601	-	-	-	-	-	7	-	-	-	-
EL	212	-	-	11092	311	-	3375	-	679	-	149	-	268
ES	1176	1219	614	30677	3164	4032	13104	102	7271	1331	360	-	242
FI	-	91	-	1035	1008	2232	1494	3177	7902	360	-	-	68
FR	2126	1453	500	10629	3172	11529	6801	303	9035	2493	736	179	1039
HR	179	-	-	1135	-	-	315	51	339	-	552	-	-
HU	84	210	-	2624	558	1179	1125	-	31	-	455	-	-
IE	-	-	-	6331	-	-	-	-	-	-	-	-	8
IT	3110	1495	411	27322	6225	3915	24759	511	11048	1278	540	-	263
LT	168	-	-801	-	-	-	-	-	27	-	990	-	-
LU	-	438	-	668	927	-	2025	-	-	-	-	-	-
LV	-	-	-	1302	-	-	810	-	-	-	-	-	-
MT	-	-	-	-	-	-	-	-	-	-	-	-	-
NL	836	197	-	735	720	5679	234	-	1761	3641	1710	-	762
PL	1338	1080	912	9158	747	5499	4131	124	3633	-	1973	-	328
PT	710	-	-	7593	225	-	1620	-	2208	-	-	-	128
RO	146	473	134	4928	270	1800	2439	-	147	-	192	-	181
SE	84	438	-	1723	126	3717	1391	3428	6372	563	-	-	-
SI	51	-	-	1015	45	-	666	-	440	-	-	-	14
SK	78	-	234	2651	1125	2592	909	-	809	-	432	-	-
UK	1060	913	-	3619	2336	7281	3240	241	5321	2102	941	-	407
EU28	**15317**	**11616**	**7970**	**153718**	**32614**	**89757**	**88606**	**9563**	**93784**	**18097**	**13062**	**1178**	**7994**

4.4.2 Calculation of excess heat potentials

Excess heat potentials can be calculated for entries in the industrial database that include information about production process and annual production, using the specific energy consumption (SEC) values and excess heat factor f on different temperature levels described in chapter 3. All these entries include information about the location of the production sites as coordinates. The production capacity is multiplied with typical sectoral utilisation rates, obtaining the annual production P in kt/a. By multiplying with the SEC per process in GJ/t, the annual fuel demand for this industrial process can be calculated. The excess heat factor *f* signifies the share of the process specific fuel demand, which can be utilised annually as excess heat EH. This factor strongly depends on the production process, the temperature the exhaust gas is cooled down to and the share of internal heat recovery:

$$EH = P \cdot SEC_{Process} \cdot f \cdot 1000 \quad (1)$$

For each relevant production process in the database, six different excess heat potentials are calculated. There are three different temperature levels the exhaust gas is cooled down to considered: Level_1 (25°C), Level_2 (55°C) and Level_3 (95°C); and for each of the possible exhaust gas temperatures one potential for the assumed status quo and for a theoretical full internal heat recovery (Level_1_r, Level_2_r, Level_3_r).

In total, 1889 sites of the relevant sectors with production data and 1653 sites with actual excess heat potentials in EU28 plus Switzerland, Norway and Island could be identified with the methodology of combining different datasets and multiplying the annual production with the excess heat factors for relevant processes. For EU28, the scope of this study, 1842 (total) and 1608 (total with quantified excess heat values) sites are identified. That means about 60% of the 4377 entries in the industrial database originating from EU ETS dataset do not list relevant processes for excess heat recovery considered in this study. For the relevant production processes, most of the entries in the industrial database list production data, which attests the matching methodology being a good method to fill data gaps and combining information originating from different datasets.

With the production data and process specifications of these sites, the annual fuel and electricity demand per site can be calculated with the defined SEC values. In Figure 7, the results of process-specific energy demand calculation for the iron and steel industry for main countries are depicted. Additionally, the corresponding annual demand as stated in Eurostat is marked as a line. It implies that almost all processes are covered by the sector database, as well as a structural underestimation of electricity demand. The slight overestimation of the fuel demand in some countries is due to the specification of production capacity instead of actual production and needs to be addressed in the calculation of excess heat potentials. The underestimation of electricity demand for most countries simply reflects the fact that many utilities like compressed air, lighting etc. as well as downstream processes are not included in the SECs.

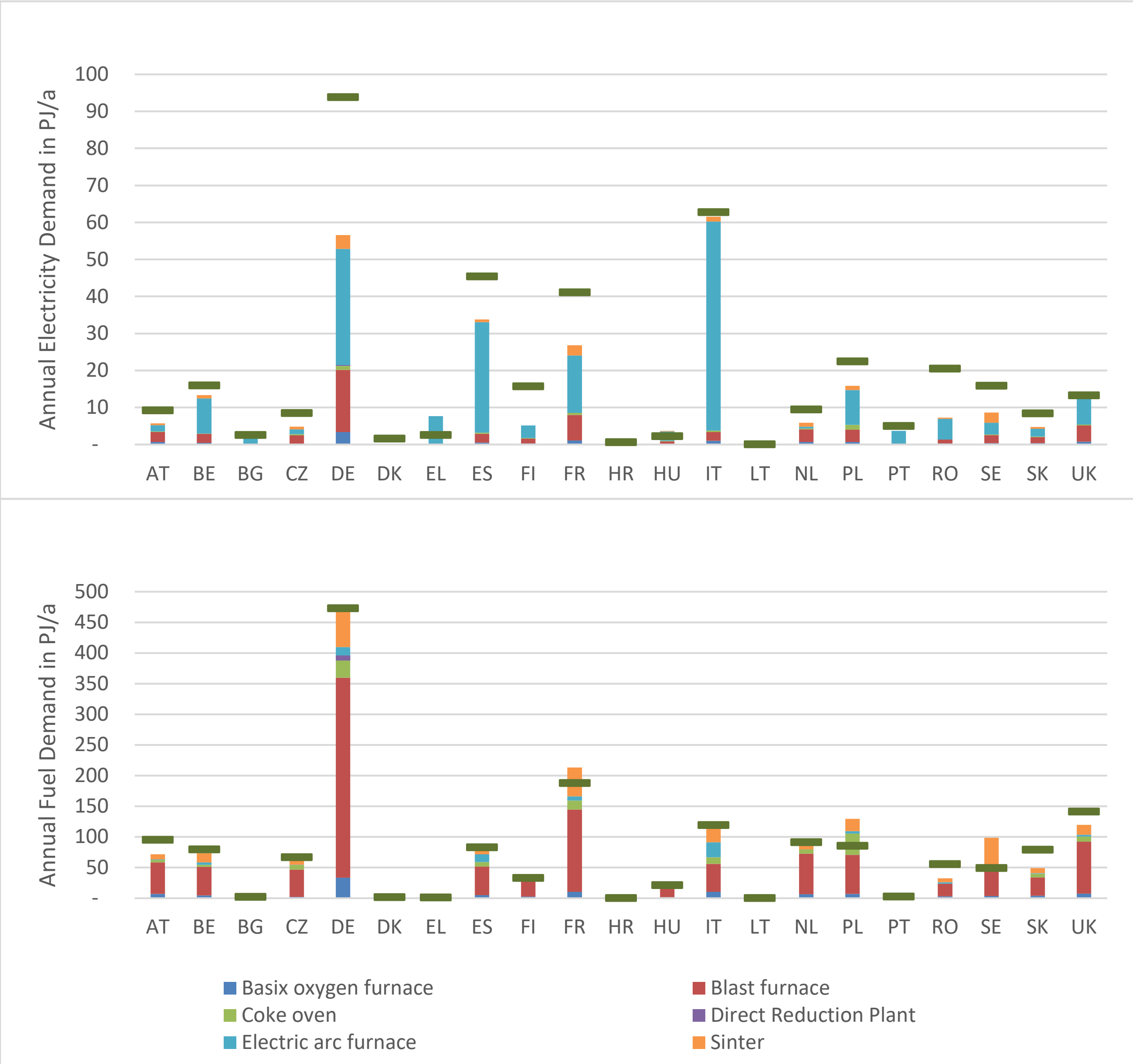

Figure 7: **Electricity (above) and fuel demand (below) in the iron and steel sector per process as calculated using the production data from the industrial site database, for main countries**

For the 1608 industrial sites in EU28, excess heat potentials ranging between 960 and 190 PJ are identified, depending on the different excess heat utilisation rates. For Level_1 (25°C) at current level of internal heat recovery the highest potential of 960 PJ was determined, full internal heat recovery reduces it to 692 PJ. If the excess heat is available at the temperature level of 55°C (Level_2), which corresponds to typical temperatures of 4th generation district heating systems, the current available potential amounts to 503 PJ, at full internal recovery reduced to 263 PJ. At temperatures of 95°C (Level_3), the typical conventional district heating system temperatures, a potential of 425 PJ and 191 currently and at full internal heat recovery respectively are identified.

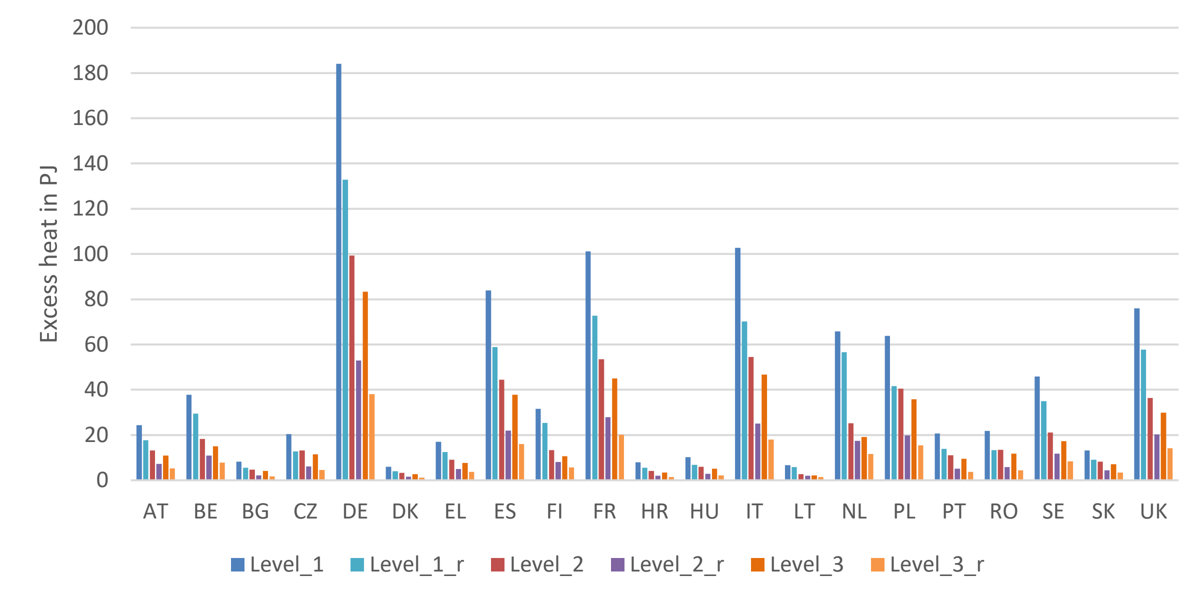

Figure 8: Total excess heat potentials in PJ, separated by heat utilisation levels, for main countries in EU28

In Figure 8, total excess heat potentials for main countries are depicted. Obviously, countries with many basic material industry locations have higher excess heat potentials. Germany has the highest excess heat potential for all utilisation levels ranging up to 184 PJ/year, as there are many steel production sites and refineries located. The same applies for France, which has the second highest potential. The main contributor for the excess heat potential in Sweden and Finland is the paper industry, in Spain non-metallic minerals and in Italy refineries.

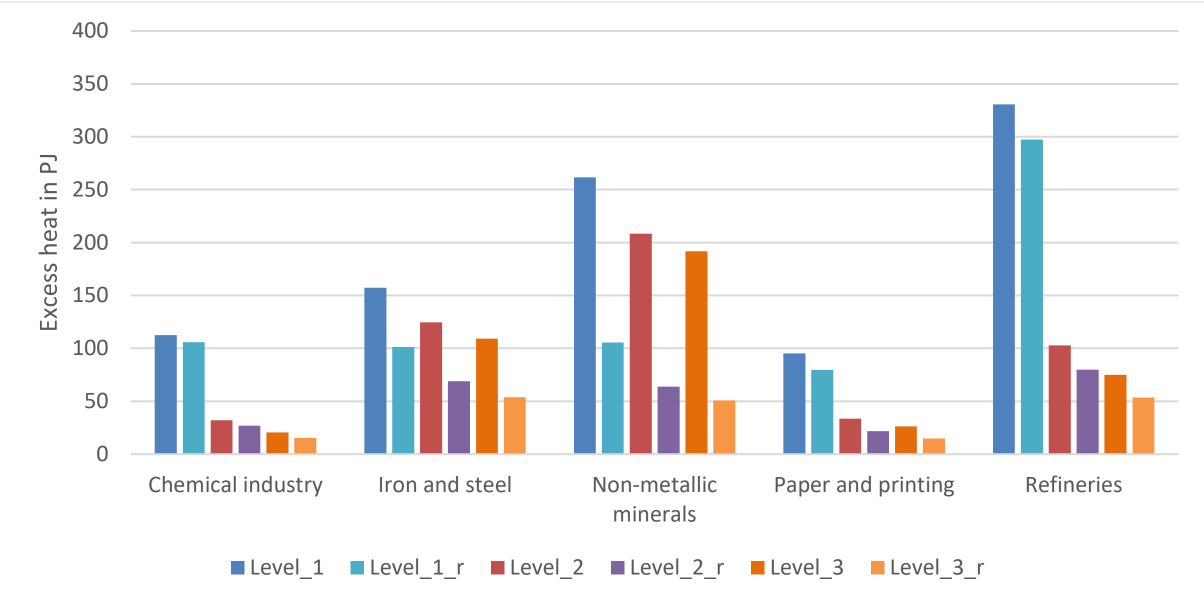

Figure 9: Total excess heat potentials in PJ in EU28, separated by heat utilisation levels, for the industrial subsectors

The sectoral total excess heat potential (Figure 9) show structural differences between the sectors. The chemical industry and refineries have high excess heat potentials for temperatures around 25°C, while the other sectors show high potentials for internal heat recovery. In general, the sectors refineries, iron and steel and non-metallic minerals have high excess heat potentials in EU28.

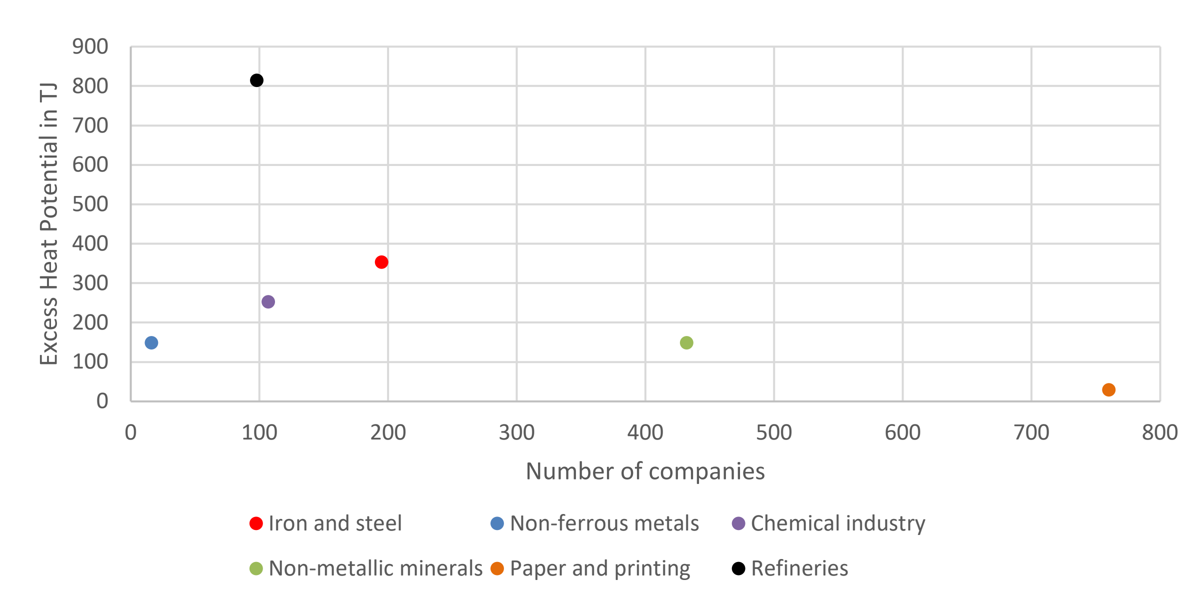

Figure 10: Average excess heat potential in PJ per site, by industrial subsector, shown for Level_2_r (55°C)

The average excess heat potentials per company, depicted in Figure 10 for the temperature of 55°C with internal recovery, represent typical process dimensions. By far the most identified industrial sites in numbers are paper production sites in the European countries, but they have a very low specific excess heat potential. Same applies for non-metallic minerals plants like glass and cement. In contrast to this, there are only about 100 refinery sites identified with a very high specific excess heat potential, leading to a high total excess heat potential.

Table 19: Excess heat potential comparison of EU28, Germany and Denmark to other studies

Study	Method	Excess heat potential in PJ/a	Tempera-ture level	Comments	Comparison with present study	Excess heat potential in PJ/a	Deviation
Brückner et al., 2017	Emission-based estimates for Germany	127	35°C	Conservative estimates for 80% of companies in Germany	Level_1_r	133	4%
		56	100°C		Level_3_r	38	-32%
Bühler et al., 2016	Exergy analysis for Denmark	8.6	40°C	22 industrial sectors included (80% of industrial energy demand)	Level_2	3.2	-62%
Persson et al., 2014	Emission-based estimates	9300	Not known	Application of estimated emission factors and recovery efficiency. Power plants included	Level_3	425	-95%
Manz et al., 2018	Process-specific SECs with excess heat factor	228	>100°C - 500°C	Conservative estimates for energy-intensive industries (no chemicals)	Level_3	425	86%

The found excess heat potentials are benchmarked with selected values found in other studies with methodologies different from the one presented here. The input data, the inclusion of industrial sectors and even the power sector, the methodology for estimation of available excess heat and the temperature levels differ greatly, which is mentioned in the Table 19. The found values in this study are within the range of conservative estimates for excess heat potentials. The greatest deviation found, compared to the values from Heat Roadmap Europe in the study of Persson et al., 2014, can be explained mainly by the exclusion of power plants and by a different methodology of excess heat calculation that is process specific leading to more precise estimates. The country specific values are comparable for Germany, and 60% lower for Denmark, as fewer industrial sectors are included in this study.

Summarized, the establishment of a extensive industrial site database and the calculation of process specific energy demand and corresponding excess heat potentials presented here can be benchmarked with other studies from EU28 calculating conservative estimations of current excess heat potential and offers a greater level of detail for process specific analyses. Besides, the emission data of sites originating from EU ETS principally enables the estimation of additional excess heat potentials, based on the CO_2 emissions. The process specific approach requires greater attention to sector specific details and data. However, it offers the possibility to calculate more precisely excess heat potentials based on physical production and additionally assess future industrial developments like switching to less carbon-intensive or carbon neutral processes as process specific analyses are possible. Among future development of the industrial structure, decommissioning or opening of large industrial facilities this is a crucial point and necessitates future research, as it will definitely change the availability of industrial excess heat for district heating. Further developments of the industrial database should be the inclusion of less energy-intensive industrial sectors and processes, further validation of unmatched sites and frequent updates on production volumes and decommissioning of sites.

5 Estimate selected excess heat potentials by district heating areas

The main objective of this part of the study is to establish the spatial relationship between the georeferenced industrial sites and urban areas characterised by high levels of heat demand densities and which meet current criteria for feasible operation of district heating systems. By performing spatial mapping and analysis of industrial sites and, what we have chosen to label, “Expected District Heating” areas (DH-E), a first selected excess heat potential is derived from the total potential by calculating distances and matches within a 10 km search radius from each industrial site and the complete array of expected district heating areas (see further section 5.1.1 below). By further establishing which of these expected district heating areas that indeed have district heating systems in operation today, a sub-dataset labelled “Actual District Heating” areas (DH-A) is derived from the expected district heating areas which constitute the basis for assessing a second selected potential.

In the following subsections, the methods, data, and main results, from this work are presented in respective order. Apart from the D5.1 dataset of georeferenced industrial sites, several other datasets are used in the mapping, some from other working groups in the sEEnergies project (e.g. the D5.2 dataset on urban areas), and some from previous EU projects (e.g. the Heat Roadmap Europe hectare grid raster dataset on residential and service sector heat demand densities for the EU28).

5.1 Method

The establishment of coherent spatial representations of current high heat demand density areas (heat demand densities above 500 GJ/ha), i.e. expected district heating areas (DH-E), constitute the first core element in this part of the study. The motivation for this is that such high heat demand density areas reflect the geographical shape, distribution, and extent, of urban areas for which district heating (second core element) may be feasibly operated at current. The underlying evidence for this assumption consists in published results from several previous studies regarding physical and economic suitability for district heating in Europe (see for example (Persson et al., 2019)).

The second core element consists of data on current European district heating systems, for which purpose the Halmstad University District Heating and Cooling database (HUDHC_v5) (Persson et al., 2017) is used in this work. In this database, the geographical locations of district heating systems are determined only by geographical coordinates of each corresponding city centre (point sources), which is a limitation since real world district heating grids are spatially distributed and spread out according to the pipe network design. The approach developed in this study therefore also serves as a means by which to assess the actual spatial outreach of these systems, thus based on the likely assumption that current district heating grids have been built and are operated in areas with high heat demand densities.

The third core element for this work is the georeferenced industrial sites themselves. By establishing the spatial linkage between these sites and expected district heating areas in Europe, without as well as with the presence of district heating systems, an assessment of selected excess heat potentials is made feasible, selected potentials which are thus based on the geographical cohesion between supply (sites) and demand (district heating areas). For this purpose, a stepwise approach, outlined in Figure 11, was developed to render quantitative and spatial output data which characterises these selected potentials.

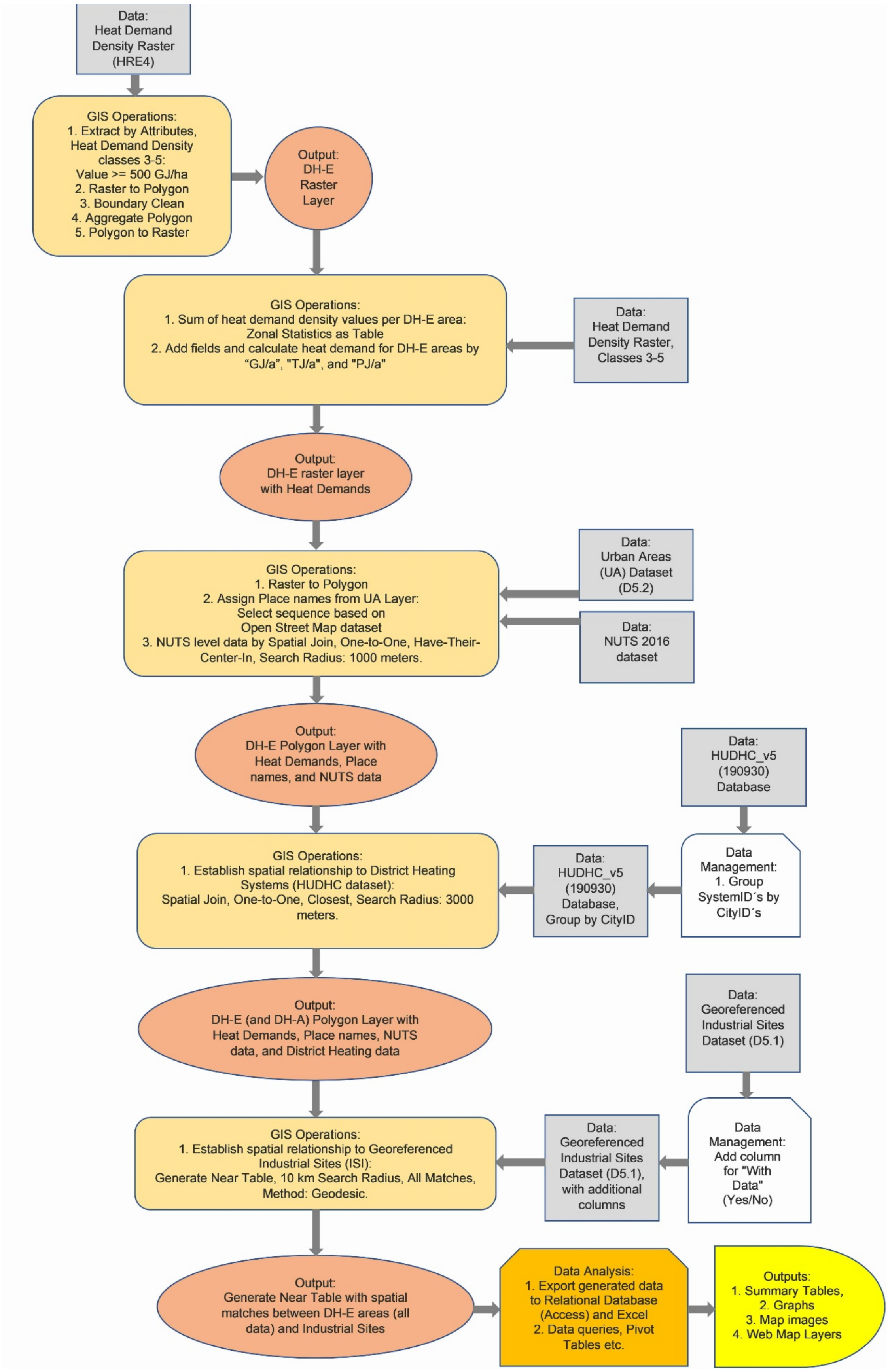

Figure 11: Principal overview flowchart of the mapping methodology, with used data, main GIS operations, and generated outputs indicated

5.1.1 Creating spatial representations of district heating areas

With reference to Figure 11, the first step of the process was to extract all raster grid cells from the Heat Roadmap Europe 4 hectare layer with heat demand density values at or above 500 GJ/ha, which correspond to heat demand classes 3, 4, and 5, as outlined in Table 20. The Heat Roadmap Europe 4 project, where these density classes were first developed and used, found that approximately 78% of all EU28 residential and service sector heat demands in 2015 originated from these three classes (Persson et al., 2019). In commentary, it may be added that classes 4 and 5 correspond to dedicated inner urban areas (dense and very dense) while class 3 typically represents outer urban areas, such as next-to city centre suburbs and multi-family building residentials districts (moderate).

Table 20: Heat demand density classification used in the Heat Roadmap Europe 4 project

Heat density class	Heat density intervals [GJ/ha]	Concentration of heat demands
0	0	No modelled heat demand
1	$0 < q_L < 200$	Very sparse
2	$200 \leq q_L < 500$	Sparse
3	$500 \leq q_L < 1200$	Moderate
4	$1200 \leq q_L < 3000$	Dense
5	$q_L \geq 3000$	Very dense

By additional GIS operations (conversion of the extracted raster dataset to a polygon layer, boundary cleaning, aggregation, and conversion back to raster format), a first raster layer of the expected district heating areas was generated, to which the sum of heat density values from the three considered density classes were added by means of Zonal Statistics. Hereby, a second output was generated, with the sum of heat demands per area added to it. After conversion back to vector format, place names were retrieved from the sEEnergies D5.2 Urban Areas (UA) dataset and added to the district heating areas dataset by a select sequence utilising Open Street Map Place names. The UA dataset was generated based on Corine Land Use Classes and is principally equivalent to Urban Morphological Zones (UMZ) (Wiechers et al., 2020). For illustration, heat demand density raster data for all five heat demand density classes and D5.2 urban areas are exemplified in Figure 12 for two different locations.

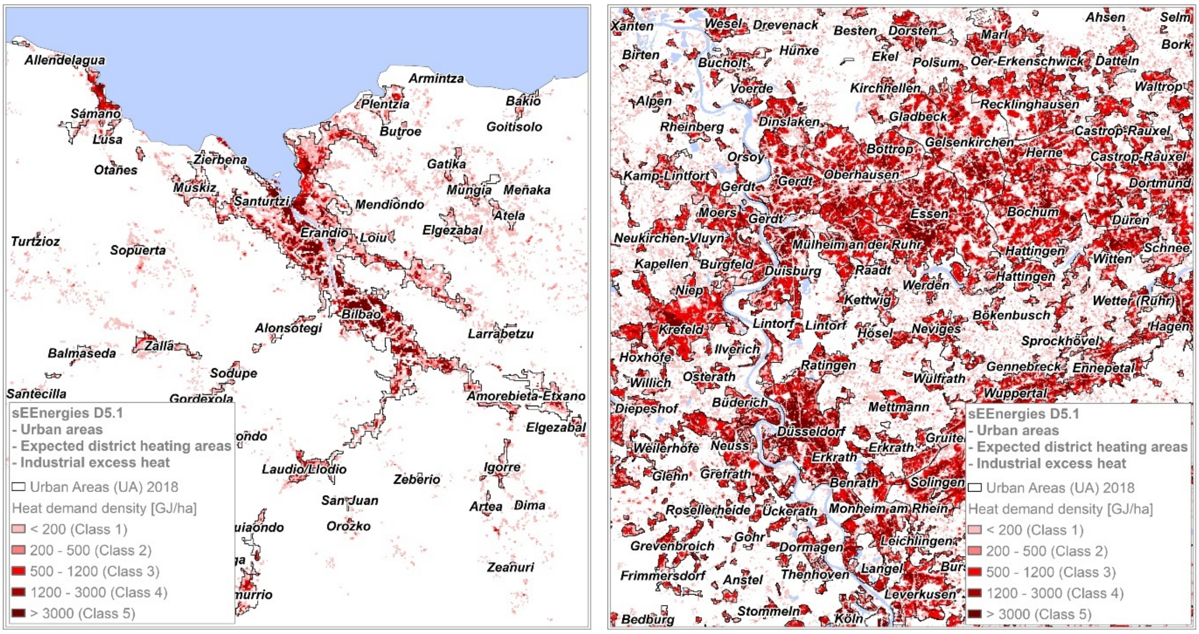

Figure 12: Heat demand densities by hectare grid cells for five classes and Urban Areas (UA), exemplified for Bilbao (ES) at left and for Düsseldorf and surroundings (DE) at right

By extracting only heat demand density grid cells with values of 500 GJ/ha and above, which thus correspond to densities suitable for current 3rd generation district heating systems (Level 3, as outlined in Figure 12 above), and by further converting these cells into (coherent, boundary cleaned, and aggregated) polygons, geometrical vector features are found that are more delimited in comparison to ordinary urban morphological zones (UMZ) and the D5.2 urban areas (UA). Hereby, the resulting expected district heating areas represent only the high heat demand density areas within these larges agglomerations and may therefore serve as spatial representations of the boundaries by which to measure distances to plausible excess heat sources, as illustrated in Figure 13.

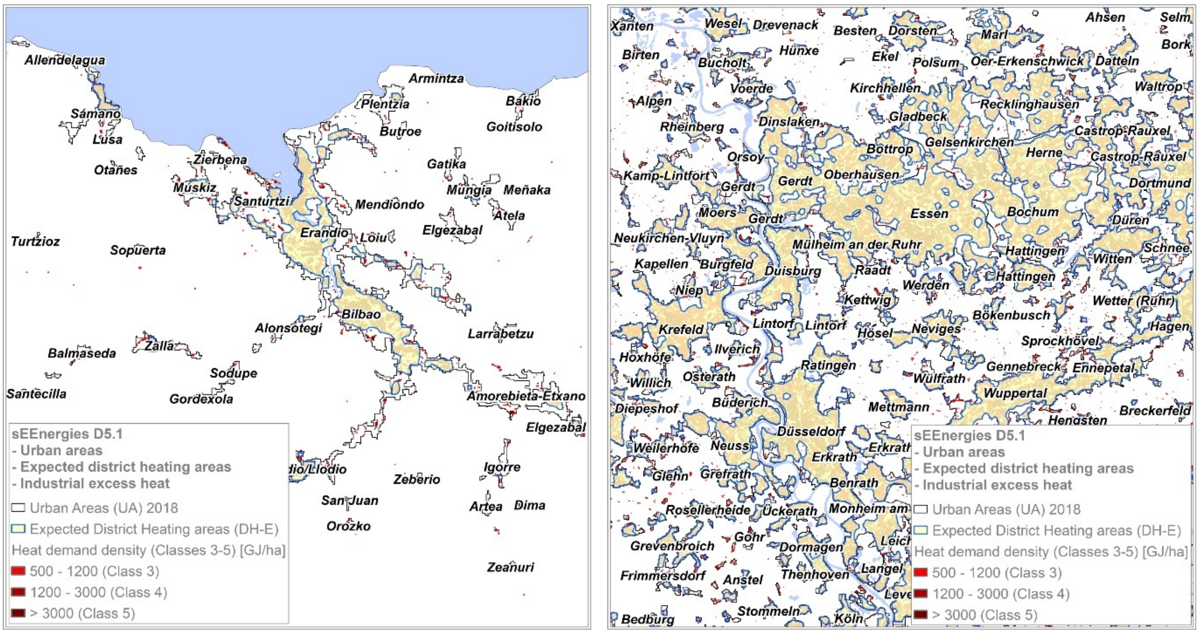

Figure 13: Expected district heating areas as coherent vector feature representations of heat demand densities of 500 GJ/ha and above, and heat demand density classes 3, 4, and 5, exemplified for Bilbao (ES) at left and for Düsseldorf and surroundings (DE) at right

After having established the sum of heat demands inside each expected district heating area, and after having associated place names as well as general NUTS data (Eurostat, 2019), the next step was to integrate the EU28 district heating dataset from Halmstad University to the district heating areas output layer. Given that the district heating systems recorded in this database each have a unique SystemID (no duplicate) as well as a CityID (duplicates), the dataset was prepared before entering the Geographical Information System (GIS) model by grouping on CityID (still counting the unique SystemID´s), serving the purpose to facilitate easier matching to the expected district heating areas. The geographical association was performed by a spatial join, one-to-one, where the coordinates of a district heating CityID (point source) was matched to the closest perimeter segment of near-by expected district heating areas within a search radius of 3 km. This particular search radius was chosen after iterative testing of various distances to obtain the highest possible rate of correct matches.

Hereby, the output expected district heating area dataset was now complete with attribute fields for sum of heat demands, place names, NUTS data, as well as selected information on district heating systems, as e.g. current presence, count of SystemID, annual heat sales etc. Noteworthy, in this process several occasions were found where one expected district heating area was matched to several district heating system CityID´s, which resulted in yet another level of grouping (of district heating systems CityID´s by expected district heating area ObjectID´s).

5.1.2 Mapping the georeferenced industrial sites

The integration of the georeferenced industrial database (shared internally as an Excel file) into the D5.1 file geodatabase and corresponding GIS model was quite straight forward. A few columns were added to the dataset before integration, for example one column indicating if data on excess heat volumes are present or not (Yes/No), another whether the country is a Member State of EU28 (Yes/No), as indicated in Figure 11. Regarding the former, excess heat volumes were not possible to calculate for a few processes since no reliable SEC values were available. Figure 14 illustrates for two different locations the projection of the industrial sites' dataset together with the final expected district heating areas layer (for the case of Düsseldorf at right also with reference to the sub-dataset of actual district heating areas).

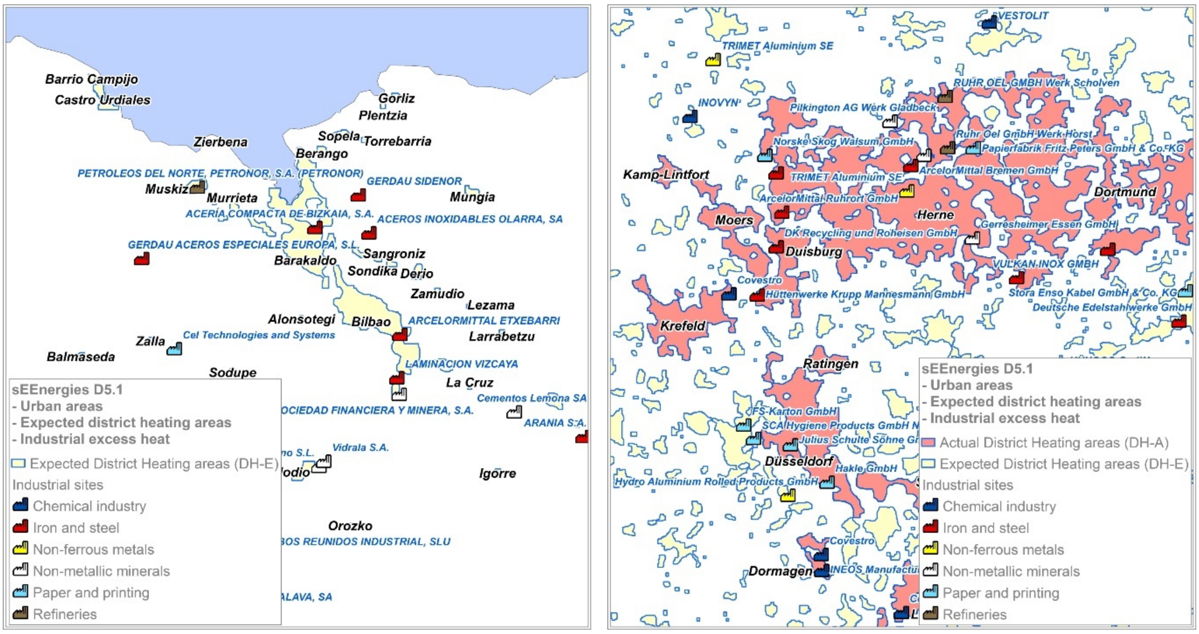

Figure 14: Industrial sites from the georeferenced industrial database and their spatial relationship to expected (DH-E) and actual (DH-A) district heating areas, exemplified for Bilbao (ES) at left and for Düsseldorf and surroundings (DE) at right

5.1.3 Generating outputs and validation

For the final step, calculating (Euclidian, i.e. straight line) distances and matches within a 10 km search radius from each industrial site and all expected district heating areas, the ArcGIS Proximity tool "Generate Near Table" was used within the context of a spatial model (Model Builder). This GIS operation produced an output table with all matches specified by distance (in meters) and by rank (inside = 0, next closest = 1, then 2, 3 etc.). The spatial model was run iteratively for a set of different search radii (e.g. 100 km, 25 km, and 10 km) that reflect plausible transition pipe lengths for excess heat recoveries, which for their feasibility depend mainly on the capacities and the magnitudes of available excess heat and corresponding heat costs. The shortest and perhaps most realistic distance by which to arrange external excess heat recoveries today, 10 km, was selected as the model default by which to also present the potential estimates and study results.

For final analysis, and to establish the selected excess heat potentials, all produced outputs were exported to a relational database for querying and further grouping, and then exported to Excel files for post-processing, i.e. validation, quality check, comparisons, and to establish summaries and aggregated tabular outputs (Pivot tables).

5.1.4 Preparing web map layers

Two output datasets (the georeferenced industrial sites and the district heating areas) were prepared as web map layers for visualisation and download access (including metadata and licencing information) by publication at the sEEnergies project Open Data Hub (hosted by sEEnergies partner Flensburg University in Germany).

5.2 Data

Three main, and two complementary, data sources have served as input to this part of the study:

- Main data sources:
    - Type: Heat demand density raster data by hectare resolution
        - Source: Pan-European Thermal Atlas (PETA 4.3) of the Heat Roadmap Europe 4 project (HRE, 2018; PETA 4.3, 2018)
        - Data year and scope: 2015, EU 27 + United Kingdom (EU28)
        - Open data: Yes (visualisation on web map)
        - References: (Persson et al., 2017; Persson et al., 2019)
    - Type: European district heating systems
        - Source: Halmstad University District Heating and Cooling database (version 5 of 2019-09-30)
        - Data year and scope: Various (mainly 2011), EU 27 + United Kingdom (EU28)
        - Open data: No (internal institutional database)
        - References: (Persson et al., 2014; Persson et al., 2017)
    - Type: Georeferenced industrial sites
        - Source: sEEnergies D5.1 dataset on industrial sites (open dataset)
        - Data year and scope: 2015, EU 27 + United Kingdom (EU28) + CH, IS, NO
        - References: This report.
- Complementary data sources:
    - Type: Urban Areas (UA) dataset
        - Source: sEEnergies D5.2 dataset (Wiechers and Möller, 2020)
        - Data year and scope: 2018, EU 27 + United Kingdom (EU28) + CH, IS, NO
        - References: (Wiechers et al., 2020)
    - Type: NUTS (Nomenclature of Territorial Units for Statistics) data for Europe
        - Source: Eurostat (NUTS_RG_01M_2016_3035)
        - Data year and scope: 2016, EU, EFTA countries and candidate countries (2017)
        - References: (Eurostat, 2019)

In the following sub-sections, these datasets and associated outputs are described in more detail.

5.2.1 Heat demand densities, urban areas, and district heating areas

In the sEEnergies D5.2 dataset, a total of 147,791 urban areas were modelled for the EU27 plus United Kingdom (EU28) scope, as shown in Table 21 with specifications for each country. The extraction of expected district heating areas resulted in a total of 47,275 unique polygon areas for the corresponding countries, which approximately equates to a 32% share albeit not perfectly comparable since the two datasets are based on different underlying input data.

By reference to the Heat Roadmap Europe 4 project results on EU28 residential and service sector building heat demands, which were assessed at 10,718 PJ for the year 2015, the calculated sum of heat demands in the expected district heating areas constitute 65% (7018 PJ), which is fairly in line with expectations: in the final publication from the work on physical (heat demand density) and economic (heat distribution costs) suitability for European district heating in the Heat Roadmap Europe 4 project (Persson et al., 2019), the accumulated heat demands for density classes 3-5 was found at ~8410 PJ (78%). The discrepancy being due to several outlying and single grid cells being omitted in the extraction process (which may be observed in Figure 12 and Figure 13.

Table 21: Overview table on Urban Areas (UA) from sEEnergies D5.2, Expected District Heating areas (DH-E), and residential and service sector heat demands from the Heat Roadmap Europe 4 project

MS	Urban Areas (UA)	Expected District Heating areas (DH-E)	DH-E Share of UA [%]	MS Heat Demands (2015) [PJ/a]	DH-E Heat Demand (2015) [PJ/a]	DH-E Heat Demand of MS [%]
AT	4090	1032	25	232.4	129.7	56
BE	2882	1699	59	324.3	210.9	65
BG	3972	242	6	68.6	32.2	47
CY	425	9	2	8.6	0.8	9
CZ	5984	1032	17	237.2	138.5	58
DE	22,960	13,452	59	2413.4	1773.2	73
DK	1528	636	42	166.6	102.6	62
EE	622	106	17	34.4	19.7	57
EL	3432	274	8	120.3	65.8	55
ES	7231	2201	30	470.8	329.1	70
FI	1758	586	33	226.4	131.8	58
FR	26,217	7497	29	1514.3	913.0	60
HR	1725	294	17	69.0	24.1	35
HU	3773	1136	30	209.9	83.9	40
IE	803	321	40	105.5	42.1	40
IT	10,583	5952	56	1276.8	880.6	69
LT	1964	116	6	45.8	22.9	50
LU	258	131	51	25.7	16.4	64
LV	909	106	12	46.0	30.5	66
MT	34	12	35	3.0	1.7	58
NL	1534	1611	105	425.3	339.9	80
PL	18,241	2023	11	657.7	310.2	47
PT	2378	289	12	62.0	23.2	37
RO	11,228	351	3	183.0	75.3	41
SE	3018	817	27	296.3	177.8	60
SI	586	122	21	39.5	16.2	41
SK	2914	396	14	95.6	48.4	51
UK	6742	4832	72	1360.1	1077.2	79
EU28	**147,791**	**47,275**	**32**	**10,718**	**7018**	**65**

As for the European database on district heating systems, the used version of the Halmstad University District heating and Cooling database (version 5 of 2019-09-30), counts a total number of 4113 unique systems for EU28, as outlined in Table 22. By the preparation process of grouping these systems by their corresponding CityID´s, as described above, these unique systems correspond to a total of 3703-point source city coordinate pairs (latitude and longitude). Noteworthy, nobody knows today exactly how many district heating systems that are currently in operation in Europe, but it is likely that the total number could be found in the interval between 5000 and 6000 systems. However, with respect to the used database, most large-size European district heating systems that have been operated over long time periods are included, while missing systems mainly should refer to smaller systems and more recent project developments. Still, as for the results and conclusions drawn from this work, it should be kept in mind that the used database on European district heating systems, in this respect, is somewhat incomplete and that there is room for future improvements.

This may also be said regarding the statistics on annual heat sales from the recorded systems in the database. For reasons of limited resources mainly, the latest updates with regards to statistics refer to data year 2016, while the main bulk of data refers to national district heating records form data year 2011. For a few countries, additionally, statistics have not been found while for some others (e.g. PL, CZ, and SK), statistics have been provided under confidentiality conditions (not to be published on system level). The latter circumstance is the reason why statistics on annual heat sales are included here in this report (national aggregates), but that they are omitted from the web map dataset.

Table 22: Overview table on the Halmstad University District Heating and Cooling database (HUDHC_version 5 of 2019-09-30) with spatial match to Expected District Heating areas (DH-E), thus Actual District Heating areas (DH-A), and recorded annual heat sales of DH-A (mainly with data from 2011)

MS	District Heating Systems in HUDHC_v5 [n]	District Heating Cities in HUDHC_v5 [n]	Recorded Heat Sales (Various years) [PJ/a]	DH-A (DH-E with District Heating Systems) [n]	Number of District Heating Systems in DH-A [n]	Recorded Heat Sales in DH-A (Various years) [PJ/a]	Share of Recorded Heat Sales in DH-A [%]
AT	473	368	0	240	312	0	0
BE	38	32	2.4	27	33	2.0	84
BG	21	21	31.3	18	18	31.2	100
CY	No data	No data	0	0	0	0	0
CZ	391	391	56.1	348	348	55.9	100
DE	254	228	277.6	215	239	278.2	100
DK	458	434	115.5	242	254	105.9	92
EE	151	142	16.7	54	63	15.5	93
EL	5	5	0.8	4	4	0.8	100
ES	17	16	0.6	14	15	0.6	100
FI	178	165	115.7	130	141	114.1	99
FR	456	378	78.6	224	266	78.4	100
HR	18	18	7.3	17	17	7.2	99
HU	109	99	0.05	100	110	0.06	133
IE	2	2	0	2	2	0	0
IT	81	80	22.6	54	54	22.0	97
LT	37	35	1.9	34	36	1.9	100
LU	1	1	0	1	1	0	0
LV	37	36	20.8	31	32	20.8	100
MT	No data	No data	0	0	0	0	0
NL	20	18	1.0	16	18	1.0	100
PL	429	428	239.7	408	409	237.4	99
PT	1	1	0	1	1	0	0
RO	75	75	0.05	62	62	0.01	13
SE	386	342	169.5	226	268	165.9	98
SI	57	57	0.0009	39	39	0	0
SK	219	219	63.3	160	160	62.0	98
UK	199	112	1.5	96	123	1.5	100
EU28	**4113**	**3703**	**1223**	**2763**	**3025**	**1203**	**98**

From Table 22, it still becomes quite clear that the recorded systems (and statistics) represent the major volumes of sold district heat in EU28 today (1223 PJ), which, by relations to the total heat demands from Table 21 (10,718 PJ), indicates an ~11% residential and service sector heat market share for district heating. This is rather consistent with international energy statistics reports from the last decade.

In terms of spatial matching, 2763 district heating CityID´s matched with expected district heating areas (3025 unique systems), which therefore constitute the actual district heating areas (DH-A) for the EU28. Together, the matching systems constitute 98% of recorded statistics on annually sold heat (1203 PJ). For a sub-set of 940 CityID's, no match was established: cities which have district heating at current, but where heat demand densities are below the extraction limit (or farther than 3 km from nearest area). After examination, it was found that most of these cities are located in countries with high shares of district heating (e.g. Scandinavia, the Baltics, Austria, and the Slovak Republic).

5.2.2 District heating areas and georeferenced industrial sites

In terms of spatial matching of the district heating areas vis-à-vis the georeferenced industrial sites, as presented in Table 23, 12,283 expected district heating areas were found with at least one match within the 10 km default search radius (EU28), which corresponds to 26% of the total count of expected district heating areas (47,275) and 52% (3678 PJ) of the total heat demand in expected district heating areas (7018 PJ). The highest matching rates with regards to areas was found for Luxembourg (56%), Slovenia (47%), and for Portugal (42%). Dittos with regards to heat demands were found in Luxembourg (91%), Portugal (78%), and Greece (77%).

As for the actual district heating areas, a sub-set from the matches found for the expected district heating areas, consisting of 724 areas with matches to industrial sites, could be derived from the output data. While the share that this sub-set represents in terms of the total count of expected district heating areas is quite small (1.5%), the same sub-set constitutes no less than 31% (2169 PJ) of the total heat demand of the expected district heating areas (EU28). For a few countries, more than 50% of the total heat demand is represented by these actual district heating areas (e.g. in Austria, Croatia, and Slovenia). For several others, the share is well above the 31% EU28 average (e.g. Lithuania, the Czech Republic, France, Bulgaria, Luxembourg, Sweden, to mention the first six by order of share magnitude). The recorded annual heat sales of the actual district heating areas with matches to industrial sites constitute 51.5% of all heat sales in actual district heating areas and 50.6% of all heat sales recorded in the Halmstad University District Heating and Cooling database.

Table 23: EU28 overview of Expected District Heating areas (DH-E) and Actual District Heating areas (DH-A) with spatial match to georeferenced industrial sites

	DH-E with match to Industrial Sites				DH-A with match to Industrial Sites					
MS	Count [n]	Share of all DH-E [%]	Heat Demand (2015) [PJ/a]	Share of all DH-E Heat Demand [%]	Count [n]	Share of all DH-E [%]	Heat Demand (2015) [PJ/a]	Share of all DH-E Heat Demand [%]	Number of District Heating Systems [n]	Recorded Heat Sales (Various years) [PJ/a]
AT	275	27	92.1	71	74	7.2	84.1	65	106	0
BE	613	36	145.9	69	15	0.9	46.7	22	17	1.4
BG	48	20	16.1	50	6	2.5	13.6	42	6	27.5
CY	No data	No data	No data	No data	No data	No data	No data	No data	No data	No data
CZ	250	24	71.1	51	85	8.2	61.9	45	85	32.5
DE	3727	28	944.7	53	95	0.7	534.9	30	109	187.6
DK	55	9	8.0	8	12	1.9	5.9	6	12	9.3
EE	4	4	0.1	1	3	2.8	0.1	0	3	0.14
EL	73	27	50.6	77	1	0.4	0.7	1	1	0
ES	558	25	201.8	61	9	0.4	81.1	25	10	0.45
FI	173	30	56.4	43	35	6.0	45.6	35	41	40.7
FR	1621	22	520.3	57	75	1.0	403.7	44	89	62.7
HR	55	19	14.0	58	5	1.7	12.9	54	5	5.9
HU	111	10	6.4	8	14	1.2	3.7	4	16	0.008
IE	16	5	0.7	2	No data	No data	No data	No data	No data	No data
IT	2206	37	567.8	64	21	0.4	219.8	25	21	17.6
LT	24	21	14.2	62	6	5.2	11.2	49	8	0.021
LU	73	56	14.9	91	1	0.8	6.5	40	1	0
LV	7	7	1.6	5	3	2.8	1.4	5	3	0.9
MT	No data	No data	No data	No data	No data	No data	No data	No data	No data	No data
NL	436	27	140.4	41	6	0.4	41.1	12	7	0.9
PL	465	23	120.6	39	92	4.5	97.8	32	93	105.0
PT	122	42	18.1	78	1	0.3	6.5	28	1	0
RO	73	21	35.0	47	14	4.0	28.8	38	14	0
SE	205	25	83.2	47	61	7.5	70.7	40	84	84.4

	DH-E with match to Industrial Sites				DH-A with match to Industrial Sites					
SI	57	47	10.7	66	17	13.9	8.7	54	17	0
SK	95	24	19.5	40	39	9.8	15.4	32	39	42.1
UK	941	19	523.8	49	34	0.7	366.7	34	52	0.82
EU28	**12,283**	**26**	**3678**	**52**	**724**	**1.5**	**2169**	**31**	**840**	**620**

5.2.3 Industrial sites data by main sectors

The D5.1 industry dataset that was internally shared for the spatial analysis performed in this section (version 4), counted a total of 1889 unique sites (including in excess of EU27 plus United Kingdom sites; 16 Swiss, 3 Islandic, 27 Norwegian, and one Turkish site). For the EU27 plus United Kingdom (EU28) context, the total count was thus found at 1842 sites, which are presented by main sectors in Table 24.

Table 24: Total potential: EU28 extract of the georeferenced industrial sites by Main Sectors, without and with excess heat data, and estimated potentials for the six Level categories

			Excess Heat Potential					
			Current Internal Heat Recovery			Max Internal Heat Recovery		
Main Sector	Industrial Sites [n]	Industrial Sites - With Excess Heat Data [n]	Level 1 (25°C) [PJ/a]	Level 2 (55°C) [PJ/a]	Level 3 (95°C) [PJ/a]	Level 1 (25°C) [PJ/a]	Level 2 (55°C) [PJ/a]	Level 3 (95°C) [PJ/a]
Chemical industry	109	107	112.5	32.1	20.4	105.9	27.0	15.6
Iron and steel	372	195	157.4	124.7	109.2	101.2	68.9	53.8
Non-ferrous metals	16	16	2.5	2.4	2.3	2.5	2.4	2.3
Non-metallic minerals	466	432	261.8	208.3	191.8	105.7	63.9	50.9
Paper and printing	781	760	95.2	33.6	26.3	79.6	21.9	15.0
Refineries	98	98	330.7	102.7	75.1	297.4	79.8	53.5
EU28	**1842**	**1608**	**960**	**504**	**425**	**692**	**264**	**191**

In Table 24 is also indicated the 1608 EU28 sites (87% of the total EU28 count) for which data on excess heat was possible to establish. As can be seen, the total annual excess heat potential (Level 1), at current rates of on-site internal heat recoveries, is just short of one exajoule per year (960 PJ). By external excess heat recovery at current 3rd generation district heating supply temperatures (Level 3), at current rate of internal heat recovery, the corresponding potential is a little less than half of the total potential (425 PJ). Given that excess heat data was missing for 234 EU28 sites, visualised at left in Figure 15, it is fair to conclude that the stipulated potentials are somewhat lower than what would have been assessed should excess heat data have been available for the complete study population.

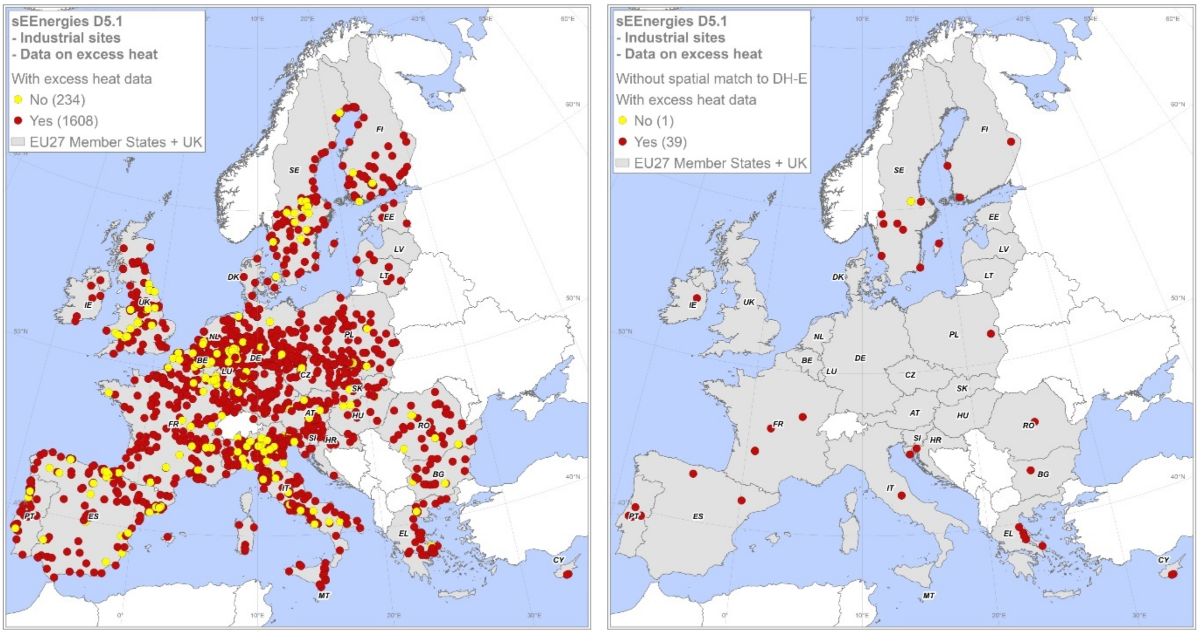

Figure 15: Visualisation of the 1608 industrial sites with excess heat data and the 234 without (left), and the 40 sites without spatial match to expected district heating areas (DH-E) out of the 1842 EU28 sites (right)

Approaching the results of this part of the study, Table 25 presents the findings related to the selected potential 1 (industrial sites with matches to expected district heating areas) by main sectors for the EU28 (the equivalent results by Member States are presented in Table 28). One major finding from this analysis should be underlined, namely that 1802 sites out of the 1842-total count (98%) indeed displays a spatial match to expected district heating areas. The first and perhaps most significant consequence of this fact is that the total annual excess heat potential and the first selected excess heat potential in principle are of the same magnitudes.

Table 25: Selected potential 1: EU28 extract of the georeferenced industrial sites by Main Sectors with spatial match to Expected District Heating areas (DH-E), without and with excess heat data, and estimated potentials for the six level categories

			Excess Heat Potential					
			Current Internal Heat Recovery			Max Internal Heat Recovery		
Main Sector	**Industrial Sites - With DH-E Match [n]**	**Industrial Sites - With DH-E Match and Excess Heat Data [n]**	**Level 1 (25°C) [PJ/a]**	**Level 2 (55°C) [PJ/a]**	**Level 3 (95°C) [PJ/a]**	**Level 1 (25°C) [PJ/a]**	**Level 2 (55°C) [PJ/a]**	**Level 3 (95°C) [PJ/a]**
Chemical industry	109	107	112.5	32.1	20.4	105.9	27.0	15.6
Iron and steel	367	191	157.1	124.5	109.0	101.1	68.8	53.7
Non-ferrous metals	16	16	2.5	2.4	2.3	2.5	2.4	2.3
Non-metallic minerals	453	419	252.2	200.6	184.9	101.1	60.8	48.4
Paper and printing	761	740	92.2	32.4	25.3	77.2	21.2	14.5
Refineries	96	96	324.2	100.6	73.6	291.5	78.2	52.4
EU28	**1802**	**1569**	**941**	**493**	**415**	**679**	**258**	**187**

In addition, with reference to the chosen 10 km search radius, it might be worthwhile commenting that among the 40 sites for which no spatial match was found, as depicted in Figure 15 at right, at least one site (Swedish Södra Cell AB paper and printing facility), located some 12 km north of the town of Varberg (Euclidian distance), is known to have external excess heat recovery in operation today (Industrial dataset site identifier: 893). For further references, see also (Persson and Werner, 2012).

For the selected potential 2, i.e. industrial sites with matches to actual district heating areas, Table 26 presents our findings by main sectors for the EU28. 866 sites, of which 752 with excess heat data, were found to be located inside or within 10 km of these areas, corresponding to a total annual excess heat potential of some 529 PJ at current rate of on-site internal heat recoveries. For external heat recovery by 3rd generation district heating systems under these conditions (Level 3), this equates to an annual potential of approximately 230 PJ.

Table 26: Selected potential 2: EU28 extract of the georeferenced industrial sites by Main Sectors with spatial match to Actual District Heating areas (DH-A), without and with excess heat data, and estimated potentials for the six level categories

			Excess Heat Potential					
			Current Internal Heat Recovery			Max Internal Heat Recovery		
Main Sector	**Industrial Sites - With match to DH-A [n]**	**Industrial Sites - With match to DH-A and Excess Heat Data [n]**	**Level 1 (25°C) [PJ/a]**	**Level 2 (55°C) [PJ/a]**	**Level 3 (95°C) [PJ/a]**	**Level 1 (25°C) [PJ/a]**	**Level 2 (55°C) [PJ/a]**	**Level 3 (95°C) [PJ/a]**
Chemical industry	63	61	70.7	20.1	12.8	66.6	17.0	9.8
Iron and steel	225	123	112.9	89.1	77.8	73.9	50.3	39.3
Non-ferrous metals	9	9	1.4	1.3	1.3	1.4	1.3	1.3
Non-metallic minerals	191	186	112.6	89.3	82.6	44.2	25.8	20.5
Paper and printing	323	318	51.5	18.3	14.3	43.0	11.8	8.1
Refineries	55	55	180.3	55.9	40.8	162.3	43.5	29.1
EU28	**866**	**752**	**529**	**274**	**230**	**391**	**150**	**108**

5.3 Results

In this section, the main results from this part of the study are presented by reference to the EU27 Member States plus United Kingdom (EU28). The three different potentials, the total, the first selected, and the second selected, are presented in tabular form and in scatter plots to provide a brief analysis of the correlation between the heat demands of district heating areas and the corresponding excess heat potentials. In the end, the section includes also an account of the publication of the major outputs (the district heating areas layer and the industrial sites layer) at the sEEnergies Open Data Hub.

5.3.1 Urban areas and district heating areas

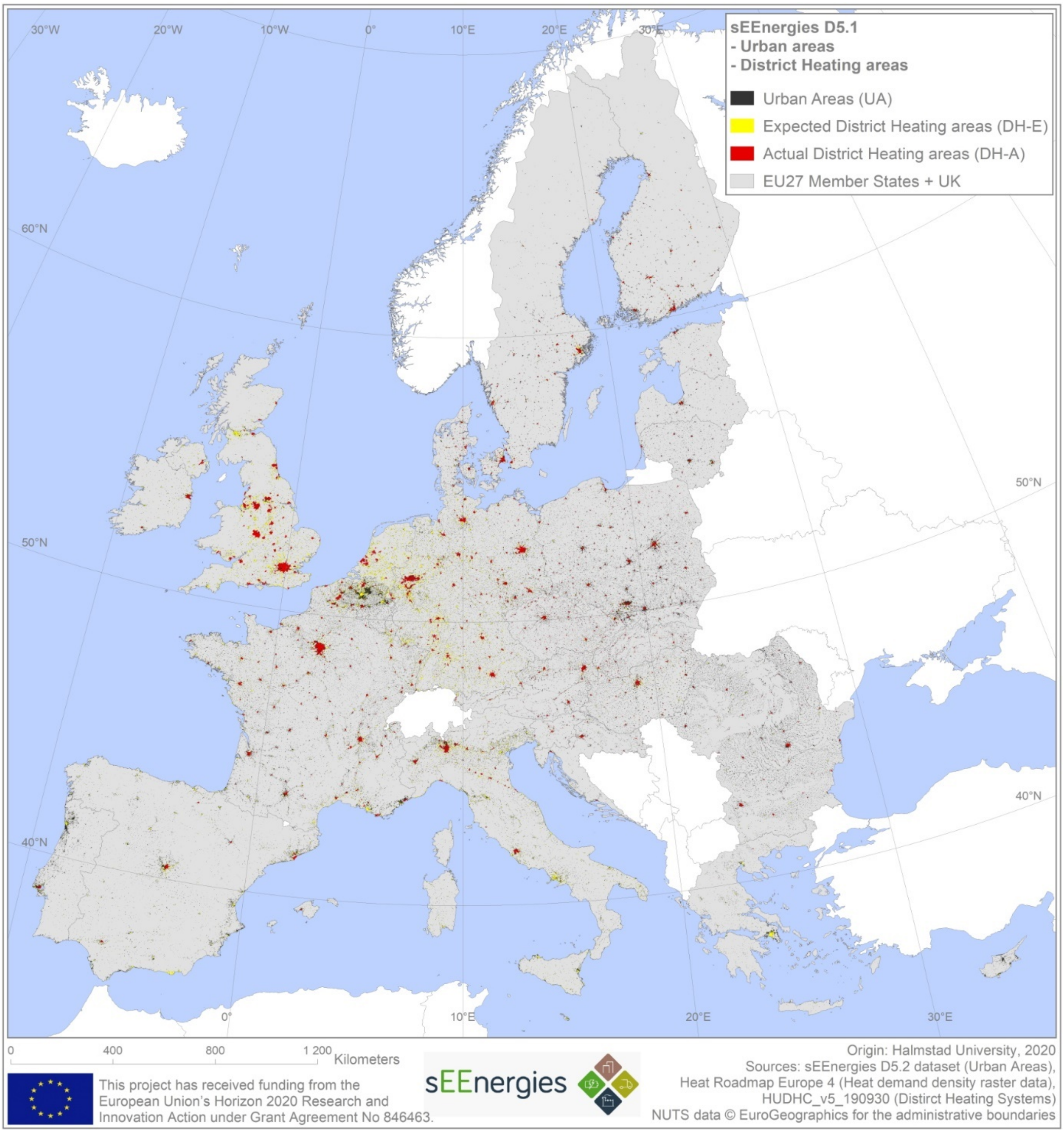

Figure 16: EU28 map of Urban Areas (UA), Expected District Heating areas (DH-E), and Actual District Heating areas (DH-A)

Figure 16 shows a European map with the urban areas and the expected and actual district heating areas. Albeit the detail is principally lost at this continental scale (see web map for full detail), the map still indicates the general distribution of these areas and is therefore included here to provide a first order visual appreciation of the district heating areas dataset.

5.3.2 Total excess heat potential

As for the industrial sites, their geographical locations and distribution, and the annual excess heat potentials associated with them, Figure 17, presents a European map with the 1842 georeferenced EU28 sites by main sectors and with the total potential (Level 1, at current rate of internal heat recovery) indicated by five legend quantity sizes.

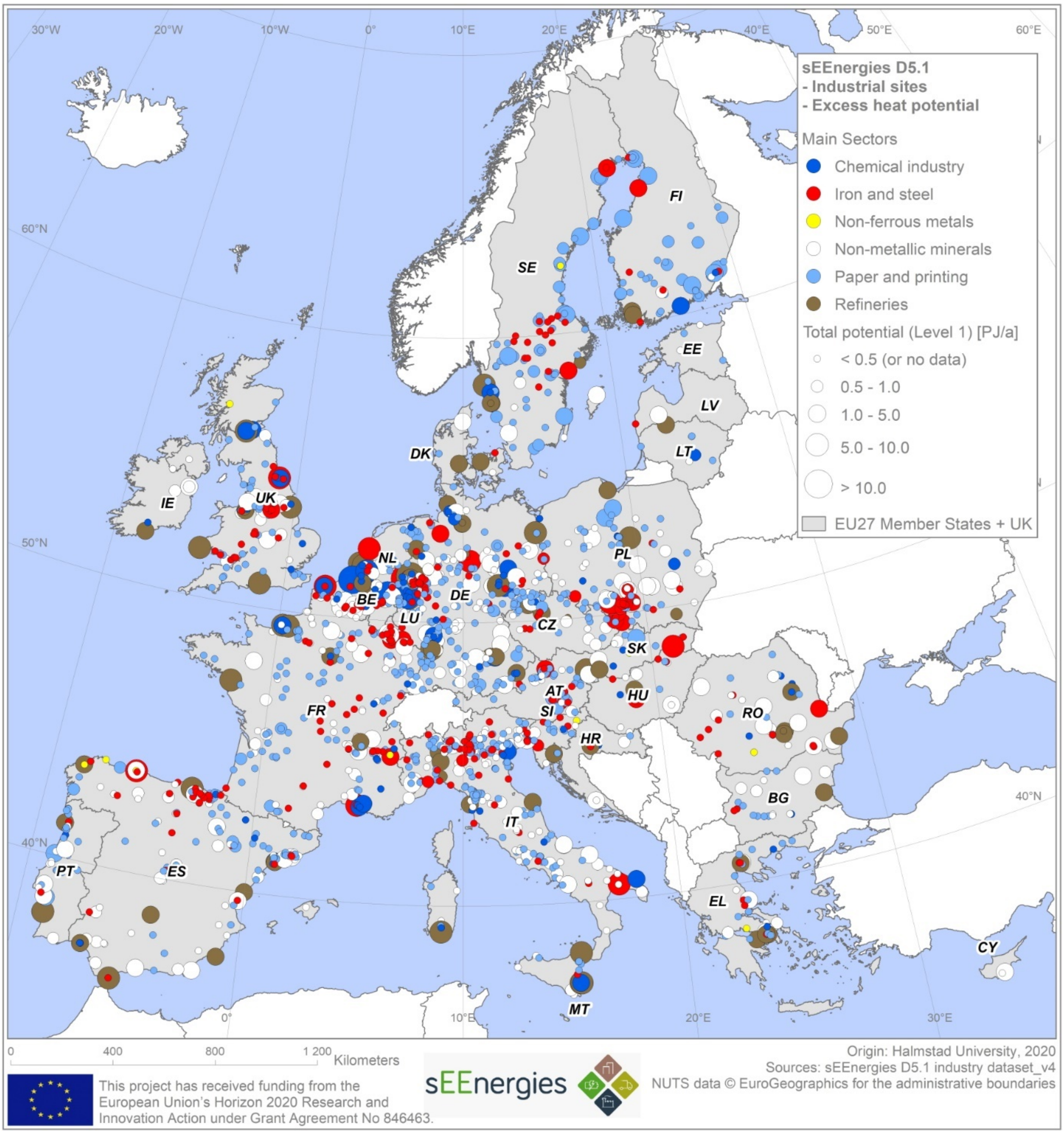

Figure 17: EU28 map of the 1842 georeferenced industrial sites by Main Sectors and with Level 1 (25°C) excess heat potential at current rate of internal heat recovery

The total annual excess heat potential presented in Figure 17 is correspondingly detailed for each Member state in Table 27, and with reference to all six established potentials. As briefly mentioned above, since sites with excess heat data represents 87% of the total EU28 count of sites, the annual potentials accounted for in Table 27 are likely a slight underestimate. Another circumstance which emphasises that the potentials for industrial excess heat here assessed are conservative is that only large-scale facilities have been mapped (and only those belonging to energy-intensive main sectors).

Table 27: Total potential: EU28 extract of the georeferenced industrial sites by Member State (MS), without and with excess heat data, and estimated potentials for the six level categories

			Excess Heat Potential					
			Current Internal Heat Recovery			Max Internal Heat Recovery		
MS	Industrial Sites [n]	Industrial Sites - With Excess Heat Data [n]	Level 1 (25°C) [PJ/a]	Level 2 (55°C) [PJ/a]	Level 3 (95°C) [PJ/a]	Level 1 (25°C) [PJ/a]	Level 2 (55°C) [PJ/a]	Level 3 (95°C) [PJ/a]
AT	48	44	24.3	13.1	11.0	17.7	7.2	5.2
BE	44	34	37.7	18.3	15.0	29.4	10.9	7.8
BG	21	19	8.3	4.7	4.1	5.5	2.2	1.7
CY	2	2	1.4	1.1	1.0	1.0	0.7	0.6
CZ	44	39	20.5	13.1	11.6	12.8	6.1	4.6
DE	343	310	184.1	99.3	83.4	132.8	53.0	38.1
DK	7	5	5.9	3.2	2.8	4.0	1.5	1.1
EE	4	4	0.7	0.5	0.4	0.5	0.4	0.3
EL	38	36	17.0	9.0	7.6	12.4	5.0	3.7
ES	171	143	84.0	44.4	37.8	58.9	22.0	16.0
FI	50	47	31.6	13.3	10.7	25.4	8.2	5.7
FR	225	197	101.2	53.5	45.1	72.8	27.9	20.1
HR	12	12	8.0	4.1	3.5	5.5	2.0	1.4
HU	17	14	10.2	6.0	5.2	6.9	2.9	2.1
IE	4	4	2.4	2.0	1.8	1.2	0.8	0.7
IT	322	275	102.7	54.5	46.8	70.1	25.1	18.1
LT	8	8	6.6	2.7	2.1	5.8	2.0	1.5
LU	9	5	3.6	2.9	2.7	1.1	0.5	0.4
LV	2	2	1.2	1.0	0.9	0.4	0.3	0.3
MT	No data	No data	No data	No data	No data	No data	No data	No data
NL	44	41	65.8	25.2	19.1	56.6	17.4	11.6
PL	107	98	63.8	40.5	35.9	41.6	19.8	15.5
PT	41	38	20.7	11.1	9.5	13.8	5.1	3.7
RO	42	36	21.9	13.5	11.8	13.4	5.8	4.4
SE	84	70	45.9	21.1	17.3	35.0	11.8	8.3
SI	15	15	1.6	1.1	1.0	0.8	0.5	0.4
SK	18	16	13.2	8.3	7.2	9.1	4.5	3.5
UK	120	94	76.0	36.4	29.9	57.8	20.3	14.2
EU28	**1842**	**1608**	**960**	**504**	**425**	**692**	**264**	**191**

The total EU28 annual industrial excess heat potential from the considered sites and sectors thus represent approximately one exajoule per year (960 PJ), given current rates of internal heat recovery. In a (future) situation where all these industries would be able to harness the energy efficiency benefits of maximum rates of internal heat recoveries, the corresponding (external) total excess heat potential is reduced to some 692 PJ (a reduction of ~28%), the Level 2 potential from 504 PJ to 264 PJ (a ~48% reduction), and the Level 3 potential from 425 PJ to 191 PJ (a ~45% reduction).

If, for the total excess heat potential considered here, the sum of heat demands originating from expected district heating areas within each respective Member State (disregarding any spatial matches between sites and areas), are plotted together with the sum of excess heat per Member State, the correlation between these two dimensions may be investigated. Figure 18 shows this comparison with regards to the total excess heat potential at current rates of internal heat recovery at left, and with regards to maximum rates of internal heat recovery at right.

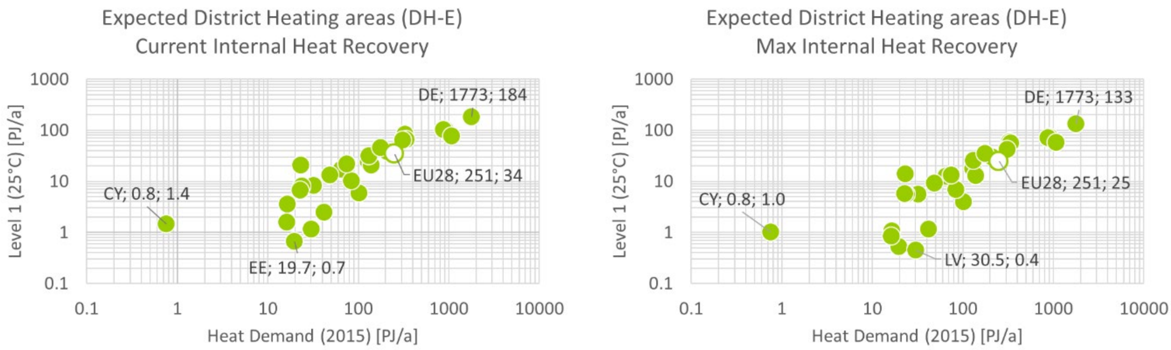

Figure 18: Total potential: Member State correlation between Expected District Heating areas (DH-E) heat demands and the corresponding industrial excess heat potential, for current rate of internal heat recovery and Level 1 temperatures (25°C) at left, and for maximum rate of internal heat recovery and Level 1 temperatures (25°C) at right. The EU28 marker represents average values

As can be seen in Figure 18 (at left), the sum of expected district heating areas heat demands per Member State range from approximately 10 PJ per year to well above 1000 PJ (excluding outlier Cyprus). Annual total industrial excess heat volumes range correspondingly from approximately 0.7 to 184 PJ per year. The average of all Member States sums values, here labelled "EU28", is found at expected district heating areas heat demand of 251 PJ at an annual industrial excess heat volume of 34 PJ, indicating an approximative 14% possible coverage of heat demands by excess heat in these areas.

For the situation with maximum rates of internal heat recovery, as displayed in Figure 18 at right, the heat demand volumes established for the district heating areas are here kept at the same level (which likely would not be the case in a future scenario where maximum rates of internal heat recoveries are implemented), but the corresponding excess heat volumes are decreased. Annual, for external use available, excess heat volumes are now found in the range between 0.4 and 133 PJ per year, with the EU28 average found at 25 PJ (~10% coverage).

5.3.3 Selected excess heat potential 1

For the first selected potential, due to the high degree of spatial matches between sites and expected district heating areas (98%, as mentioned above), annual excess heat volumes are principally found at the same order of magnitude as for the total potential. The sum of heat demands for the associated expected district heating areas per Member State, however, are here significantly reduced in comparison, since only those district heating areas with spatial matches to industrial sites are considered.

Table 28 presents the first selected annual industrial excess heat potential for EU28. The full potential under these conditions (Level 1) is only marginally lower than the total potential (941 PJ), given current rates of internal heat recovery. In a situation where these industries would be able to operate at maximum rates of internal heat recoveries, the corresponding (external) Level 1 excess heat potential is reduced to 680 PJ (an equivalent reduction of ~28% as in the case of the total potential), the Level 2 potential from 493 PJ to 258 PJ (a ~48% reduction also here), and the Level 3 potential from 415 PJ to 187 PJ (a ~55% reduction). A possible response to the relatively larger reduction of excess heat volumes at the third level (under maximum rates of internal heat recovery), is for future external heat recoveries to be made at Level 2 conditions, which would correspond to 4th generation district heating supply temperatures (Lund et al., 2014).

Table 28: Selected potential 1: EU28 extract of the georeferenced industrial sites by Member State (MS) with spatial match to Expected District Heating areas (DH-E), without and with excess heat data, and estimated potentials for the six level categories

			Excess Heat Potential					
			Current Internal Heat Recovery			Max Internal Heat Recovery		
MS	**Industrial Sites - With DH-E Match [n]**	**Industrial Sites - With DH-E Match and Excess Heat Data [n]**	**Level 1 (25°C) [PJ/a]**	**Level 2 (55°C) [PJ/a]**	**Level 3 (95°C) [PJ/a]**	**Level 1 (25°C) [PJ/a]**	**Level 2 (55°C) [PJ/a]**	**Level 3 (95°C) [PJ/a]**
AT	48	44	24.3	13.1	11.0	17.7	7.2	5.2
BE	44	34	37.7	18.3	15.0	29.4	10.9	7.8
BG	20	18	7.6	4.1	3.6	5.2	2.0	1.5
CY	No data	No data	No data	No data	No data	No data	No data	No data
CZ	44	39	20.5	13.1	11.6	12.8	6.1	4.6
DE	343	310	184.1	99.3	83.4	132.8	53.0	38.1
DK	7	5	5.9	3.2	2.8	4.0	1.5	1.1
EE	4	4	0.7	0.5	0.4	0.5	0.4	0.3
EL	33	31	15.7	8.0	6.7	11.7	4.5	3.4
ES	166	138	81.5	43.3	36.9	57.1	21.4	15.5
FI	47	44	25.9	11.4	9.3	20.4	6.8	4.8
FR	221	193	101.1	53.4	45.0	72.7	27.9	20.1
HR	10	10	7.6	3.8	3.2	5.3	1.9	1.3
HU	17	14	10.2	6.0	5.2	6.9	2.9	2.1
IE	3	3	1.8	1.5	1.3	0.9	0.6	0.5
IT	321	274	102.4	54.2	46.6	70.0	25.0	18.0
LT	8	8	6.6	2.7	2.1	5.8	2.0	1.5
LU	9	5	3.6	2.9	2.7	1.1	0.5	0.4
LV	2	2	1.2	1.0	0.9	0.4	0.3	0.3
MT	No data	No data	No data	No data	No data	No data	No data	No data
NL	44	41	65.8	25.2	19.1	56.6	17.4	11.6
PL	106	97	63.8	40.5	35.9	41.6	19.8	15.5
PT	36	33	20.1	10.8	9.3	13.4	5.0	3.6
RO	41	35	20.6	12.5	10.9	12.8	5.5	4.1
SE	75	62	41.3	17.9	14.6	32.5	10.6	7.4
SI	15	15	1.6	1.1	1.0	0.8	0.5	0.4
SK	18	16	13.2	8.3	7.2	9.1	4.5	3.5
UK	120	94	76.0	36.4	29.9	57.8	20.3	14.2
EU28	**1802**	**1569**	**941**	**493**	**415**	**679**	**258**	**187**

Figure 19 presents a similar comparison as in Figure 18, but here with reference to the first selected potential for two different cases of external heat recovery: at 3rd generation district heating supply temperatures at left (Level 3 at current rate of internal heat recovery), and at 4th generation district heating supply temperatures at right (Level 2 at maximum rate of internal heat recovery).

The sum of heat demands by expected district heating areas per Member State is now found at 3678 PJ for EU28 (as outlined in Table 23 above), which is related to the Level 3 potential of 415 PJ at left (at current rate of internal heat recovery) and to the Level 2 excess heat potential of 258 PJ at right (at maximum rate of internal heat recovery).

For both cases, it can be seen that no sum of excepted district heating areas heat demands by Member State exceeds the 1000 PJ per year level, and that, for the first case, associated annual excess heat volumes never exceed 100 PJ (maximum at 83 PJ for Germany), and, for the second case, basically not so for the 50 PJ level (Germany with highest value at 53 PJ). The corresponding EU28 average values (averages established on the basis of all Member State sum values) are 131 PJ (average heat demand of expected district heating areas with spatial matches to sites) and, for the first case at left: 15 PJ (~11% coverage)), and, for the second case at right, 9 PJ (~7% coverage).

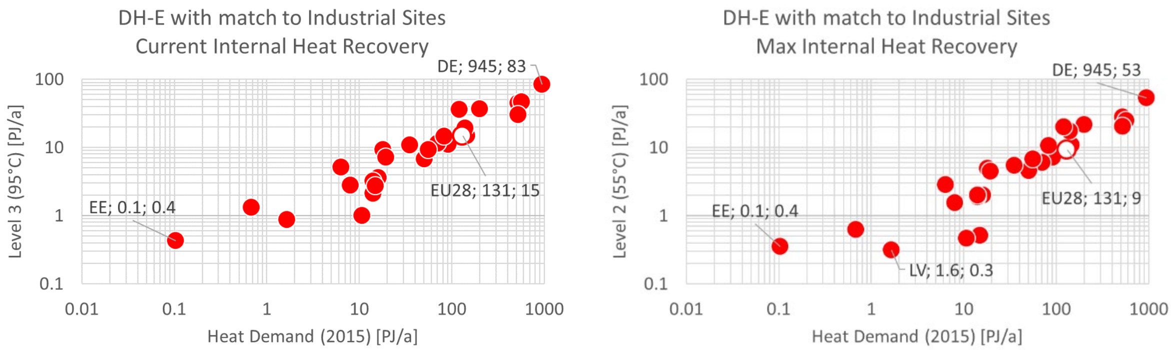

Figure 19: **Selected potential 1: Member State correlation between matching Expected District Heating areas (DH-E) heat demands and the corresponding industrial excess heat potential, for current rate of internal heat recovery and Level 3 temperatures (95°C) at left, and for maximum rate of internal heat recovery and Level 2 temperatures (55°C) at right. The EU28 marker represents average values**

5.3.4 Selected excess heat potential 2

Considering the second selected excess heat potential, Table 29 presents the results for all industrial sites (866 in total, 752 with data) with spatial matches to actual district heating areas, which, as presented in Table 23 above, consists of 724 areas with a total heat demand sum of 2169 PJ.

Table 29: **Selected potential 2: EU28 extract of the georeferenced industrial sites by Member State (MS) with spatial match to Actual District Heating areas (DH-A), without and with excess heat data, and estimated potentials for the six level categories**

			Excess Heat Potential					
			Current Internal Heat Recovery			Max Internal Heat Recovery		
MS	**Industrial Sites - With match to DH-A [n]**	**Industrial Sites - With match to DH-A and Excess Heat Data [n]**	**Level 1 (25°C) [PJ/a]**	**Level 2 (55°C) [PJ/a]**	**Level 3 (95°C) [PJ/a]**	**Level 1 (25°C) [PJ/a]**	**Level 2 (55°C) [PJ/a]**	**Level 3 (95°C) [PJ/a]**
AT	44	40	23.87	12.83	10.69	17.48	7.12	5.14
BE	34	26	36.76	17.65	14.42	28.92	10.74	7.68
BG	11	10	4.73	2.26	1.92	3.34	1.06	0.74
CY	No data	No data	No data	No data	No data	No data	No data	No data
CZ	43	38	19.94	12.77	11.20	12.62	6.00	4.55
DE	156	142	119.76	63.63	52.83	90.03	36.47	26.21
DK	6	4	3.93	2.61	2.31	2.19	1.06	0.81
EE	3	3	0.64	0.48	0.43	0.50	0.35	0.30
EL	1	1	0.00	0.00	0.00	0.00	0.00	0.00
ES	26	21	5.94	4.27	3.93	2.59	1.16	0.88
FI	40	38	24.24	10.81	8.80	19.03	6.42	4.53
FR	111	102	58.25	29.24	24.29	42.80	15.32	10.67
HR	6	6	5.64	2.56	2.11	4.28	1.43	1.02
HU	14	12	8.87	4.89	4.15	6.47	2.73	2.05
IE	No data	No data	No data	No data	No data	No data	No data	No data
IT	59	47	9.28	7.16	6.55	3.92	2.14	1.64
LT	8	8	6.63	2.68	2.12	5.76	2.01	1.48
LU	4	2	2.42	1.91	1.83	0.66	0.23	0.17
LV	2	2	1.15	0.96	0.88	0.44	0.31	0.25
MT	No data	No data	No data	No data	No data	No data	No data	No data
NL	11	10	33.73	11.00	8.09	29.83	8.06	5.29
PL	85	76	51.50	31.36	27.55	35.17	16.07	12.48
PT	3	3	0.44	0.36	0.34	0.13	0.06	0.04
RO	20	18	13.65	7.55	6.49	9.03	3.39	2.42
SE	67	54	35.21	15.48	12.56	27.88	9.23	6.46
SI	14	14	1.57	1.12	1.01	0.84	0.46	0.37
SK	18	16	13.19	8.28	7.17	9.06	4.49	3.46
UK	80	59	48.12	22.25	17.91	38.32	13.48	9.32
EU28	**866**	**752**	**529**	**274**	**230**	**391**	**150**	**108**

The full excess heat potential under these conditions (Level 1, current rate of internal heat recovery) is found at 529 PJ per year, an annual volume of which principally 53% originates from only four countries: Germany (120 PJ), France (58 PJ), Poland (52 PJ), and the United Kingdom (48 PJ). Compared to the total and the first selected potentials, the relative reduction of annual excess heat volumes at this second selected potential is approximately minus 45% with regards to both instances (only marginal difference between the two), and in terms of district heating areas heat demands, a minus 69% reduction compared to the total potential and a minus 41% reduction compared to the first selected potential (with reference to Table 23).

At Level 3 conditions, reflecting current 3rd generation district heat distribution conditions with supply temperatures at 95°C, i.e. the present-day situation in actual European district heating areas, a total of 230 PJ of industrial excess heat should be within reach of existing district heating systems (at current rates of internal heat recovery). This result, in itself, may also be pronounced as a major finding emanating from this work. As a reference, albeit somewhat outdated, Persson and Werner assessed that ~25 PJ of industrial excess heat was recovered in European district heating systems in 2008 (Persson and Werner, 2012). A hands-on estimate on this basis would suggest that current industrial excess heat volumes inside or within 10 km of actual district heating areas is nine times that which is indeed recovered today.

As for the two previous potentials, the Member State correlations are plotted also for the second selected potential, see Figure 20. Thus, only focusing on actual district heating areas with matching industrial sites, it can be seen that the main bulk of Member State heat demands range from 0.07 to just above 500 PJ per year (Germany with the highest value at 535 PJ and the EU28 average at 77 PJ). At current rates of internal heat recovery (at left), annual excess heat volumes range from approximately 0.0003 PJ (Greece) to 53 PJ with an EU28 average at 8.2 PJ, and at maximum rates of internal heat recovery (at right), from 0.0003 PJ to 36 PJ with an EU28 average at 5.3 PJ. In the latter case, the comparison is made to Level 2 conditions, i.e. 4th generation district heat distribution conditions, to emphasise the possibilities for increased industrial excess heat recoveries in the future. For 3rd generation systems (i.e. Level 3), this future setting reduces the annual excess heat potential to some 108 PJ, which, however, still is more than four times anticipated current external recovery levels.

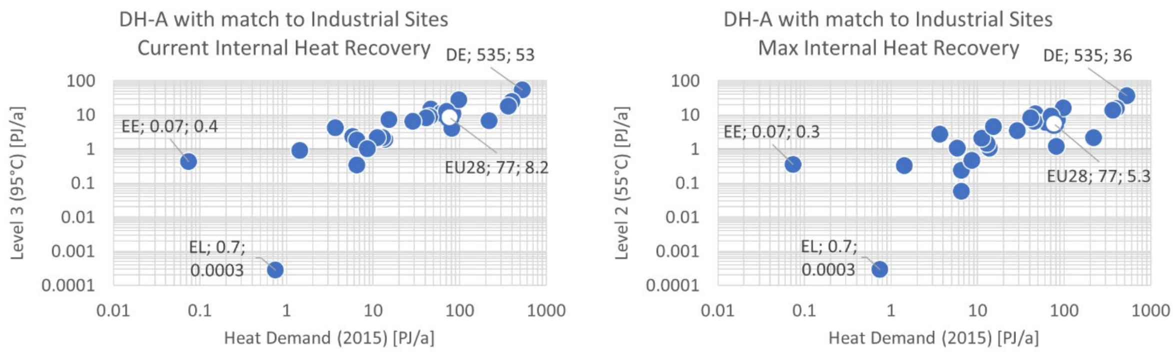

Figure 20: Selected potential 2: Member State correlation between matching Actual District Heating areas (DH-A) heat demands and the corresponding industrial excess heat potential, for current rate of internal heat recovery and Level 3 temperatures (95°C) at left, and for maximum rate of internal heat recovery and Level 2 temperatures (55°C) at right. The EU28 marker represents average values

Finally, to add further perspective to the above presented results, the total count of spatial matches between the 1802 considered industrial sites and the 47,275 expected district heating areas, as resulting from the “Generate Near Table” operation, amounted to 21,638 total matches within the given 10 km search radius limit. As mentioned above, 98% of all EU28 industrial sites investigated (1802 out of 1842) were found to have at least one spatial match at these settings, but the fact is that most industrial sites are located inside or within only a few kilometres from the 12,283 targeted expected district heating areas.

By categorising all measured distances within the 10 km default search radius by ten distance classes, from zero meters (Inside), from zero to one kilometre (0-1km) and so on up to the 10 km limit, as displayed in Figure 21, this interesting characteristic of current EU28 industrial sites is revealed. In terms of total counts, at left in Figure 21, 803 of the 1802 sites (45%) are actually located inside the area perimeters of the associated district heating areas, and another 582 sites (32%) are found within just one kilometre from the borders of these areas. One might fairly conclude that 1549 sites (86%) are located inside or within 2 km – which also is a major finding from this work.

In terms of annual excess heat volumes, here considering the first selected potential at Level 1 and at current rates of internal heat recoveries (941 PJ, as presented above in Table 25 and Table 28), Figure 21 (at right) indicates the corresponding concentration of these volumes to sites located inside or only at a few kilometres from the corresponding expected district heating areas.

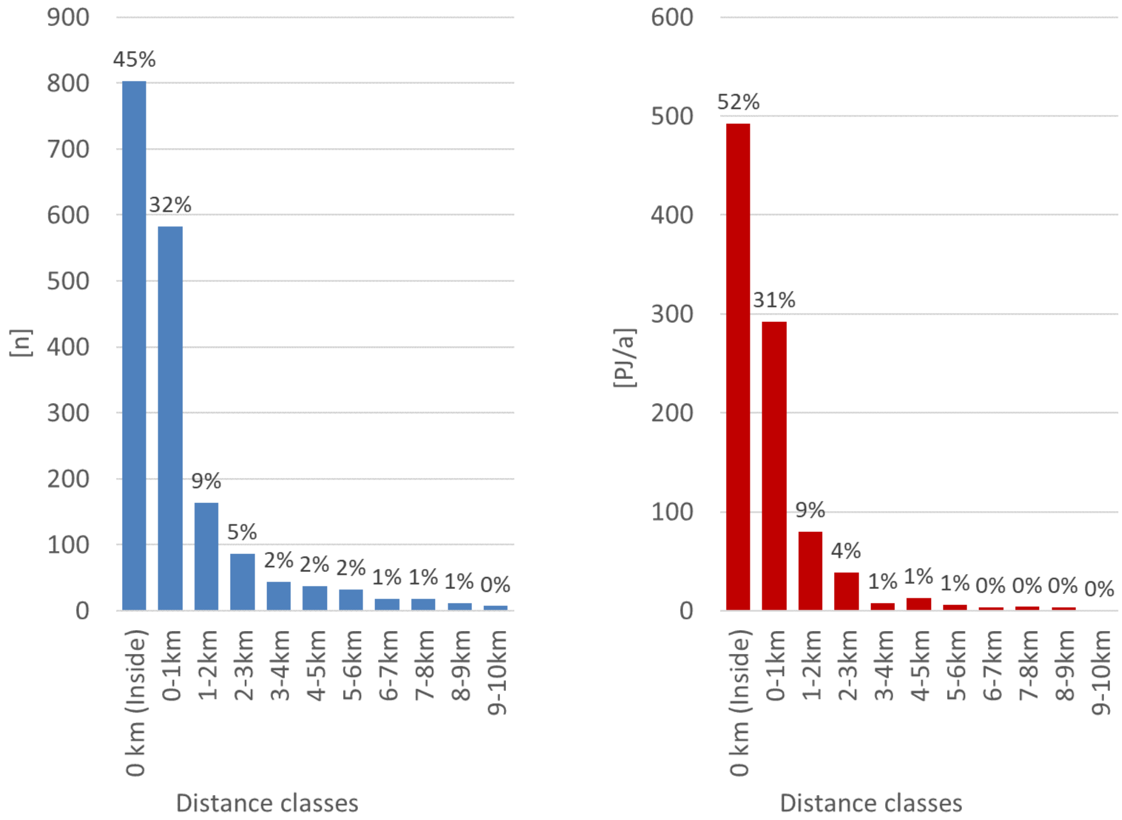

Figure 21: Distribution by first rank match of the 1802 industrial sites with spatial matches to expected district heating areas by ten distance classes, for total count of sites (at left) and for the first selected excess heat potential, Level 1, at current rate of internal heat recovery (at right)

A similar presentation regarding only those industrial sites with spatial matches to actual district heating areas is presented in Table 30, which reflects the results from a separate model run exclusively establishing spatial matches within the 10 km default radius between the 1608 sites with excess heat data and the 2763 actual district heating (DH-A) areas. In Table 30 it can be seen that the distribution of spatial matches is somewhat more evenly spread out over the ten distance classes, while still 206 sites (27%) are located inside, 108 within one km, and another 79 within 2 km, of these areas, giving a total of 393 sites (52% of the 752 sites identified within the 10 km default distance) inside or within two kilometres of these areas. The same pattern is correspondingly reflected with regards to the annual excess heat potential, here represented by the second selected potential at 95 ˚C and at current rates of internal heat recovery (Level 3). As can be seen in the table, 114 PJ, or some 50% of the 230 PJ total excess heat potential available at these conditions within the 10 km default distance, originates from sites located inside or within only two kilometres of these areas.

Table 30: Industrial sites with exclusive match to actual district heating areas (rank 1 matches within the 10 km distance limit), by ten distance classes for count of sites and second selected excess heat potential, Level 3, at current rate of internal heat recovery

Distance classes	0 km (Inside)	0-1 km	1-2 km	2-3 km	3-4 km	4-5 km	5-6 km	6-7 km	7-8 km	8-9 km	9-10 km	Grand Total
Sites [n]	206	108	79	63	53	47	48	40	35	36	37	752
Share [%]	27%	14%	11%	8%	7%	6%	6%	5%	5%	5%	5%	100%
Sel. Pot. 2 (L3) [PJ/a]	54	29	31	26	17	9	15	12	9	13	15	230
Share [%]	24%	13%	13%	11%	8%	4%	6%	5%	4%	6%	7%	100%

6 Conclusions and recommendations

Our results show a total potential of 425 PJ of industrial excess heat available at a temperature of 95°C, with 960 PJ available at a lower temperature (25°C). This equals about 4% and 9% of total industrial final energy demand in 2015, respectively. This is calculated for a total of 1608 sites from the energy-intensive industries.

Matching this potential with a GIS analysis of heat demand densities and current (actual) district heating systems reveals that 230 PJ of excess heat could be used within a 10km range at a temperature of 95°C, which is compatible with most existing district heating systems (*Selected potential 2*). As district heat today has a total final energy consumption of 1,945 PJ, this means that about 12% of district heating in the EU28 could be supplied by excess heat sources from energy-intensive industries.

While this is already a substantial potential, many excess heat sources remain untapped, particularly in countries with low district heating use. We therefore projected future expected district heating areas based on a GIS analysis of heat demand densities for all EU28 countries. Expected district heating areas are defined as coherent areas with heat demand densities above 500 GJ/ha. These areas meet current economic suitability criteria for district heating[4].

The results indicate that district heating systems would be economically viable in most urban areas in Europe and could cover as much as 65% of heat demand in buildings in the residential and service sectors. This represents an enormous increase compared to today's use of district heating, which accounts for about 9% of total heating and cooling energy demand in the EU28 residential and service sectors (Fleiter et al. 2018). If district heating systems were expanded, they could use almost all the available excess heat from the industrial sites analysed. 98% of these are within 10km, allowing the exploitation of 415 PJ of heat at 95°C (*Selected potential 1*). In fact, a majority of sites are located inside or within only a few kilometres of these areas.

In the future, low-temperature district heating systems, often referred to as 4th generation district heating, are expected to diffuse further, which will increase the amount of excess heat available. For example, at a temperature of 25°C, the exploitable excess heat potentials will more than double from 415 PJ (95°C) to 940 PJ (25°C). This low-temperature heat could either be used in cold district heating systems with decentralised heat pumps, or in centralised large-scale heat pumps to supply district heating systems at higher temperatures (see for example Popovski et al. 2019).

To summarize, our analysis reveals a significant potential of mostly untapped excess heat from energy-intensive industries that could be used in district heating systems as well as a huge potential to increase the use of district heating systems in Europe. Combining excess heat sources and the deployment of district heating systems should therefore be a central element in the transition towards a sustainable and CO_2-neutral heating and cooling sector in Europe. However, the analysis also shows that industrial excess heat alone will not be sufficient, and the major heat source for district heating will need to come from renewable energy sources (locally, this might be different in highly industrialised areas).

[4] The areas correspond to heat demand density classes 3, 4, and 5, as established in the Heat Roadmap Europe 4 project

It is essential to underline that inherent to the bottom-up approach taken, there is always a certain excess heat potential that remains outside the system boundary of our analysis. In particular this includes

- smaller industrial facilities,
- activities with comparably lower energy demand (e.g. furnaces in downstream steel or other metals processing, products like ceramics, bricks, chemical products, food industry),
- non-industrial activities with low temperature heat demand like wastewater treatment plants, metro stations or data centers.
- excess heat sources beyond the waste heat losses from exhaust gases, such as waste heat from solid and liquid streams, cooling water, and radiation and conduction heat losses.

Including such additional excess heat sources would certainly increase the potential available, particularly at the lower temperatures. However, the excess heat potential within the scope of this study comprises the most relevant potentials, because they are large major point sources and often provide heat at high temperature levels. Thus, exploiting sources beyond our system boundary would probably involve higher specific costs, because smaller excess heat streams would need to be addressed. Still, further research should also include such excess heat sources that probably will also become more attractive with the diffusion and technical learning of heat pumps.

While we focused on the spatial availability and use of excess heat on an annual basis, the sub-annual availability e.g. with daily or hourly resolution is another important restriction for the use of excess heat and should be addressed by further research (see for example Bühler et al. 2018).

Another aspect of our modelling which could be improved in future research is the determination of distances to be used for spatial matching of industrial sites (supply) and expected district heating areas (demand). While a fixed 10-kilometre search radius was used in this context, alternative approaches could be developed where the distances to be considered instead are resulting outputs from cost-optimisation modelling based on acceptable heat distribution costs (answering the question: up to what distance can excess heat from a given site be feasibly transferred while meeting certain cost constraints?). Such approaches could possibly also take into consideration other influential factors, for example that different user sectors (residential, service, industrial etc.) may represent different levels in terms of acceptable heat distribution costs.

A fourth item for future research contains potential structural changes that might take place while the industry sector transforms towards a CO_2-neutral production. This can mean a shift from primary to secondary production, the use of synthetic fuels via new processes like direct reduction of iron ore based on hydrogen, a more efficient use of energy, electrification, etc. All these changes will affect the availability of excess heat, subject to other analyses in the sEEnergies project.

References

Ammar, Y.; Joyce, S.; Norman, R.; Wang, Y.; Roskilly, A. P. (2012): Low grade thermal energy sources and uses from the process industry in the UK. Applied Energy, 89(1), 3-20.

Aydemir, A., Doderer, H., Felix, H. & Braungart, S. (2019). Abwärmenutzung in Unternehmen - Studie für das Ministerium für Umwelt, Klima und Energiewirtschaft Baden-Württemberg.

BCS Inc. (2008): Waste heat recovery: technology and opportunities in U.S. industry. U.S. Department of Energy, Office of Energy Efficiency and Renewable Energy, Industrial Technologies Program Washington, DC, USA.

Blesl, M.; Kempe, .S; Ohl, M.; Fahl, U.; König, A.; Jenssen, T.; Eltrop, L. (2008): Wärmeatlas Baden-Württemberg: Erstellung eines Leitfadens und Umsetzung für Modellregionen, Forschungsbericht, FZKA-BWPLUS; 2008.

Blesl, M.; Ohl, M.; Fahl, U. (2011): Ganzheitliche Bewertung innovativer mobiler thermischer Energiespeicherkonzepte für Baden-Württemberg auf Basis branchen- und betriebsspezifischer Wärmebedarfsstrukturen Programm Lebensgrundlage Umwelt und ihre Sicherung (BWPLUS), durchgeführt vom Institut für Energiewirtschaft und Rationelle Energieanwendung (IER). Universität Stuttgart.

Boddy, J.H. (1994): Sources of heat, in: Institution of Electrical Engineers. Profiting from low-grade heat: thermo- dynamic cycles for low-temperature heat sources. U.K: Crook AW (ed).

Bonilla, J. J.; Blanco, J. M.; Lopez, L.; Sala, J. M. (1997): Technological recovery potential of waste heat in the industry of the Basque Country. Applied Thermal Engineering, 17(3), 283-288.

Boulamanti, A.; Moya, J.A. (2017): Energy efficiency and GHG emissions: Prospective scenarios for the chemical and petrochemical industry. EUR 28471 EN, doi:10.2760/20486.

Brückner, S.; Arbter, R.; Pehnt, M.; Laevemann, E. (2017): Industrial waste heat potential in Germany – a bottom up analysis. Energy Efficiency 10, 513–525.

Brückner, S.; Miró, L.; Cabeza, L. F.; Pehnt, M.;Laevemann, E. (2014): Methods to estimate the industrial waste heat potential of regions–A categorization and literature review. Renewable and Sustainable Energy Reviews, 38, 164-171.

Bühler, F.; Nguyen, T.; Elmegaard, B. (2016): Energy and exergy analyses of the Danish industry sector. Applied Energy 184, 1447–1459.

Bühler, F.; Petrović, S.; Holm, Müller, F.; Karlsson, K.; Elmegaard, B. (2017). Industrial excess heat for district heating in Denmark. Applied Energy 205, S. 991-1001.

Bühler, F.; Petrović, S.; Holm, F. M.; Karlsson, K.; Elmegaard, B. (2018): Spatiotemporal and economic analysis of industrial excess heat as a resource for district heating. Energy 151, S. 715–728. DOI: 10.1016/j.energy.2018.03.059.

Cronholm, L.; Grönkvist S.; Saxe, M. (2009): Spillvärme fran industrier – och värmeatervinning fran lokaler. Svensk Fyärrvärme. [http://www.svenskfjarrvarme.se/Global/FJ%C3%84RRSYN/Rapporter%20och%20resultatblad/Rapporter%20omv%C3%A4rld/2009/Spillv%C3%A4rme%20fr%C3%A5n%20industrier%20och%20lokaler%20.pdf]

Dengler, J.; Köhler, B.; Dinkel, A.; Bonato, P.; Azam, N.; Kalz, K. (2016): Mapping and analyses of the current and future (2020 - 2030) heating/cooling fuel deployment (fossil/renewables). Work package 2: Assessment of the technologies for the year 2012. Prepared for the European Commission.

Ecofys; Fraunhofer Institute; Öko-Institut. (2009): Methodology for the free allocation of emission allowances in the EU ETS post 2012 – Sector report for the pulp and paper industry, by order of the European Commission, Utrecht, Berlin, Freiburg.

Ecoheatcool (2006): Ecoheatcool work package 1. The European heat market. Final report.

Element Energy; Ecofys & Imperial College (2014): The potential for recovering and using surplus heat from industry. Final Report for DECC. Londen.

Energetics (2004): Energy use, loss, and opportunities analysis. U.S manufacturing & mining. U.S. Department of Energy.

Enova (2009): Utnyttelse av spillvarme fra norsk industry – en potensialstudie.

European Cement Research Academy (ECRA); Cement Sustainability Initiative (CSI) (2017): "Development of State of the Art - Techniques in Cement Manufacturing: Trying to Look Ahead". Düsseldorf, Germany.

European Environment Agency (a): European Union Emissions Trading System (EU ETS) data from EUTL (EU Transaction Log). Available at (2020-02-25): https://www.eea.europa.eu/ds_resolveuid/DAT-21-en

European Environment Agency (2020b): The European Pollutant Release and Transfer Register (E-PRTR), Member States reporting under Article 7 of Regulation (EC) No 166/2006. Available at (2020-02-25): https://www.eea.europa.eu/ds_resolveuid/DAT-26-en

European IPPC Bureau. (2013a): Best available techniques (BAT) reference document for iron and steel production. Industrial Emissions Directive 2010/75/EU (Integrated Pollution Prevention and Control). Seville, Spain, European Commission, Joint Research Centre, Institute for Prospective Technologies Studies.

European IPPC Bureau (2013b): Best available techniques (BAT) reference document for the manufacture of glass. Industrial Emissions Directive 2010/75/EU (Integrated Pollution Prevention and Control). Seville, Spain, European Commission, Joint Research Centre, Institute for Prospective Technologies Studies.

European IPPC Bureau (2013c): Best available techniques (BAT) reference document for the production of cement, lime and magnesium oxide. Industrial Emissions Directive 2010/75/EU (Integrated Pollution Prevention and Control). Seville, Spain, European Commission, Joint Research Centre, Institute for Prospective Technologies Studies.

European IPPC Bureau (2015): Best available techniques (BAT) reference document for the refining of mineral oil and gas. Industrial Emissions Directive 2010/75/EU (Integrated Pollution Prevention and Control). Seville, Spain, European Commission, Joint Research Centre, Institute for Prospective Technologies Studies.

Eurostat (2019): NUTS 2016 (NUTS_BN_01M_2016_3035). Download date: 2019-09-24. Eurostat - Your key to European statistics. Luxembourg.

Eurostat (2020a): Complete energy balances (nrg_bal_c).

Eurostat (2020b): Statistics on the production of manufactured goods. Total production by PRODCOM list (NACE Rev. 2) - annual data (DS-066342).

Fakhrai, R. (2002): Black liquor combustion in Kraft recovery boilers-Numerical modelling. Doctoral thesis. Royal Institute of Technology, Stockholm, Sweden.

Fleiter, Tobias; Elsland, Rainer; Rehfeldt, Matthias; Steinbach, Jan; Reiter, Ulrich; Catenazzi, Giacomo et al. (2017): Profile of heating and cooling demand in 2015. Heat Roadmap Europe 4. Fraunhofer ISI; TEP Energy; Utrecht University; Armines. Karlsruhe, Zürich, Utrecht, Paris.

Fleiter, T.; Manz, P.; Neuwirth, N.; Mildner, F.; Persson, U.; Kermeli, K.; Crijns-Graus, W.; Rutten, C. (2020): sEEnergies D5.1 Dataset Web-App. sEEnergies ArcGIS Online Web-Apps hosted by Europa-Universität Flensburg. Available at (2020-02-24): https://tinyurl.com/sEEnergies-D5-1.

Fydrich, M. (2017): Assembly of a Site-specific Database for the European Basic Materials Industry – Application for Regional CO2 Storage Potential. Master's Thesis, Karlsruhe Institute of Technology.

Glatzel, W.D.; Langniß, O.; Pehnt, M. (2001): Energie im Wandel: Politik, Technik und Szenarien einer nachhaltigen Energiewirtschaft Abwärme – die vergessene Eigenenergie: Ein Blick zurück und in die Zukunft, pp. 151-164. Berlin Heidelberg New York: Springer-Verlag.

Hammond, G.; Norman, J. (2012): Heat recovery opportunities in UK manufacturing. In International Conference on Applied Energy (ICAE2012). University of Bath.

Heat Roadmap Europe (HRE) (2017): Baseline scenario of the heating and cooling demand in buildings and industry in the 14 MSs until 2050. WP.3: D3.3 and D3.4. www.heatroadmap.eu

Hendricks T.; Choate W.T. (2006): Engineering scoping study of thermoelectric generator systems for industrial waste heat recovery, Industrial Technologies Program, U.S. Department of Energy.

Hough, G. (1985): Chemical Recovery in the Alkaline Pulping Process. TAPPI press, Atlanta, United States.

HRE (2018): Heat Roadmap Europe - A low-carbon heating and cooling strategy for Europe. Available at (2018-11-21): https://heatroadmap.eu/

International Energy Agency (IEA) (2000): CO2 abatement in oil refineries: fired heaters. IEA Greenhouse Gas R&D Programme. Report Number PH3/31.

Jörissen, J.; Turek, T.; Weber, R. (2011): Chlorhestellung mit Sauerstoffverzehrkathoden. Chem. Unserer Zeit, 45, pp. 172-183.

Kattenstein, T.; Drath T.; Ziolek A.; Unger H.; Wagner, H.J. (2002): Validierung und kommunale Disaggregierung des Expertensystems HERAKLES. Abschlussbericht: Ruhr-Universität Bochum.

Kermeli, K.; E. Worrell, W.; Crijns-Graus, W.; Corsten. M. (2017): Energy efficiency and cost savings opportunities for ammonia and nitrogenous fertilizer production. An ENERGY STAR Guide for energy and plant managers. United States Environmental Protection Agency (U.S. EPA).

Kramer, K.J.; E. Masanet, E.; Worrell. E. (2009): Energy efficiency opportunities in the U.S. pulp and paper industry. Conference: World Energy Engineering Congress 2008. United States.

Land, A.L.; Feldhusen Tvärne, H.A.; Cronholm, L.A.;Sundlof, C. (2002): Industriell spillvärme – Processer och potentialer. Svenska Fjärrvärmeforeningens Service AB.

Lopez, L.; Blanco, J. M.; Bonilla, J. J.; Bacza, S.; Sala, J. M. (1998): Determination of energy and exergy of waste heat in the industry of the Basque Country. Applied thermal engineering, 18(3), 187-197.

Lund, H.; Werner, S.; Wiltshire, R.; Svendsen, S.; Thorsen, J.E.; Hvelplund, F. et al. (2014): 4th Generation District Heating (4GDH): Integrating smart thermal grids into future sustainable energy systems. Energy. 2014;68(0):1-11.

Lundqvist, P. (2009): Mass and energy balances over the lime kiln in a kraft pulp mill. Uppsala Universitet.

Manz, P.; Fleiter, T.; Aydemir, A. (2018): Developing a georeferenced database of energy-intensive industry plants for estimation of excess heat potentials. Eceee industrial summer study proceedings, 239 - 247.

McKenna, R. (2009): Industrial energy efficiency: Interdisciplinary perspectives on the thermodynamic, technical and economic constraints (Doctoral dissertation, University of Bath).

McKenna, R. C.; & Norman, J. B. (2010): Spatial modelling of industrial heat loads and recovery potentials in the UK. Energy Policy, 38(10), 5878-5891.

Miro, L.; Brückner, S.; Cabeza, L.F. (2015): Mapping and discussing Industrial Waste Heat (IWH) potentials for different countries. Renewable and Sustainable Energy Reviews 51, 847–855.

Norbom, H.R. (1985): Minor, inexpensive kiln upgrades yield major gains in performance. Pulp and paper (59), pp. 118-123.

Pehnt, M.; Boedekery, J.; Arens, M.; Jochem, E.; Idrissora, F. (2010): Die Nutzung industrieller Abwärme – technisch-wirtschaftliche Potenziale und energiepolitische Umsetzung Wissenschaftliche Begleitforschung zu übergreifenden technischen, ökologischen, ökonomischen und strategischen Aspekten des nationalen Teils der Klimaschutzinitiative FKZ 03KSW016A und B.

Persson, U.; Werner, S. (2012): District heating in sequential energy supply. Applied Energy. 2012;95:123-31.

Persson, U.; Möller, B.; Werner, S. (2014): Heat Roadmap Europe: Identifying strategic heat synergy regions, Energy Policy 74. 663–681.

Persson, U. (2014): Stratego, Work Package 2, Background Report 7: Quantifying the Excess Heat Available for District Heating in Europe.

Persson, U.; Möller, B.; Wiechers, E. (2017): Methodologies and assumptions used in the mapping. Deliverable 2.3: A final report outlining the methodology and assumptions used in the mapping. August 2017. Heat Roadmap Europe 2050, A low-carbon heating and cooling strategy. Available at (2018-12-10): https://heatroadmap.eu/wp-content/uploads/2018/11/D2.3_Revised-version_180928.pdf

Persson, U.; Wiechers, E.; Möller, B.; Werner S. (2019): Heat Roadmap Europe: Heat distribution costs. Energy. 2019;176:604-22.

PETA 4.3 (2018): Pan-European Thermal Atlas 4.3 (PETA 4.3). Europa-Universität Flensburg, ArcGIS Online. Heat Roadmap Europe - A low-carbon heating and cooling strategy for Europe. Available at (2018-11-22): https://heatroadmap.eu/peta4

Popovski, E.; Fleiter, T.; Santos, H.; Leal, V.; Fernandes, E. (2018): Technical and economic feasibility of sustainable heating and cooling supply options in southern European municipalities-A case study for Matosinhos, Portugal. In: Energy, Volume 153, 15 June 2018, Pages 311-323; https://doi.org/10.1016/j.energy.2018.04.036.

Popovski, E.; Aydemir, A.; Fleiter, T.; Bellstädt, D.; Büchele, R.; Steinbach, J. (2019): The role and costs of large-scale heat pumps in decarbonising existing district heating networks – A case study for the city of Herten in Germany. In: Energy, Vol. 180, August 2019, pp. 918-933.

Ray, H.S.; Singh, B.P.; Bhattacharjee, S.; Misra, V.N. (2005): Energy in minerals and metallurgical industries. Allied Publishers PVT LTD. New Delhi, India.

sEEnergies (2020): sEEnergies Open Data. Europa-Universität Flensburg. Available at (2020-02-24): https://tinyurl.com/sEEnergies-Hub.

United States Department of Energy (U.S. DOE) (2002): Steam system opportunity assessment for the pulp and paper, chemical manufacturing, and petroleum refining industries. Office of energy efficiency and renewable energy. United States.

United States Environmental Protection Agency (U.S. EPA) (2009): Technical support document for the lime manufacturing sector: proposed rule for mandatory reporting of greenhouse gases. Office of air and radiation, U.S. EPA.

Vakkilainen, E.K. (2005): Kraft recovery boilers – principles and practice. Suomen Soodakattilayhdistys r.y. Helsinki.

Wiechers, E.; Möller, B.; Persson, U. (2020): D5.2 Documentation and dataset from the analysis and mapping of cities with similar topography and demography and the relation to energy efficient transport and mobility. sEEnergies - Quantification of Synergies between Energy Efficiency First Principle and Renewable Energy Systems. Horizon 2020 Project No. 846463.

Wiechers, E.; Möller, B. (2020): sEEnergies D5.2 Dataset Web-App. sEEnergies ArcGIS Online Web-Apps hosted by Europa-Universität Flensburg. Available at (2020-02-24): https://tinyurl.com/sEEnergies-D5-2.

Worrell, E.; Kermeli, K.; Galitsky, C. (2013): Energy efficiency improvement and cost saving opportunities for cement making. Washington DC: United States Environmental Protection Agency (U.S. EPA).

Xu, T.; Sathaye, J.; Kramer, K.J. (2012): Bottom-up representation of industrial energy efficiency technologies in Integrated Assessment models for the U.S. pulp and paper sector.Ernest Orlando Lawrence Berkeley National Laboratory (LBNL), Environmental Energy Technologies Division. DE-AC02-05CH11231.